Manufacturing of thick-walled composites

Curado de composites gruesos

Ángel Rodríguez Gil

Ingeniería Industrial

Supervisor (Universidad Carlos III de Madrid):

Dr. José Manuel Torralba Castelló

Supervisor (Delft University of Technology):

Ir. Jordy M. Balvers

Ángel Rodríguez Gil
Septiembre 2010

INDEX

1 INTRODUCTION 2

1.1 BACKGROUND 3
1.2 OBJECTIVE 4
1.3 SCOPE 5

2 LITERATURE REVIEW 6

2.1 EXPERIMENTAL WORK 6
2.2 CURE SIMULATION 13
2.2.1 Available models 13
2.2.2 Submodels: Material parameters 15
2.3 OPTIMISATION ROUTINES 19
2.3.1 Minimization of temperature gradients 20
2.3.2 Prediction of temperature overshoots 22
2.3.3 Isothermal step in the thermal profile optimisation 24
2.3.4 Reduction of stresses and cycle time 26
2.3.5 Cure cycle optimisation with genetic algorithm 32

3 CURE KINETICS MODEL 34

3.1 CURE KINETICS 34
3.2 THE MODEL IN COMSOL MULTIPHYSICS 46

4 EXPERIMENTAL WORK 49

4.1 PREPARATION OF THE MOULD 50
4.2 LAYOUT OF GLASS FIBRE LAYERS AND THERMOCOUPLES 50
4.3 PROCEDURE 51
4.4 DENSITY AND VOLUME FRACTION CALCULATION 51

5 SIMULATION OF THE RTM CURING PROCESS AND ITS RESULTS 54

5.1 PARAMETERS SETTINGS AND EQUATIONS 54
5.2 CALCULATION OF THE SSE AND THERMAL DIFFUSIVITY 57
5.3 CALCULATION OF THERMAL CONDUCTIVITY 62
5.4 EFFECT OF CURE CYCLE IN THERMAL CONDUCTIVITY CALCULATION 68

6 MODELISATION AND ITS RESULTS 71

6.1 ONE DIMENSION (1D) 71
6.1.1 Influence of MVF 71
6.1.2 Influence of the thickness 74
6.2 TWO DIMENSIONS (2D) 75
6.2.1 Influence of edge effect 76
6.2.2 Influence of curvature 80
6.2.3 Influence of edge effect in curved parts 82
6.2.4 Influence of cure cycle 87
6.2.5 Influence of thermal conductivity ratio 91
6.3 TWO DIMENSIONS (2D). T-JOINT 93
6.4 THREE DIMENSIONS (3D) 95
6.4.1 Influence of edge effect 97

7 CONCLUSIONS 102

8 FUTURE WORK 104

9 APPENDIX 1. SSE AND THERMAL DIFFUSIVITY CALCULATION 105

10 APPENDIX 2. CALCULATION OF THE FITTEST THERMAL CONDUCTIVITY 119

11 REFERENCES 124

Acknowledgements

I would like to express my sincere gratitude to all those who helped me on the way to achieve my thesis.

Firstly, I want to thank Jordy M. Balvers for his work focused on my thesis, all the help he offered to me and time spent during my working period.

Also, I want to thank Irene Fernández Villegas because she gave me the great opportunity to run the thesis at the Aerospace Engineering Faculty of TUDelft.

I want to take the opportunity to thank Adriaan Beukers, Lisette Volmer and technicians from the laboratory for all their work and time.

To end this chapter, I would like to give my special thanks to my Family, everything is because of you.

1 Introduction

1.1 Background

The manufacturing of thick-walled composites has problems related to the exothermic reaction of the resin. This problem causes not only internal stress but also other structural defects. Not only this problem but many others emphasize the necessity of improving the understanding of different phenomena occurring in the manufacturing process of thick-walled structures [1].

Manufacturer's Recommended Cure Cycle (MRCC) is not going to be implement because produce peak temperatures and thermal gradients. Both affect the structural integrity of the composite and thus a different approach is needed. During the RTM process, the mould is usually heated to initiate a curing reaction, which is an exothermic resin polymerization phenomenon that cross-links the resin and results in a composite structure.

In order to improve the quality of thick composites, processing temperatures need to be controlled to minimize thermal gradients throughout the part. This means the mould temperature must be lower for thick parts than for thin ones, which is one of the goals of the optimisation. The reinforcing fibres are not really affected during the process cycle, but the polymer matrix can shrink during cross-linking, in some cases by as much as 9%.

During processing, different thermal behaviors produce residual stresses. During the cure of fibre-reinforced composites, the residual stresses generated can have considerable effects on the part quality and on its mechanical properties, phenomena like warpage or initiating matrix cracks and delamination can appear. The processing of thick composites at a lower temperature should reduce thermally induced residual stresses.

In the processing of composite materials by Resin Transfer Moulding (RTM), the three key processing parameters are curing time, temperature and pressure. Appropriate choice of these parameters will produce a material which is fully cured, well compacted and of high quality [2].

Thermosetting resins are polymerized by applying temperatures and pressures for some length of time. The reason of apply pressure during the curing period is why excess resin need to be squeezed out of the composite. Internal heat is also generated by chemical reactions.

In the literature most of the natural fibre composites studied are produced by hand lay-up or press moulding techniques. Very little research is available for industrial processes such as resin transfer moulding (RTM). The RTM process is commonly used in the aerospace and automotive industry. The process consists

of mixing resin with a hardener and injecting at low pressure the combination into a mould, which contains fibres. The resulting part is cured at room temperature or above till the end of the curing reaction. Several types of resins (epoxy, polyester, phenolic and acrylic) can be used for this process as long as their viscosity is low enough to ensure a proper wetting of the fibres [16].

A great number of studies can be found in the literature concerning the RTM process. Number of simulations of the mould filling process and cure processes are proposed, and many experimental data sets have been presented. The knowledge of all the operating steps is very important to obtain high quality parts.

1.2 Objective

The objective of this work is to obtain proper and educated values of thermal conductivity of the composite material, study which phenomena appear during the manufacturing process and which setting parameters affect to the final manufactured plate.

It is necessary to obtain proper and educated values of thermo physical parameters of the resin and the glass fiber and study phenomena during the manufacturing process. To achieve this goal, some experiments were run at the laboratory in order to generate profile temperature data along the through-thickness of the manufactured plate and volume fraction of the resin (Matrix Volume Fraction) and fibre (Fibre Volume Fraction).

The work carried out at the laboratory is going to be focused on the RTM experiment. Problems related to the manufacturing process also need to be solved, in order to achieve valid experiments and useful data.

With values obtained with the experimental work, simulations are taken over to study the behavior of the plate. Solutions given by the model of cure kinetics and experimental work need to be compared, in order to generate a value of thermal conductivity, which gives the best agreement between them. With MATLAB software the simulation of RTM curing process were run, and its verification with experiments at the laboratory.

The goal is to obtain an average value of thermal conductivity, and use it in future simulations. Also, those simulations behave as a design tool, which helps to establish the best process strategy to manufacture thick-walled composites.

The simulation tool COMSOL Multiphysics is going to be used as a tool to simulate the behavior of composite parts during the manufacturing process. The goal of this part of the work is to generate knowledge about phenomena occurring during the process, keys of the manufacture, values of peak temperature and times of the overshoots.

Models of one, two and three dimensions are going to be evaluated, and models of real life structures like T-shaped structures and curved shapes.

1.3 Scope

The second main point is a summary of the papers read before starting the work. In the literature review, some explanations about work carried out in laboratory can be read. Different models of cure simulation used in the past are also explained. Optimisation routines are developed, its objectives and the strategies followed.

On chapter three an introduction of the model used to face the simulations and the cure kinetic model used can be read.

Chapter number four gives an explanation of the work carried on the laboratory, the procedures followed to run the RTM experiment and measurements registered during the experiment.

The following chapter, number five, develops deeply the simulations run during the analysis work, acquired data at the laboratory and its explanations. (For further explanations, go to Appendix).

On the other hand, modelisation process is explained in chapter number six, results generated during this part and conclusions obtained along this study.

Final conclusions from the whole work are displayed on chapter seven and future work applications of this technique are written on chapter eight.

Last main points of the report corresponds with the appendix.

2 Literature review

In this part of the work, appear a summary of the theoretical background acquired to face the work. Specialized literature was studied in order to understand experimental work done by other research programs, to note about guidelines used by other researchers, or get knowledge about constrains in optimization routines carried out in the past. Articles from journals, proceeding and internet sites were used to introduce in the work.

Therefore, the chapter is going to be divided in three main points. Experimental work is going to be raised in the first part, as a second point simulation will be explained. To end, optimisation routines are going to be explained.

2.1 Experimental work

Different configurations have been implemented at the laboratory in other research programs. Depending on the experiment, the configuration and materials differ from the others.

For fibre reinforced polymer composites, which has a complex manufacturing process due to the two different material systems, following layout is implemented [3]:

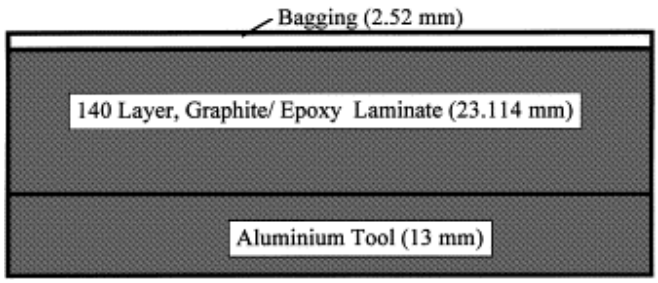

Fig. 1. Cross-section of a 140 layer, AS4/3501-6, graphite epoxy, prepreg laminate fabrication assembly.

The bagging consist on one layer of release film, two of breathers and one of nylon. The cross-section of composite is made of 140 layers of graphite epoxy.

In a work carried out to create an equation model predictive control strategy, for an autoclave composite processing, the following process technique was implemented [4].

There is a group of different processing techniques to produce thermoset composites, however, only a few are successfully. Historically, manufacturing of thick-walled composites has been assisted by autoclave molding process.

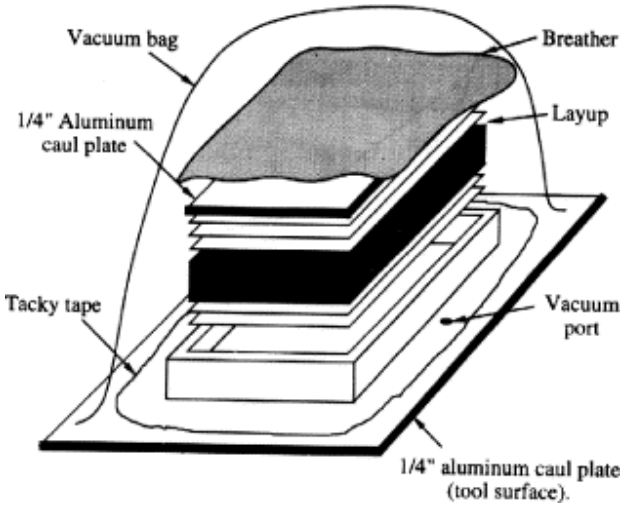

Fig. 2. Composite layup

The vacuum assisted autoclave molding presented above produce composites with the following characteristics:

- strong
- high quality
- high FVF
- low void fractions
- high capital cost requirement autoclave unit
- process time between 4 and 6 hours

The final composite shape is defined by the picture frame; layers of “prepreg” are placed in the mold and become the composite portion of the layup. They are sheets of unidirectional fibers impregnated with partially cured resin. Vacuum is achieved helped by a sealed and impermeable vacuum bag.

After vacuum achievement, temperature and pressure controls can be initiated to start the experiment. Increasing those values, it helps to reduce resin viscosity and initiate its polymerization. Also, aids the evacuation of excess resin from prepreg to consolidate the laminate.

Having a look into another experiment, the following layout was carried out at the laboratory to verify the validity of simulation. The unidirectional glass/epoxy prepreg used in this work was UGN150. Dimensions of laminate are 100 mm x 100 mm x 20mm. Its final thickness is 15 mm, and it is covered by the cault plate and dams, and all is covered by the release film. [10]

The assembly is bagged with a standard nylon bagging flim and cured in an autoclave with the conventional cure cycle:

- first stage: consolidation at 80˚C, with the rate of 4˚C/min and kept for 30 min.

- second stage: full cure at 125˚C, with the rate of 3˚C/min and kept to 120 min.

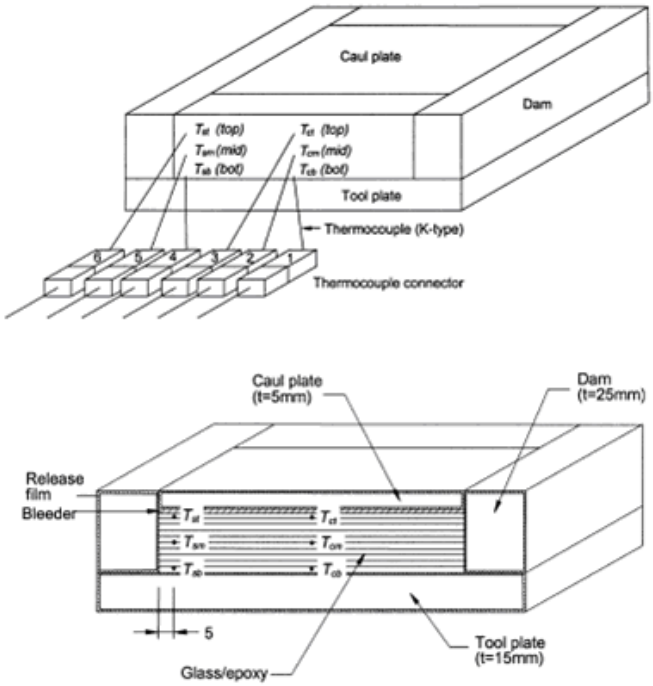

Fig. 3. Schematic diagram of experimental setup. Mold assembly

Thermocouples are installed each at the 10th ply above the bottom, at the centre of the laminate and at 10th below the top of the laminate. 6 thermocouples are installed inside the laminate. Figure 3 shows the measurement points.

For calculation of thermal dispersion term and local heat transfer coefficient between resin and fibre, experiment of non-isothermal mold filling were conducted using a non-reactive fluid called palatinol. [5]

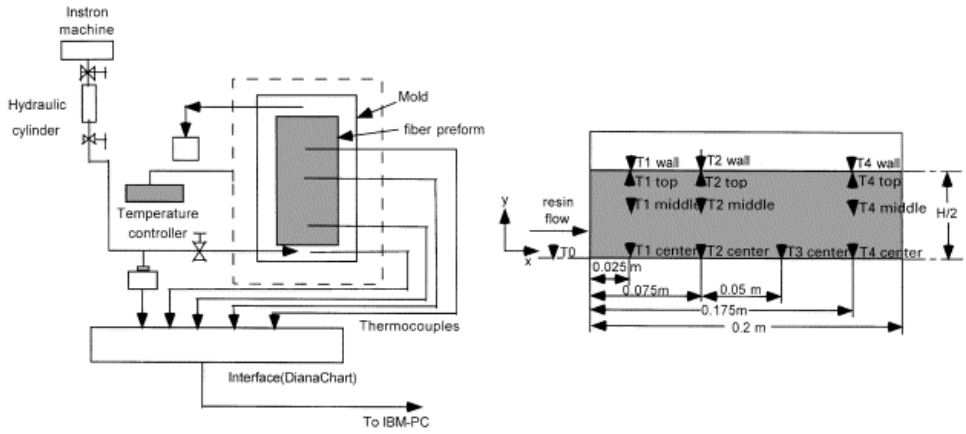

Fig. 4. Schematic of experimental setup and thermocouple distribution

There is a mould cavity of 21 cm x 7.63 cm x 0.8 cm. 14 thermocouples are placed at different locations which measure the temperature distribution in that cavity. Also, are going to measure temperatures at the mould. To prevent resin leakage, the entire assembly was clamped by a group of screws.

The mold wall temperature is achieved by a temperature controller, and heat loss problem was solved by covering with an insulating layer. A hydraulic cylinder controls the fluid injection at a constant flow rate.

Data acquisition was carried out by a group of thermocouples connected to a computer data acquisition system. Temperature data was acquired continuously until several minutes after the mold was filled.

A similar implementation has been carried out to obtain data for a finite element modeling. This time, work was done with natural fibre. There were randomly oriented and the resin solution was circulated to impregnate the fiber with the solution. A release agent was prayed over the metallic mould before applying the ten prepreg plies inside the mould.

To verify the modeling, 5 temperatures were measured through the experiment and compared with the numerical results. [6]

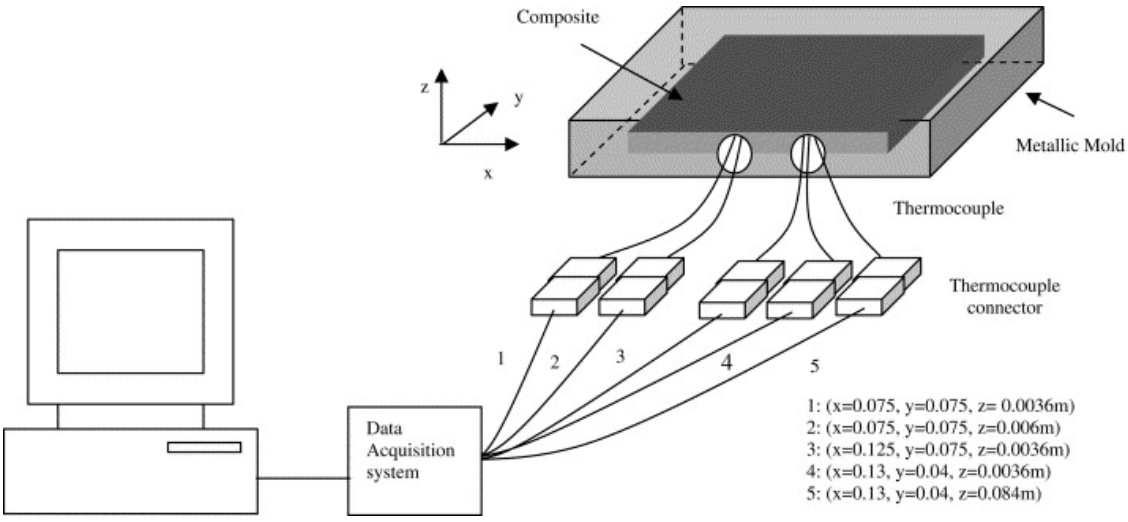

Fig. 5. Schematic diagram of the experimental set-up

Figure 5 illustrates the schematic diagram of the implemented set-up. Thermocouples are placed at different locations inside the mould. Its temperature was set to 175˚C and kept for 25 min under constant pressure.

This other experiment shows the layup implemented to carry out the experiment. Also here, prepregs need to be placed on a smooth tool surface in a predetermined fibre orientation for each layer. The bleeder is an absorbent material placed on both sides of the composite. And the Teflon porous layer is

installed in order to make easier the removal procedure. A metal lid covers the bleeder, and an air breather is placed on top of the lid. To finish the complete assembly, a plastic vacuum bag cover was used. Experience says that, for thick laminates, the understanding of the occurring consolidation and curing process is critical to guide the composite manufacturing prerequisites [7].

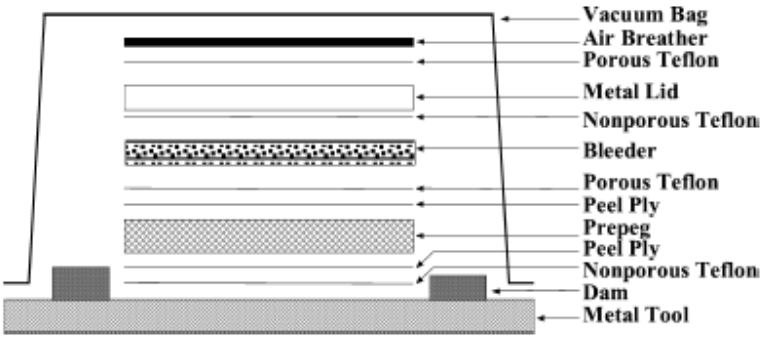

Fig. 6 Cross-section the composite lay-up

The exothermic reaction produces hot spots, which can affect to resin distribution. The control of resin flow is not that easy, because is a function of the temperature and reaction kinetics. Combination of low thermal conductivities and large thickness yields lower temperatures in the core than in regions close to the borders, it leads in a limited flow on the centre and because of the high viscosity.

In a work carried out to calculate the DOC (degree of cure), a bag-moulding process was implemented. As can be seen in the process explained above, is almost the same process. And is the most common technique used for curing composites. An advanced fiber-reinforcement composite was used on that experimental work. The prepreg is a ready-to-mould thin sheet of fibres uniformly impregnated with a partially cured polymeric matrix. This setup is similar to the one explained in figure 6.

Looking into another configuration, vacuum-assisted resin transfer moulding (VARTM) is going to be explained. It is an open-mould polymer-matrix composite manufacturing process. [8]

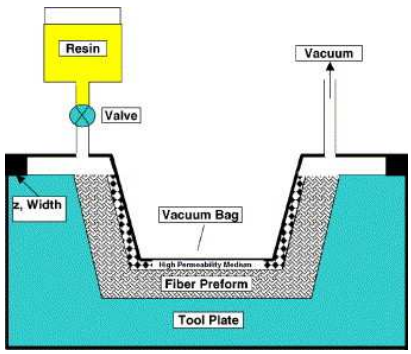

Fig. 7. Schematic of the vacuum-asisted resin transfer molding process

This procedure, widely used in industry since years ago, is based on the use of a single rigid mould with a layup of fibre-reinforcement and assembled with a vacuum bag.

Procedure starts when the preform is infiltrated with resin using vacuum pressure, then the mould is heated in order to obtain the curing of the resin. Advantages of this procedure are the following:

- low tooling cost
- low emission of volatile organic chemicals
- processing flexibility
- low void-content in parts
- potential for fabrication large parts

In summary, there are two types of VARTM depending on the type of resin distribution system used.

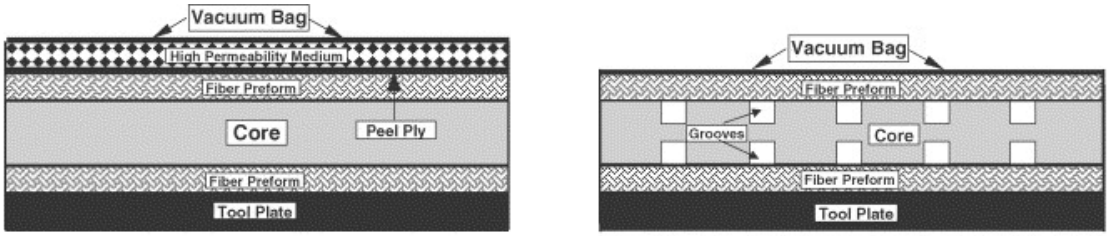

Fig. 8. High-permeability medium based system, grooves based system

Most critical stage of this procedure is the resin infiltration step. Ideal case should have a complete resin infiltration in a short period.

For the simulation of the curing process in a RTM of natural fibre reinforced composites, a system was implemented to work in the data acquisition of a RTM process. [9]

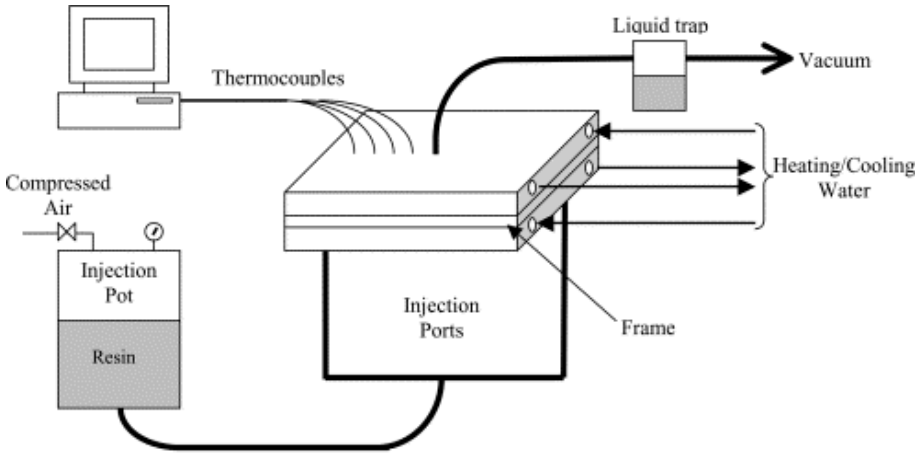

Fig. 9. Diagram of RTM equipment

The mould, was done in aluminum, and has two inlet connections in the low part. There is a vent or outlet connection placed in the upper part. The mould is kept at constant pressure by water flowing inside its upper and lower section. Temperature is controlled by a temperature controller connected to a thermocouple and an immersion heater. The thickness of the plate is defined by a frame placed between the upper and lower mould sections, and can be modified in further experiments.

Getting in touch with another experimental work, a smart autoclave processing was implemented to find a curing process optimization technique to minimize local temperature increase and residual stress. For this experiment, the carbon fibre/epoxy resin prepreg called MR50K/#982. [11]

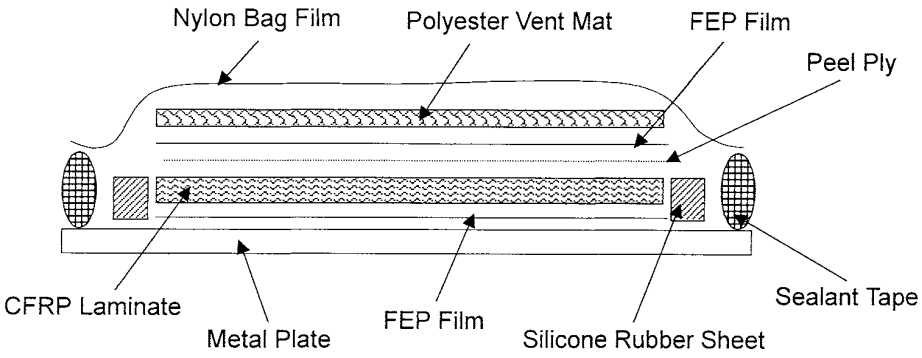

Fig. 10. Layup of implemented assembly

The control of the composite parts temperature is made by the thermocouples fixed to the plies and with the insulation of the bag film. Peak temperature can be lowered by decreasing the temperature ramp rate, but introduces an extra time during curing which makes the experiment longer.

The next experiment was run to verify the validation of simulation of the cure process. The carbon/epoxy prepreg used in this work was T300/HD03. The prepreg plies were stacked to the tool plate, then is covered by the release film. A standard nylon bagging film covers the entirely assembly, and has the following appearance. [12]

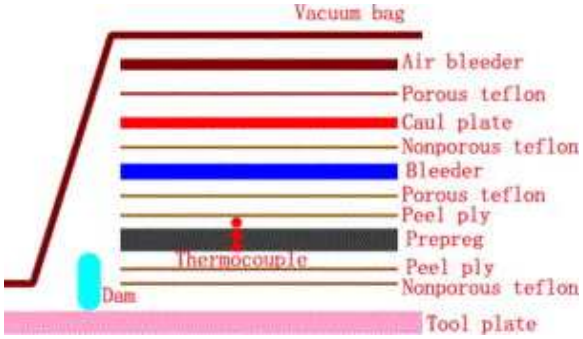

Fig. 11. Typical layup of an autoclave composite implementation

2.2 Cure simulation

Resin Transfer Moulding is an efficient process for high performance composite material with low cost manufacturing. The composite cure stage in the process is characterized by the process of the exothermal cure reaction activated by the conductive heat transport from the heated mold walls. During this process, the liquid resin releases the heat. The degree of cross-linking is referred to as a degree of cure.

There have been many studies on the curing of thick thermoset matrix composites. Bogetti and Gillespie developed a two dimensional cure simulation analysis of thick thermoset composites and predicted the temperature and degree of cure distributions.

In most of previous studies, temperature and degree of conversion were predicted correctly helped by one-dimensional finite different analysis or two dimensional finite element analyses.

A modeling of the curing process for thermosetting composites was first presented by Loos and Springer (1983), and also basing in physical laws, they presented a model developed by a thermochemical flow model. Lindt presented a consolidation model based on lubrication theory, Gutowski and Dave presented a squeezed-sponge three dimensional flow model with coupled vertical and horizontal directions and one dimensional consolidation of the composite.

The models which are going to be used in the future should be capable of providing information on temperature, pressure, degree of cure of the resin, and resin viscosity, in terms of spatial distribution within the composite and time development.

This chapter explains in detail models used in other research programs.

2.2.1 Available models

A modeling of the curing process for thermosetting composites was first presented by Loos and Springer (1983). Other authors have been investigating different aspects of the modeling.

There is a model that combines two equations. First one describes the energy balance, which includes both the conductive term and cure reaction contribution:

$$\rho_c C_{pc} \frac{\partial Tc}{\partial t} = k_{zc} \frac{\partial^2 Tc}{\partial z^2} + \rho_r H_r (1 - V_f) \dot{\alpha}$$

Equation. 1

Where suffices r, f and c refers to the properties of the resin, the fibres and the composite respectively. Other parameters are explained below:

$H_r =$ Heat generated by the curing reaction
$\dot{\alpha} =$ Rate of reaction
$V_f =$ Fibre Volume Fraction (FVF)
$\rho =$ Density
$Cp =$ Specific Heat Capacity
$k =$ Thermal conductivity

Thermal conductivity values are important because they manage the relation and heat transfer behaves between mould and resin.

Second equation couples with the first one. It is related to the resin kinetic model that describes the rate at which the cures. At the same time, is a function of the degree of cure, time and temperature:

$$\frac{\partial T_c}{\partial t} = \frac{k_{zc}}{\rho_c C_{pc}} \frac{\partial^2 T_c}{\partial z^2} + \frac{\rho_r H_r (1 - V_f)}{\rho_c C_{pc}} \dot{\alpha}$$

Equation. 2

$$\frac{d\alpha}{dt} = \dot{\alpha} = f(\alpha, t, T)$$

Equation. 3

As can be seen, the equation number 2 is characterized by three different terms, the change in internal energy of the composite is in the left side, the conduction of heat through the composite and the generations of heat within the composite due to the exothermic reaction are in the right side.

For the model of one equation, and with the assumption that the thermo-physical properties of the resin and composite are considered to be independent of the degree of cure, the transient non-isothermal heat transfer is governed by the following equation:

$$\rho_c Cp_c = \frac{\partial}{\partial_{xx}} (K_{xx} \frac{\partial T}{\partial_{xx}}) - \rho_r V_r H_R \frac{\partial \alpha}{\partial t}$$

Equation. 4

Where ρ_c , Cp_c and K_{ii} are density, specific heat capacity and thermal conductivity of the material in three orthogonal directions, respectively. The right side of the equation corresponds to the internal heat consumption sink term, and it can be directly related to the rate of cure, ignoring the effect of resin flow in the material.

Here, ρ_r is the density of the resin, V_r is the resin volume fraction of the composite, and H_R is the total heat of reaction, and α is the degree of cure.

2.2.2 Submodels: Material parameters

For the study of the resin cure, a heat conduction equation is used. But, some submodels are necessary to obtain values of thermo-physical parameters from resin and fibre. Depending on the case of study, some submodels are implemented.

Values of density and specific heat capacity can be obtained by calculations given by the product provider, but those parameters are related to the temperature, that means to the state of the resin. It is necessary to introduce fixed values in the calculation to start the work and find an educated value for each one.

The rule of mixture was used in some research programs to obtain the effective properties of the composite. Values of density and specific heat capacity were calculated using this equation:

$$\tilde{C}p = Cp_r w_r + Cp_f w_f$$

Equation. 5

$$\tilde{\rho} = \frac{\rho_r \rho_f}{\rho_r w_r + \rho_f w_f}$$

Equation. 6

Also, thermal conductivity of the resin can be calculated by this rule, and is related to the weight volume fraction. The relation is given by these two equations:

$$\tilde{k} = \frac{k_r k_f}{k_r w_r + k_r w_r}$$

Equation. 7

$$w_r = \frac{\phi / \rho_f}{(\phi / \rho_f) + (1 - \phi / \rho_r)} \qquad w_f = (1 - w_r)$$

Equation. 8

Where ϕ is the porosity and w_r , w_f denote the weight fractions of resin and fibres, respectively.

This way of calculation can be assumed to be valid for the physical and thermal properties of the composite. But, for the transverse conductivity, the Tsai-Halpin model was used: [13]

$$\frac{k}{k_m} = \frac{k_f + k_m + (k_f + k_m)V_f}{k_f + k_m - (k_f - k_m)V_f}$$

Equation. 9

For a finite element nodal control volume, the change in material properties as thermal conductivity can be calculated using the following equation:[14]

$$\frac{1}{k_c} = \frac{m_f}{k_f} + \frac{m_r}{[(1-\alpha_T)k_r^u + \alpha_T k_r^s]}$$

Equation. 10

Where $m_f = v_f(\frac{\rho_f}{\rho_c})$, $m_r = 1 - m_f$, and superscripts u and s represent uncured and fully cured resin respectively.

The Springer-Tsai model can also be used to calculate the ratio that relates the transverse and longitudinal thermal conductivity coefficient:

$$\frac{\lambda_T}{\lambda_L} = \left(1 - 2\sqrt{\frac{V_f}{\pi}}\right) + \frac{1}{B}\left[\pi - \frac{4}{\sqrt{1-\left(B^2 V_f/\pi\right)}} \tan^{-1} \frac{\sqrt{1-\left(B^2 V_f/\pi\right)}}{1 + B\sqrt{V_f/\pi}}\right]$$

Equation. 11

Where $B = 2\left(\lambda_r / \left(\lambda_f - 1\right)\right)$, V_f is the fibre volume fraction, λ_r is the conductivity of resin and λ_f is the conductivity of the fibre.

On the other hand, to obtain the thermo-physical properties of the composite in a work of finite element modeling of polymer curing in composites, the following equation were used. Densities of cured and non-cured resin were measured; density of composite can be calculated by the rule of mixture. The variation of the fibre's heat capacity can be fitted quite well by a polynomial of the second order: [15]

$$C_{pf} = C_1 T^2 - C_2 T + C_3$$

Equation. 12

Where T is the absolute temperature. For the resin heat capacity, the following equation was used:

$$C_{pr} = 0.0149T + 0.459$$

Equation. 13

Also, the heat capacity of the composite should be calculated to predict the temperature variations in the composite. The heat capacity is required, rule of mixture as follows was used:

$$C_{pc}(T) = C_{pf}(T) * v_f + C_{pr}(T) * (1 - v_f)$$

Equation. 14

Where v_f is the volume fraction of the fibre.

For thermal conductivities calculation, the transverse value for the composite, K_t, was applied the thermal-electrical analogy technique for elliptical filaments and square packing array unit cell model, which can be expressed as follows:

$$\frac{K_t}{K_m} = 1 - 1/c + \pi/2d - c/d\sqrt{d^2 - c^2} \ln\left|\frac{d + \sqrt{d^2 - c^2}}{c}\right|$$

Equation. 15

Where K_m is the thermal conductivity of the matrix. $c = \sqrt{\pi\mu / v_f}/2$, $d = \mu(1/\beta - 1)$, and $\beta = K_f / K_m$. Where μ is the geometry ratio of the filler $(\mu = a/b)$, where a and b are the axial lengths of the ellipse along the x-axis and y-axis, respectively, v_f is the fibre volume fraction of the composite and K_f is the conductivity of fibre.

In another research work where an experimental approach of the heat transfer of fibre in RTM, the heat transfer coefficient k may be dependent on: [17]

- type of the fibre
- type of the resin
- degree of filling g
- thickness of the cavity d
- fibre volume fraction c_F
- flow velocity w of the resin

$$k = f(materials, g, d, v_f, w)$$

Equation. 16

The heat between two points at different temperature can be transported by conduction, convection and radiation. For typical temperatures as applied in liquid composite moulding radiation is not relevant. Therefore, the effective thermal conductivity can be expressed as follows:

$$k = k_c + k_d = k_c * (1 + x)$$

Equation. 17

Where k_d is the thermal dispersion parameter and x expresses the influence of dispersion on thermal conductivity.

For another study of numerical modeling of mold filling and curing, the Chang's model was used to calculate the composite thermal conductivity:

$$\frac{k_e}{k_f} = \frac{(2-\varepsilon_f)k_s / k_f + 1}{2 - \varepsilon_f + k_s / k_f}$$

Equation. 18

But, can also be find the simplest alternative for a two-component composite. If we assume that materials are arranged in either parallel or series with respect to heat flow, the upper or lower bounds of effective thermal conductivity can be calculated. For the parallel conduction model: [18]

$$k_c = (1-\phi) * k_m + \phi * k_f$$

Equation. 19

Where c is related to composite, m to matrix, f to filler and ϕ to volume fraction of the filler.

For a series conduction model:

$$\frac{1}{k_c} = \frac{1-\phi}{k_m} + \frac{\phi}{k_f}$$

Equation. 20

Those equations can be applied for different distributions, e.g., for a parabolic distribution the following modifications were done to apply the model above:

$$\frac{1}{k_c} = \frac{1}{\sqrt{C(k_f - k_m)[k_m + B(k_f - k_m)]}} \times \ln \frac{\sqrt{k_m + B(k_f - k_m)} + \frac{B}{2}\sqrt{C(k_f - k_m)}}{\sqrt{k_m + B(k_f - k_m)} - \frac{B}{2}\sqrt{C(k_f - k_m)}} + \frac{1-B}{k_m}$$

Equation. 21

Where for both equation:

$$B = \sqrt{3\phi / 2} \qquad C = -4\sqrt{2/(3\phi)}$$

Equation. 22

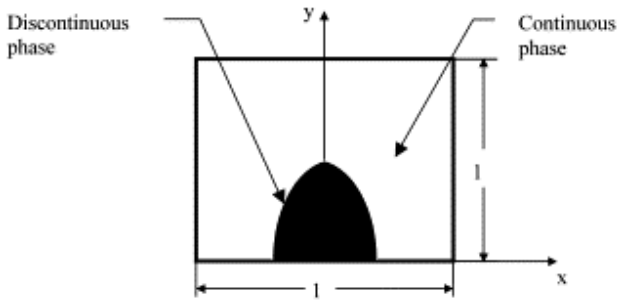

Fig. 12. Parabolic distribution of the discontinuous phase

Other researchers, Lewis and Nielsen modified the Tsai-Halpin model in order to introduce the shape of the particles and the orientation or type of packing: [19]

$$k_c = k_m \left[\frac{1 + AB\phi}{1 - B\phi\psi} \right]$$

Equation. 23

Where:

$$B = \frac{\frac{k_f}{k_m} - 1}{\frac{k_f}{k_m} + A}$$

Equation. 23

$$\psi = 1 + \left(\frac{1 - \phi_m}{\phi_m^2} \right) \phi$$

Equation. 24

2.3 Optimisation routines

The optimisation routines of the composite cure process consist on fitting the characteristics to obtain the best manufacturing process on thick composites. Parameters like thermal gradients, final degree of conversion (DOC) or the length of the whole process need to be the fittest if a good optimisation wants to be achieved.

Some methodology was followed in the past by other research programs in order to minimize thermal gradients, make the experiment shorter or increase the final quality of the plate. Some of them are going to be explained on this chapter.

2.3.1 Minimization of temperature gradients

One of the goals of an optimisation is to predict and control thermal gradients during the RTM experiment, especially at the instant the resin gels and solidifies. When the plate is covered by the mould, the variables that can control to drive the process towards a controlled scenario are the cure chemistry or the adjustment of the mould wall temperature boundary conditions. A prediction of the mould wall temperature history gives the opportunity an uniform activation of the cure reaction along the plate. If the mould is filled under uniform pressure, it simplifies the analysis because the temperature filling history does not affect the temperatures profiles during composite consolidation; therefore, the temperature only varies along the thickness direction.

The following figure explains the procedure applied in one case of study: [20]

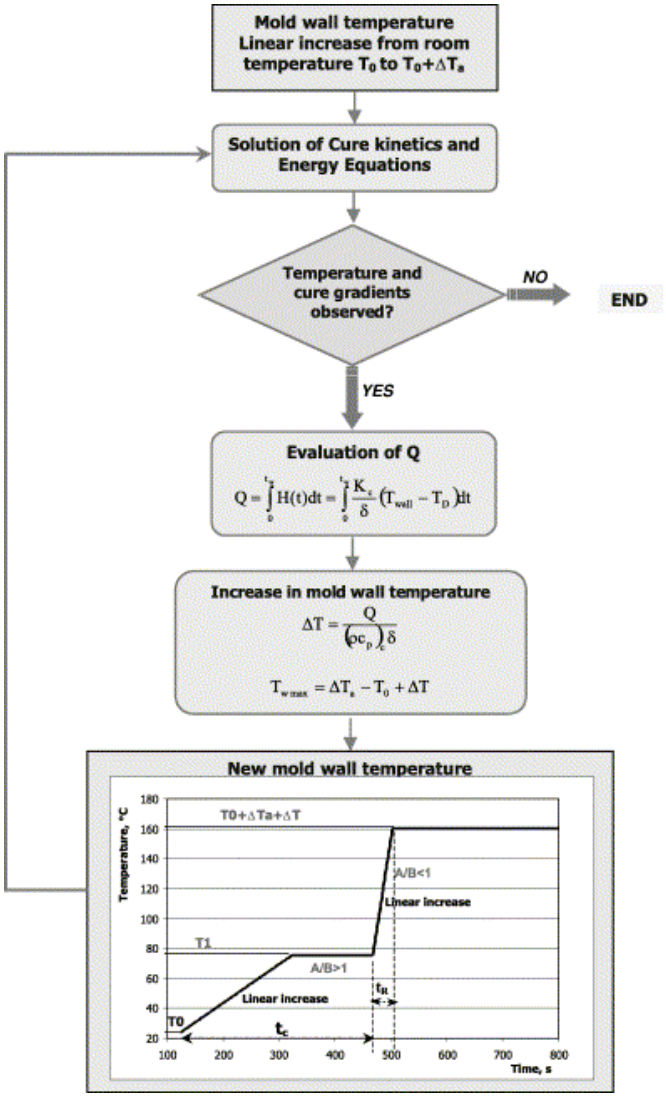

Fig. 13. Flow chart of the optimisation

After increasing the mould temperature, possible thermal gradients across the thickness of the plate need to be observed. In case of they appear, it is mandatory to impose a new mould wall temperature profile and the introduction of a flat plateau. Values of maximum wall temperature and time of the plateau can be set by employing a methodology based on the rate of energy balance principle.

$$Q = \int_0^{t_w} H(t)dt$$

Equation. 25

in which

$$H(t) = \frac{k_{zc}}{\delta/4}(T_{wall} - T_D)$$

Equation. 26

Where t_w is the duration of the conductive heat flow applied to the mould. And T_D is the temperature of the location at 25% of half of the thickness from the wall. Once Q is defined, the maximum temperature increase needs to be obtained as follows:

$$\Delta T = \frac{Q}{(\rho c_p)_c \delta}$$

Equation. 27

Finally, maximum temperature in the mould walls comes from the expression $\Delta T + (T_0 + \Delta T_a)$. The plateau is introduced at T_1, when the contribution of the heat from the reaction is insignificant. The duration is set to amount of time that allows the composite to achieve temperature values across the thickness that is close to each other.

The last figure shows two ramps along the profile temperature. During the first one, the reaction rate is small, t_R is high and $A/B > 1$. In the second region, t_R is small due to the high reaction rate hence A/B is small. Therefore, in the first region the conductive heat transport is quite big compared to the polymerisation reaction. On the other hand, in the second ramp, the reaction contribution becomes more significant.

Reading back, for a given temperature firstly, $(T_0 + \Delta T_a + \Delta T) - T_1$, the slope of the ramp which needs to be applied is defined by the time the reaction takes to reach the peak at its centre, related to a high rate of curing. In this way, lower thermal gradients are expected.

2.3.2 Prediction of temperature overshoots

It is interesting to add in a conventional cure cycle the possibility of prevention in case of being a temperature overshoot. Those phenomena yield quality degradation and increases the process time if the want to be solved.

One of the most important goals of the optimisation is to obtain a high quality product characterized by a full consolidation. To achieve this target, the required time for full consolidation needs to be calculated. By an analysis carried out in the research work this time can be obtained. [10]

In order to prevent temperature overshoots, steps of cooling and reheating were introduced into the profile temperature of the cure cycle. Need to taken into

account, that temperatures at bottom and top of the plate suffer less overshoot compared with the middle part, but for a proper optimisation, it should be conducted considering all the inside temperatures of the laminate.

Following variables are necessary for the design:

$$X = (T_{cs}, T_{ce}, T_{he}, t_{cs}, t_{ce}, t_{he})$$

Equation. 28

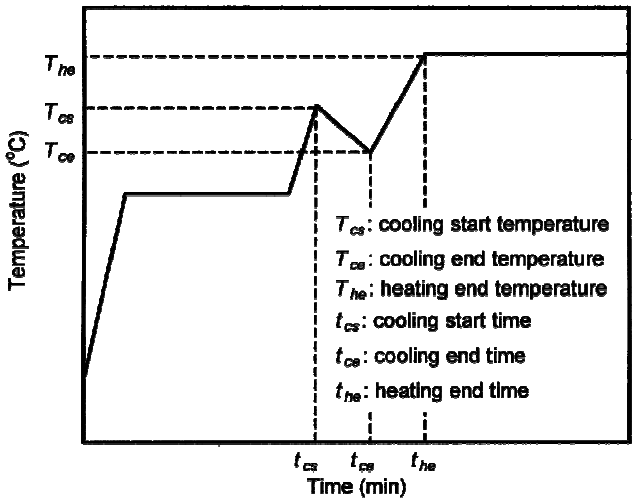

Fig. 14

In order to obtain the optimum value for the figure above, the target temperature was chosen as the temperature in the laminate calculated without exothermic reaction, and the objective function is defined by the following equation:

$$Objective\ function = \sum_{i=1}^{n} \sum_{t=0}^{t=t_{end}} (T_i^t - T_{iref}^t)^2$$

Equation. 29

Where the X vector, which minimizes the objective function, is the objective. The equation above is subjected to $X_{\min} \le X \le X_{\max}$ and $T_i^t \le T_{g\infty}$ and where i, n and t are the node number of the laminate, total node number and elapsed time respectively. Finally, T_{ref} and $T_{g\infty}$ are the target temperature and glass transition temperature for fully cured resin, respectively.

For this work, an optimisation technique provided by ANSYS was used to solve the problem. The following figure compares results obtained after its optimisation:

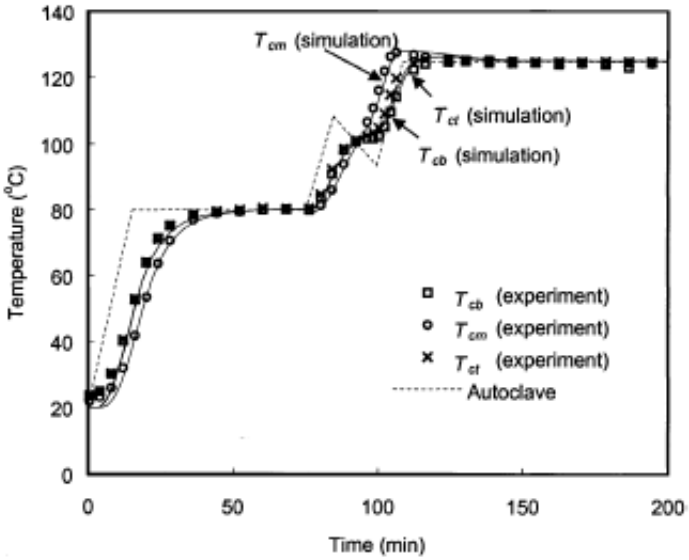

Fig. 15. Temperature profile at the centre section

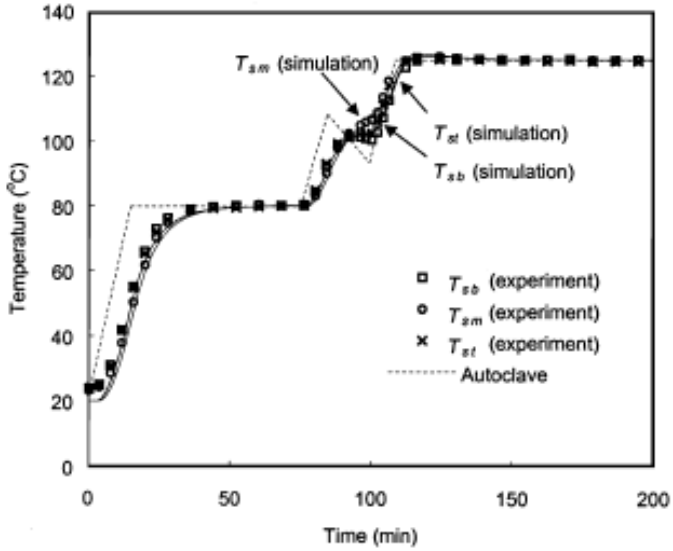

Fig. 16. Temperature profile at the side section

Six points were obtained during the simulation, and the comparison is done between those values and the experimental ones. The temperature overshoots at the midpoint as well as the top and the bottom are negligible, and profile temperatures have a well agreement with the experimentally obtained.

2.3.3 Isothermal step in the thermal profile optimisation

Usually, a thermal profile involves a heating up step followed by a plateau isothermal segment, and can be characterised by two parameters:

- the ramp up rate
- the isothermal temperature, subject of the optimisation

In a research work of inverse heat transfer, this goal was studied to achieve the optimisation.[21] The fitness function gives the parameter values, which reduce the duration of the curing stage (isothermal temperature step), but at the same time increases the time to reach a conversion of 0.84. The implemented function is the following:

$$Fitness = \frac{1}{t_c}$$

Equation. 30

which is subject to the constraint:

$$\left|\frac{dT}{dz}\right|_{\max} < 2.5^{o}C/mm$$

Equation. 31

for $\alpha > 0.6$

Constrain is related to the fractional conversion when the material has reached the rubbery state and the residual stress can build up. Also, maximum thermal gradients need to be kept lower than in other experiments.

This algorithm is considered to have converged when the individuals of a generation have very small variation, i.e. the average percentage difference between the members of the population and the average is lower than 0.5%. The following figure compares results obtained in conventional profiles and optimised.

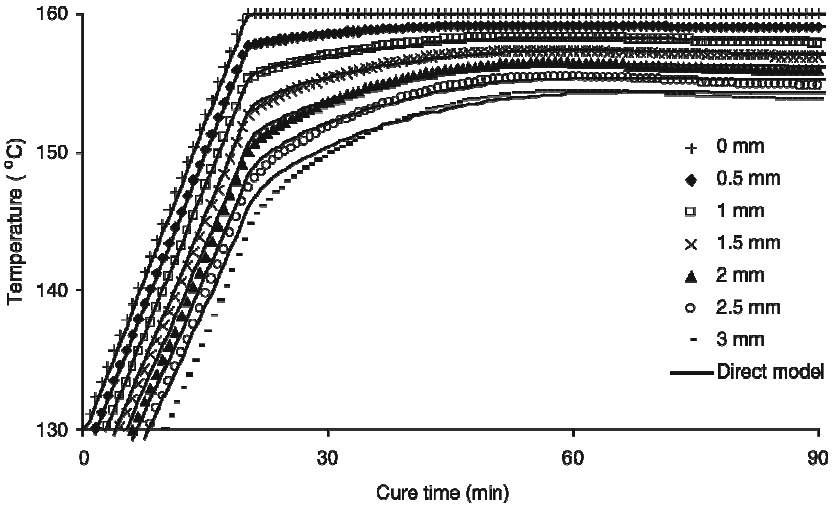

Fig. 17

2.3.4 Reduction of stresses and cycle time

The minimization of the mould filling and the curing time reduce the consumption of energy during the process. Of course, the election of the fittest parameters leads in the following characteristics:

- minimum number of defects in the final plate
- less delamination
- less warpage

Those characteristics are shared in all the optimisation goals explained before, but one is added to the list, reduction of cooling stresses.

An optimisation routine should be based in an algorithm based as well on the physics of the curing process in order to provide educated results. Then, a objective function is the target of the optimisation routine to reduce internal stresses. This function is constructed from physical information on the cure and temperature gradients, cure and cooling stresses, cycle time and maximum allowed exothermic temperature [22]. To achieve the minimization of the function, a strategy based on a Genetic Algorithm (GA), were used.

The following figure is the flow chart of the work process:

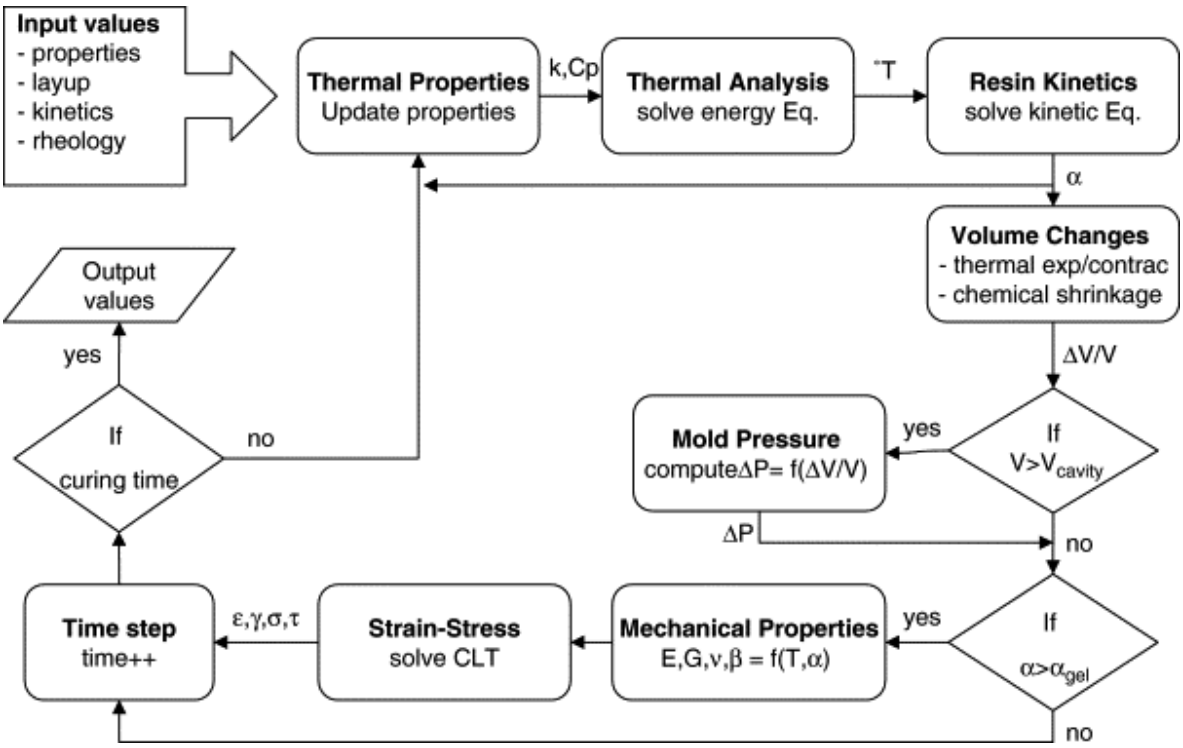

Fig. 18. Flow chart of the optimisation

Seven functions are used as partial objectives before the minimization of the final fittest function. Those function are listed below:

(1) Maximum final extent of cure
(2) Minimum processing time
(3) Minimum exothermic peak temperature
(4) Minimum curing internal stresses
(5) Minimum cooling stresses
(6) Constant through-thickness degree of cure at After Gel Point (AGP) level
(7) Minimum through-thickness curing gradients after AGP level

The optimisation was carried out with procedures from Evolutionary Algorithms (EA), which are characterized by:

- low convergences rates
- possible huge amount of evaluations required

Gauss-Sigmoid fitness function was used in order to increase the learning speed of EA. Also, sub-objective functions were written varying from 0 to 1 to increase the convergence rate.

Also, an important goal always in mind is the maximisation of the degree of polymerization to obtain good mechanical properties. Hence, a minimum value of

degree of cure $\alpha_{\min}$ needs to be reached before cooling stage. A value of $\alpha_{\min}$ is required to be set before the start of the optimisation.

1. Maximum final extent of cure

The objective function of the final resin cure is written below:

$$J_{fc} = \frac{A_{fc}}{B_{fc} + e^{-g_{fc}}} \quad \text{with} \quad g_{fc} = \frac{C_{fc}}{(\alpha_{ult} - \alpha_{\min})}$$

Equation. 32

where α_{ult} is the final degree of conversion (i.e. $\alpha_{ult} = 0.95$). Parameters A_{fc}, B_{fc} and C_{fc} are coefficients of sigmoid function.

α_{last} is the final degree of conversion, which value goes from 0 to $\alpha_{\min}$. The following figure shows how the sigmoid function permits to increase the learning speed of the algorithm used.

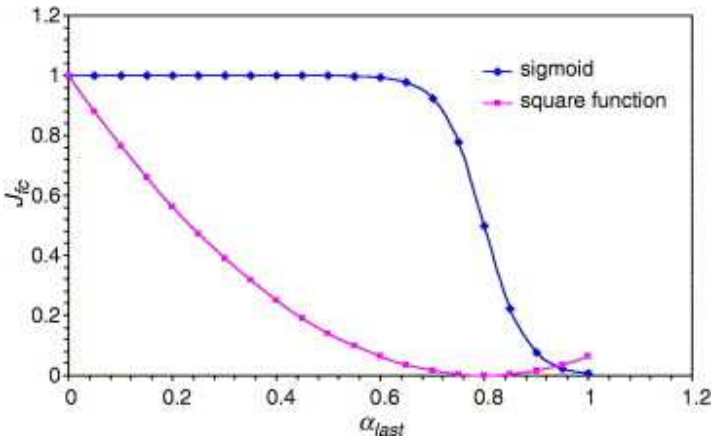

Fig. 19

At the end of the sigmoid line, can be seen that the value of $J_{fc} = 1$, because a final degree of cure below $\alpha_{\min}$ is not appropriate.

The objective function decreases with values of $\alpha_{last} = \alpha_{\min}$ to $\alpha_{last} = 1$ in a Gaussian form. On this algorithms, sigmoid function returns low survival probability of the variables used for the design if $\alpha_{last} \leq 0.6$, thus increasing the convergence for $\alpha_{last} > \alpha_{\min}$.

2. Maximum exothermic peak temperature

This part of the optimisation assures the obtaining of the high enough exothermic peak temperature to degradate the resin. This following function tries to control the cancelation of polymer degradation:

$$J_{T\max} = \frac{A_{T_{\max}}}{B_{T_{\max}} + e^{-g_{T_{\max}}}} \quad \text{with} \quad g_{T_{\max}} = \frac{(T_{exot} - T_{exot}^{\min})}{(T_{exot}^{\max} - T_{exot}^{\min})} C_{T\max}$$

Equation. 33

where T_{exot} is the exothermic peak temperature, $T_{exot}^{\max}$ is maximum value allowed and $T_{exot}^{\min}$ is the minimum value desired (i.e. $T_{exot}^{\min} = 120^{o}C$).

3. Cross-over at after gel point objective. Minimization of cure cycle time

It is experimentally demonstrated that mechanical properties begin to develop after the resin has reached an important degree of polymerization. The time before the resin starts its polymerization induces an increment in the cure cycle time. The minimization of this time results in a cure cycle time minimization. At the same time, degree of cure should be closed to the AGP level to reduce curing stresses.

$$J_{AGP} = \frac{A_{AGP}}{B_{AGP} + e^{-g_{AGP}}} + D_{AGP} \qquad g_{AGP} = C_{AGP}\left[\frac{\alpha_{surface}^{AGPcore} - \alpha_{AGP}}{\alpha_{AGP}}\right]^2$$

Equation. 34

where α_{AGP} is the degree of cure at the AGP, and $\alpha_{surface}^{AGPcore}$ is the degree of cure at the part surface when the core reaches the AGP level.

4. Reduce curing stresses.

The variations of chemical shrinkage through the thickness of the part are proportional to changes in the resin degree of cure along the through thickness direction. Hence, the chemical shrinkage and the mechanical properties of the resin should increase uniformly through the thickness, if a curing stress reduction wants to be obtained. For a desired degree of cure in the centre, the cure difference between the surface and the centre can be computed as follows:

$$J_{cure} = \frac{A_c}{B_c + e^{-j_{cure}}} \qquad j_{cure} = \frac{\sum_{i=1}^{Np} g_c^i}{Np}$$

Equation. 35

$$g_c^i = \frac{A_c}{B_c + e^{-C_c \tau_c}} + D_c \qquad \varepsilon_c^i = \left|\frac{\alpha_{surface}^i - \alpha_{core}^i}{\alpha_{AGP}}\right|^{1/2}$$

Equation. 36

where α_{core}^{i} is the desired degree of cure in the core, $\alpha_{surface}^{i}$ is at the surface at time i and Np is the number of points in the α_{core}^{i} discretization.

5. Curing and cooling down stress reduction

Curing stresses can be considered as the maximum internal stresses. If the process is not thermally balanced through the thickness, differential material contractions will create internal stresses. Under these two assumptions, cooling stresses can be minimized:

- low curing temperature
- small cooling ramp

The objective function is written below:

$$J_{stress} = \frac{A_{stress}}{B_{stress} + e^{C_{cooling} S_{TW}^{L}}} \qquad J_{cooling} = \frac{A_{cooling}}{B_{cooling} + e^{C_{cooling} S_{TW}^{L}}}$$

Equation. 37

where S_{TW}^{L} is the minimum Tsaï-Wu safety factor at layer L (the Tsaï-Wu safety factor theory for composites is implemented).

6. Processing time objective

The goal knowledge is considered to identify a target cycle-time for a given part. The following cuadratic form is:

$$J_{time} = \left[\frac{T_{cycle}}{t_{cycle}^{\exp}} \right]^2$$

Equation. 38

where $t_{cycle}^{\exp}$ is the expert desired cycle time and t_{cycle} is the calculated cycle time for a given set of design variables.

7. Final function

The objective group of functions need to be evaluated all together. The degree of success of a set of design parameters can be quantified by a weighted function of these objectives. The cure cycle optimisation is presented below:

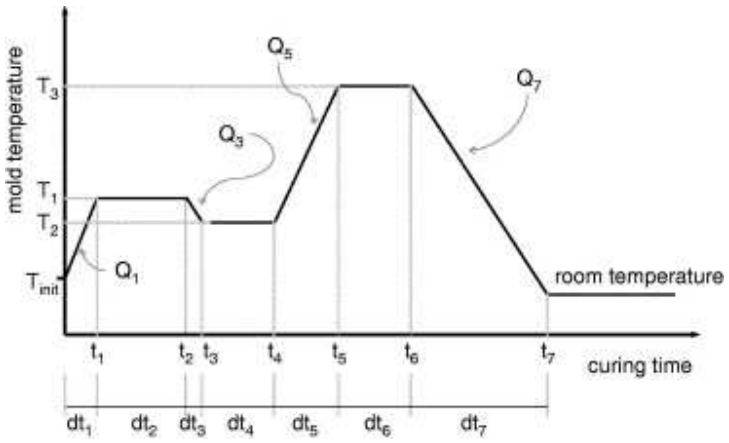

Fig. 20

The sigmoid function to minimize is:

$$F_f(Vd) = \frac{A_f}{B_f + e^{-F_\omega C_f}} + D_f$$

Equation. 39

$$F_\omega = \omega_{fc} J_{fc} + \omega_{T_{\max}} J_{T_{\max}} + \omega_{AGP} J_{AGP} + \omega_{cure} J_{cure} + \omega_{stress} J_{stress} + \omega_{cooling} J_{cooling} + \omega_{time} J_{time}$$

Equation. 40

subject to $Vd \in Cs$

where $F_f(Vd)$ is the fitness function to be optimized, parameters Cs represents constrains of the design vector, ω are the weighting coefficients for each sub-objective function implemented.

Finally, to minimize the fitness function $F_f(Vd)$, an optimisation algorithm called Logical Evolutionary Curing Optimization and Quenching (LeCoq) was developed. Following figure shows the flow of LeCoq code:

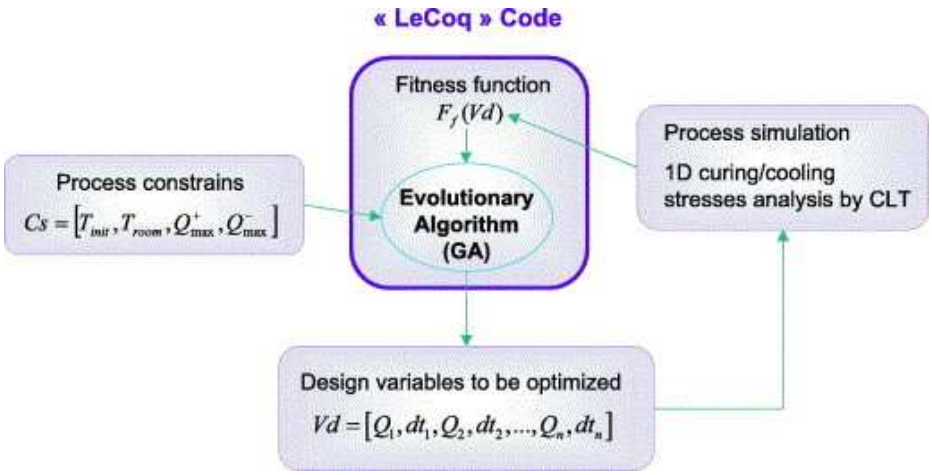

Fig. 21. Flow chart of LeCoq

2.3.5 Cure cycle optimisation with genetic algorithm

In another research work, the internal stresses generated during the resin cure, were tried to minimize. Hence, the degree of polymerization through the thickness should remain constant at each instant. Also, some parameters were considered to decrease curing stresses:

- minimization of chemical induced strain gradients
- minimization of through-thickness thermal gradients

Working on the manufacturing of a plate of 15 mm thickness, these are results obtained during the simulation:

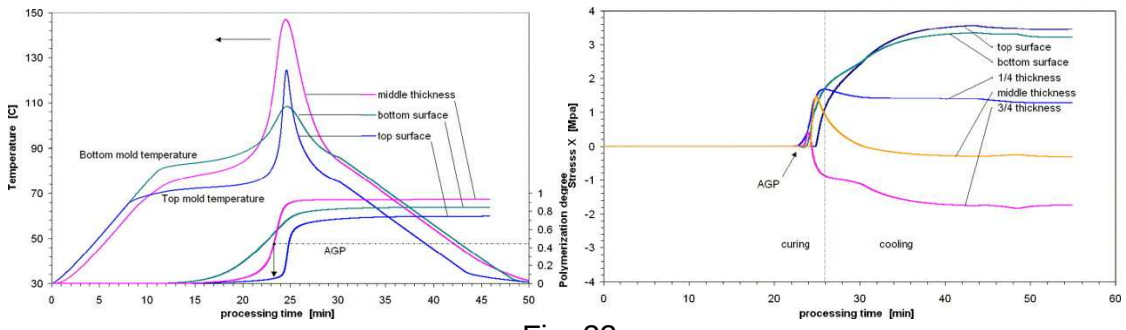

Fig. 22

Having a look into the temperature profiles can be seen that curing temperature can be higher without really increasing the exothermic peak, which can deny in a reduction of time (goal of the optimisation). The internal stresses are showed on the right figure. Around minute 24, the internal stresses grow up especially in regions closed to the boundaries (top, bottom and ¼ thickness) during the polymerization of the resin. Focuses of internal stresses are placed.

Next figures show the calculation and results obtained by the application of an optimisation methodology based on the genetic algorithm. [4] Focusing on the

optimisation of the mould temperatures. First one shows the numerical results obtained in a 15 mm thickness of internal temperature and degree of conversion. The second one illustrates how curing and cooling stresses are reduced by the approach. Those profile temperatures belong to the evolution of the curing in the plate from inside to outside cure scenario.

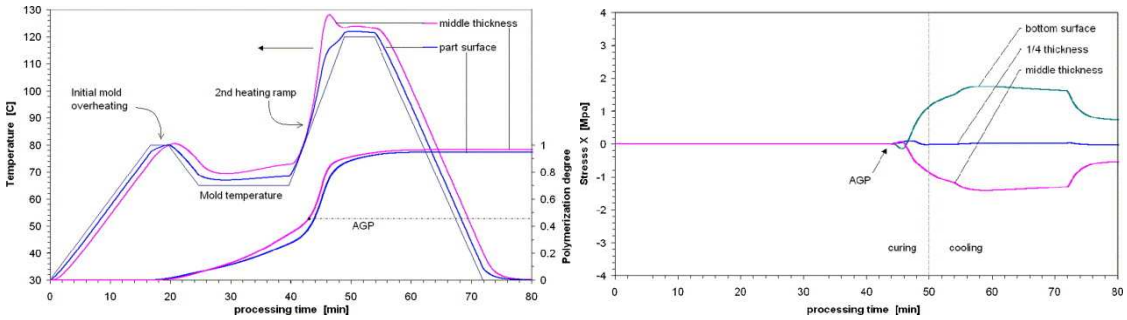

Fig. 23

In the profile temperature figure, the initial overheating at the end of the first ramp helps to decrease the processing time and minimize the through-thickness thermal and curing gradients. To obtain the objective degree of conversion, the second ramp to reheat up the mould is necessary, and avoids high exothermic temperature peaks. Those peaks appear during the second ramp and before its end (in surface and middle thickness). The figure in the right shows the internal stresses measured. Making a comparison with the stresses obtained in the previous simulation, cooling and curing stresses are significantly reduced by the numerical optimisation of the thermal boundary conditions.

3 Cure kinetics model

3.1 Cure kinetics

The models are used to make a comparison between experimental and simulation. Data collected from the experiments carried out at the laboratory are faced to the solution given by the model and a comparison can be made. These experiments have been performed for cure kinetics, specific heat capacity and density of the resin.

Four different cure kinetics models are available to compare results. Results obtained at the laboratory were run on simulations with all cure kinetics of bicomponents RTM6 system. These tests were conducted at two different laboratories, National Research Council Canada (NRC) and Delft University of Technology (TUD) [23].

At NRC some experiments were performed to calculate the total heat for different heating rates, to determine the residual heat and the fractional conversion and to determine the instantaneous glass transition temperature.

Besides, at TUD experiments were also run to calculate the total heat for different heating rates and the heat released during curing.

At the NRC, the fractional degree of conversion is determined by the following formula:

Fractional degree of conversion = (Total heat – Residual heat) / Total heat

Some plots of experimental results are done in each experiment:

- Figure 1: Fractional degree of conversion vs. time
- Figure 2: Instantaneous glass transition temperature vs. time
- Figure 3: Instantaneous glass transition temperature vs. fractional degree of conversion
- Figure 4: Modified fractional degree of conversion vs. time

Figure 26 is a combination of plotting the instantaneous glass transition temperature vs. the fractional degree of conversion. In the same plot the results of fitting to the diBenedetto equation is shown. Furthermore the model of the monocomponent RTM 6 resin system is also shown.

The DiBenedetto equation is given as:

$$T_g = T_{g,0} + \frac{(T_{g,\infty} - T_{g,0})}{1-(1-\lambda)\alpha}$$

Equation. 41

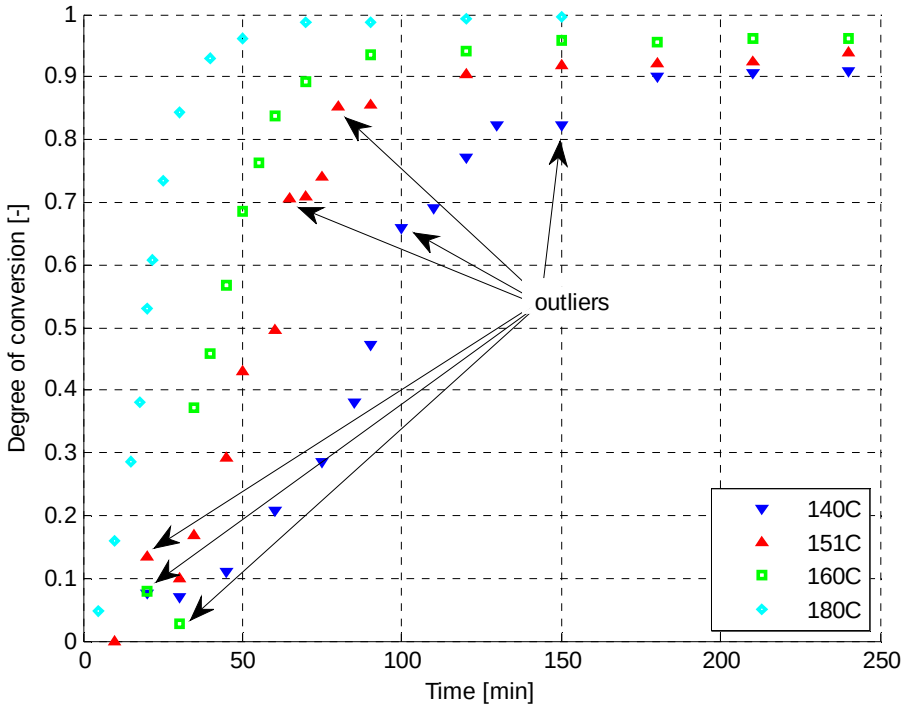
Degree of conversion [-]
Time [min]
outliers
140C
151C
160C
180C

Fig. 24

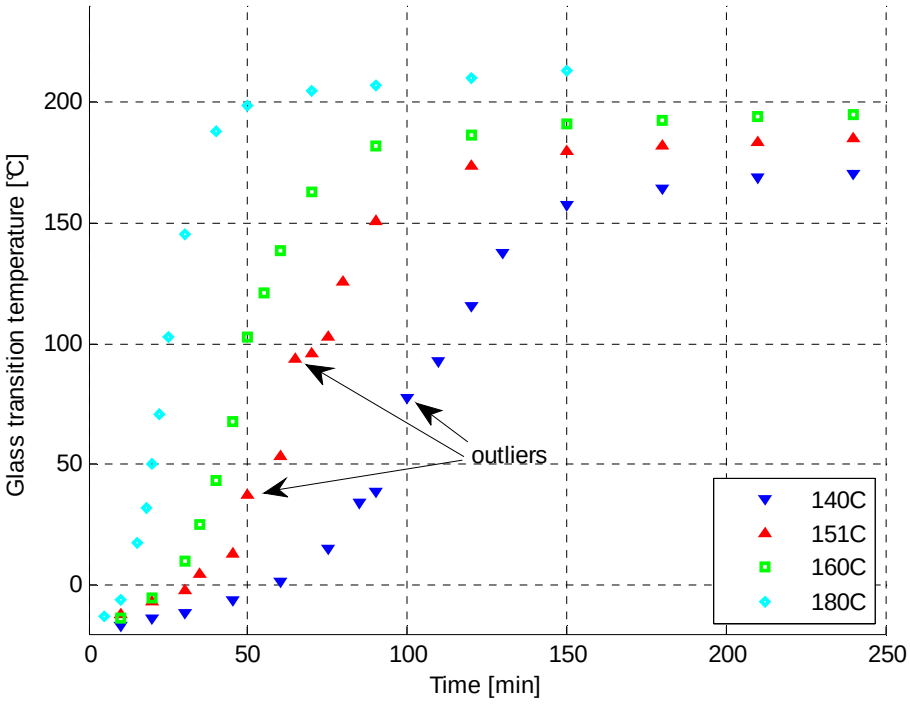
Glass transition temperature [°C]
Time [min]
outliers
140C
151C
160C
180C

Fig. 25

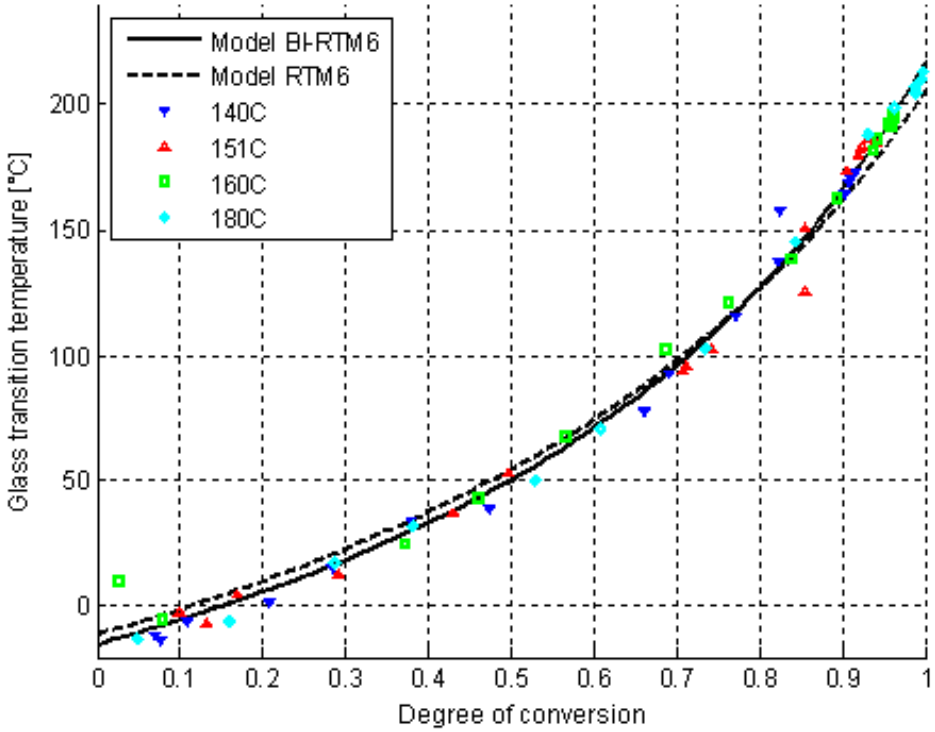
Model BI-RTM6
Model RTM6
140C
151C
160C
180C
Glass transition temperature [°C]
Degree of conversion
200
150
100
50
0
0
0.1
0.2
0.3
0.4
0.5
0.6
0.7
0.8
0.9
1

Fig. 26

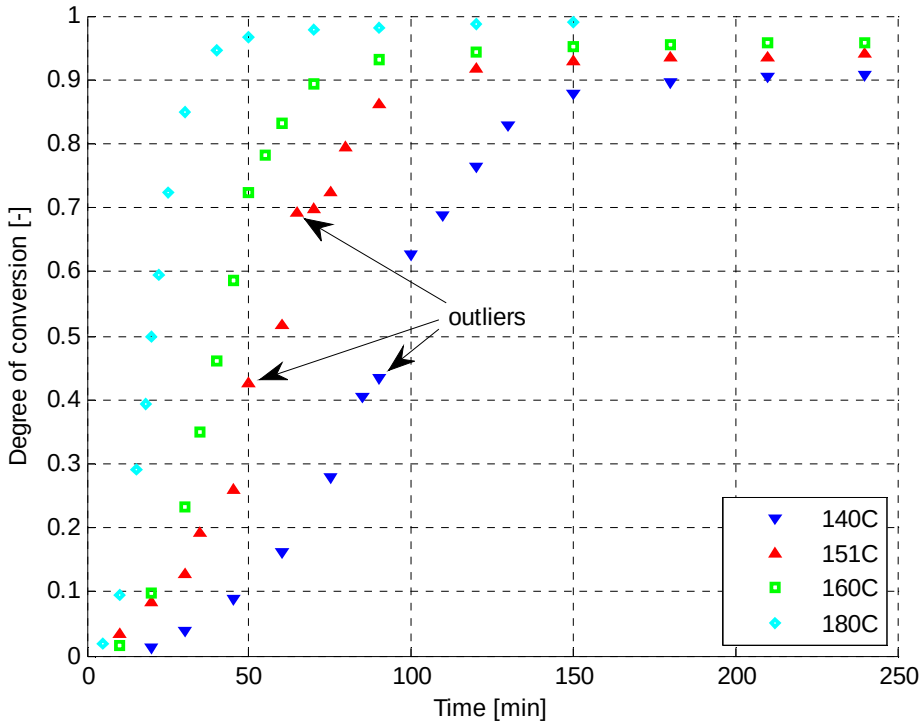
outliers
140C
151C
160C
180C
Degree of conversion [-]
Time [min]
1
0.9
0.8
0.7
0.6
0.5
0.4
0.3
0.2
0.1
0
0
50
100
150
200
250

Fig. 27

Obtained data is analyzed at NRC guided by the following guidelines:

- Each measurement is been performed for the unreacted resin system (to determine heat flow) and for the reacted resin system (to get a baseline).
- The baseline heat flow was subtracted from the measured heat flow during reaction.
- The reaction rate was obtained by dividing the heat flow by the sample mass and total heat of reaction.
- By integrating the reaction rate degree of conversion was obtained.
- It should be noted that some 'beautifying' was needed for the initial part of the curves. By plotting the LN (dα/dt) as a function time, the first part of the curve becomes linear. Using a linear extrapolating function the curve was extrapolated t=0min.
- Starting point is determined by extrapolating the heating ramp to the isothermal cure temperature.
- It should be noticed that he cure temperature was not instantaneously reached. It takes up to 5 minutes to reach the cure temperature. An initial difference of 3.5˚ was observed.

Some plots of experimental results are done in each experiment:

- Figure 2: Temperature difference vs. time
- Figure 3: Reaction rate vs. time
- Figure 4: Degree of conversion vs. time

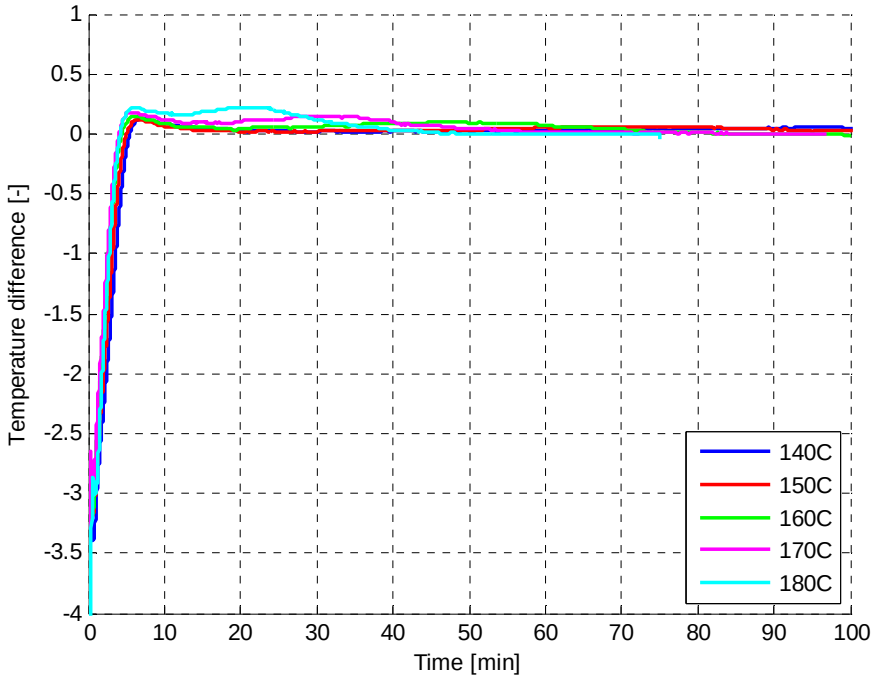

Fig. 28

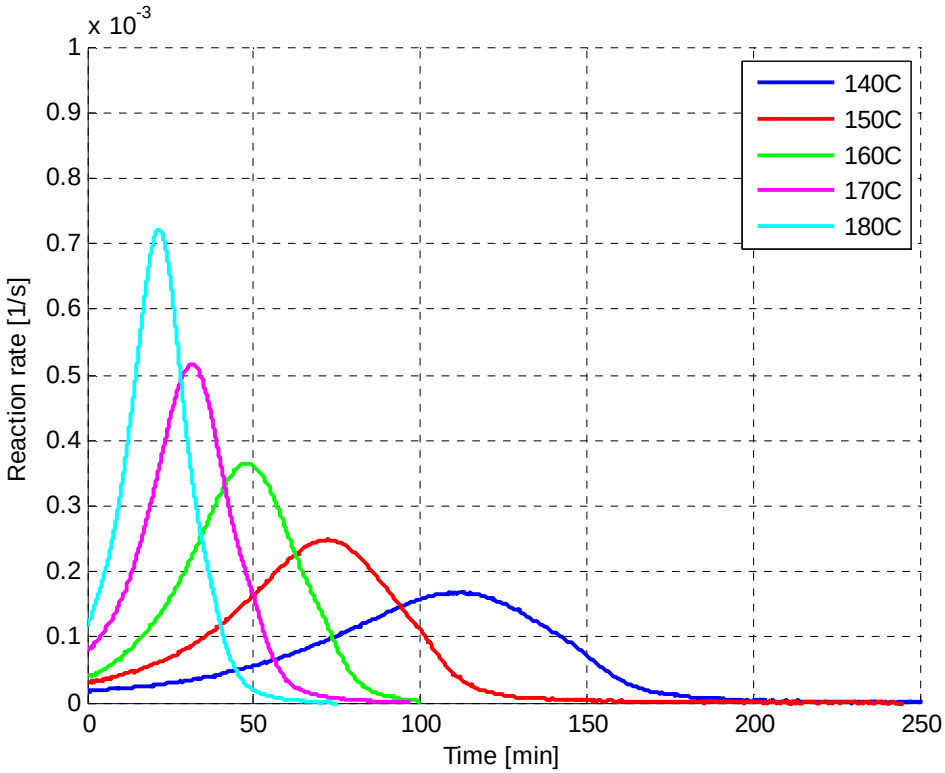
x 10^-3
Reaction rate [1/s]
Time [min]
140C
150C
160C
170C
180C

Fig. 29

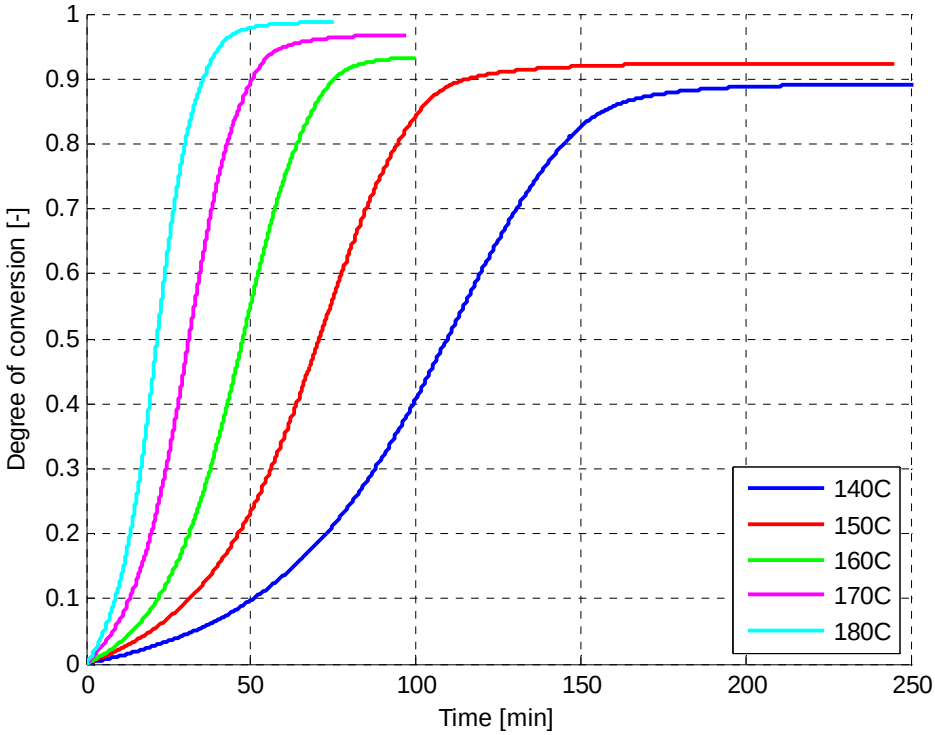
Degree of conversion [-]
Time [min]
140C
150C
160C
170C
180C

Fig. 30

If we compare data sets, a difference can be seen easily. The lower the cure temperature the larger the time gap between the two sets of experiment. Also, some effects can be causing a deviation.

- Difference in heating rates (100˚C/min (NRC) vs. 25˚C/min (TUD))
- Stabilisation problem with TUD experiments
- Choice of starting point

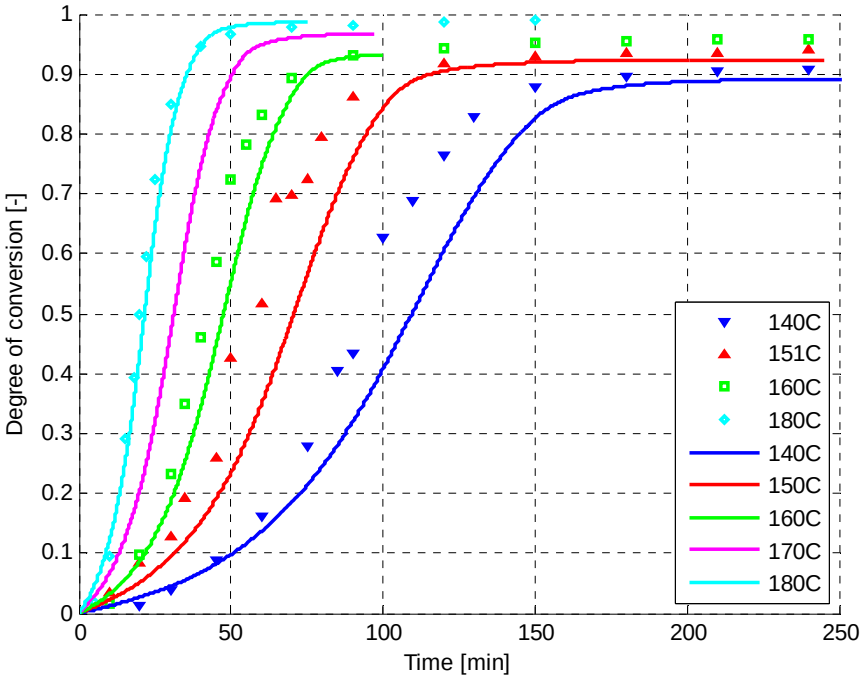

Fig. 31

For the modeling of the cure kinetics 4 models were implemented. 2 of them are from NRC and the other 2 from TUD. It is going to be explained each one

Model 1 TUD DATA: It is based on the Kamal-Sourour equation:

$$\frac{d\alpha}{dt} = (K_1 + K_2\alpha^m)(1-\alpha)^n$$

Equation. 42

In which:

$$K_i = A_i \exp(\frac{-E_i}{RT}) \qquad \text{for } i = 1,2$$

Equation. 43

Plot natural logarithm of the reaction rate as a function of the reciprocal of reaction temperature at low degree of conversions give a linear relation in which the slope equals $\frac{-E_1}{R}$ and the starting value is $LN(A_1)$.
The procedure starts with the calculation of the vitrification for each test, continue with plotting natural logarithm of reaction rate as function of cure time. Fit parabolic equations left and right of vitrification region is necessary to determine the intersection.

Some plots of experimental results are done in each experiment:

- Figure 1: Parameter estimation
- Figure 2: Model 1: reaction rate vs. time
- Figure 3: Model 1: degree of conversion vs. time
- Figure 4: Model 1: reaction rate vs. degree of conversion

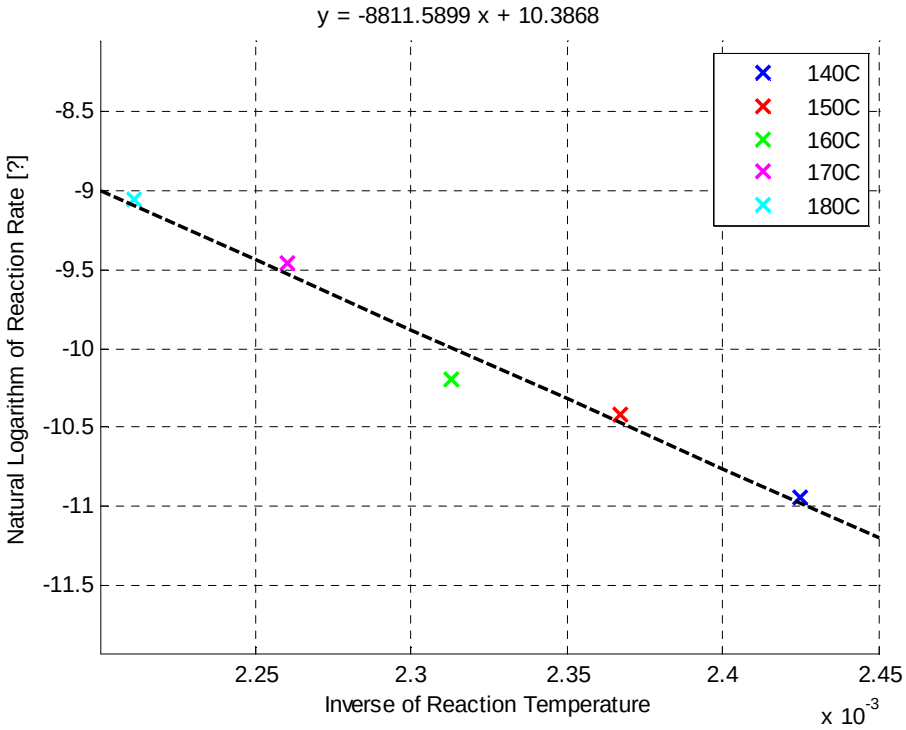

Fig. 32

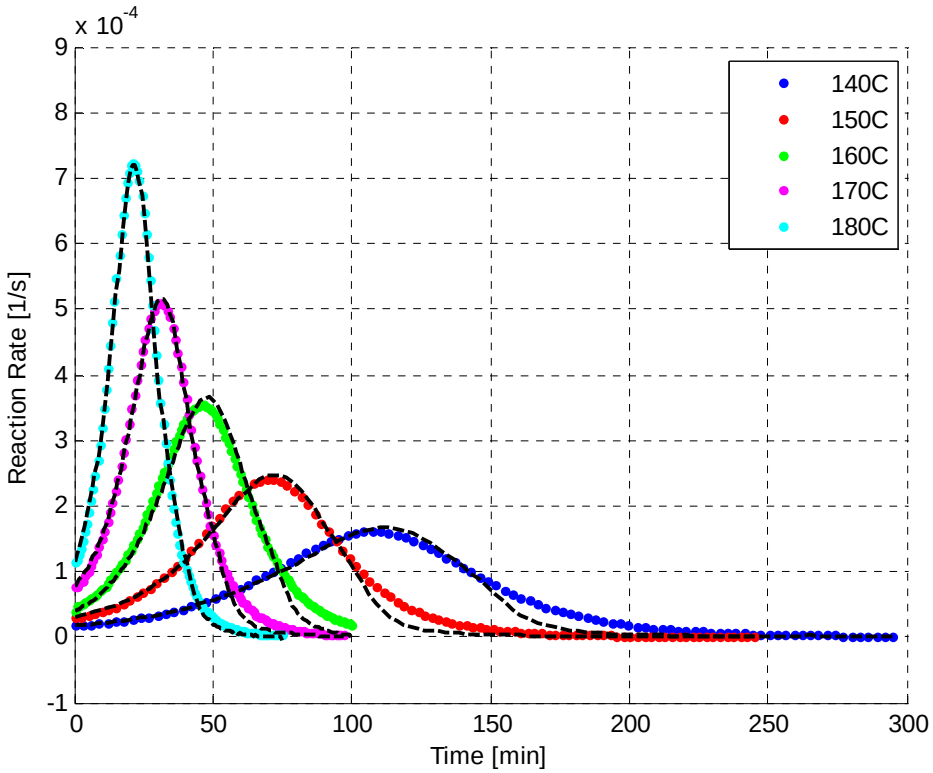
x 10^-4
Reaction Rate [1/s]
Time [min]
140C
150C
160C
170C
180C

Fig. 33

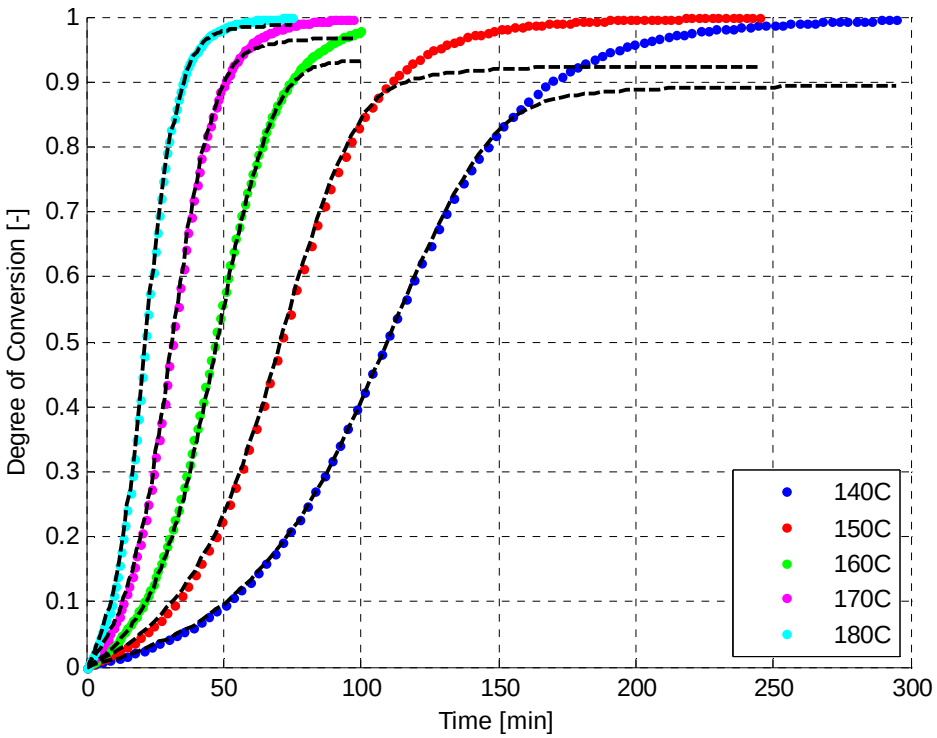
Degree of Conversion [-]
Time [min]
140C
150C
160C
170C
180C

Fig. 34

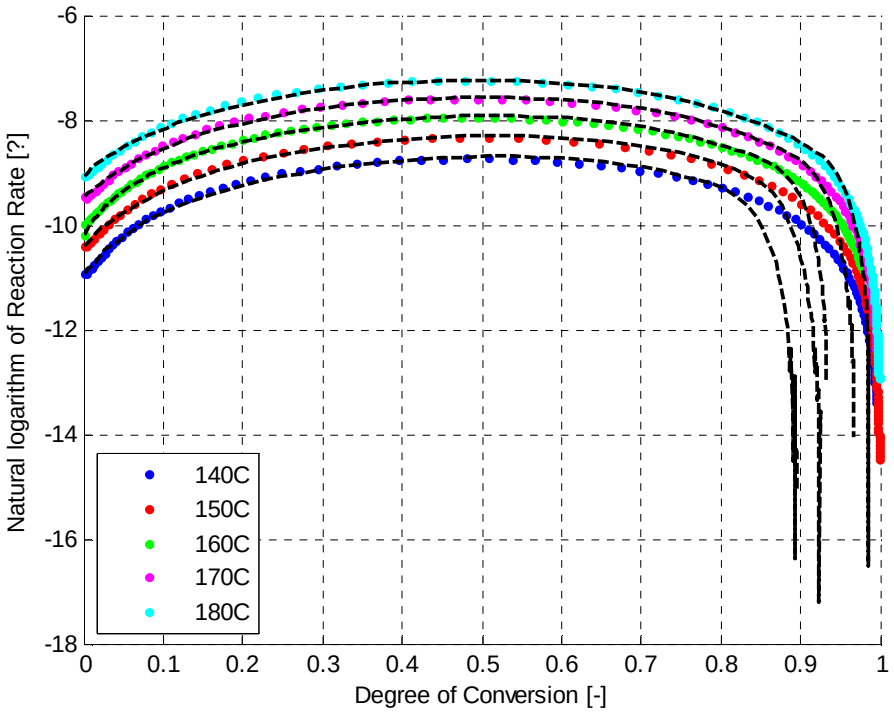

Fig. 35

As can be seen, the Kamal-Sourour estimates pretty well the cure kinetics of the bicomponent RTM 6 resin system. However, only a function has to be added for the vitrification region.

Model 2 NRC DATA: This model is also based on the Kamal-Sourour equation:

$$\frac{d\alpha}{dt} = (K_1 + K_2\alpha^m)(1-\alpha)^n$$

Equation. 44

In which:a

$$K_i = A_i \exp(\frac{-E_i}{RT}) \qquad \text{for } i = 1,2$$

Equation. 45

Making a comparison can be seen that there is a clear difference between the two sets of experiments. In this way, the coefficients of the Kamal-Sourour equation will also differ.

Parameters:	E_1	A_1	E_2	A_2	m	n	R
	[kJ/mol]	10^3 [1/s]	[kJ/mol]	10^3 [1/s]	[-]	[-]	[J/(mol-K)]
	73.26	36.05	57.49	17.63	1.1818	1.1886	8.314472

Table. 1

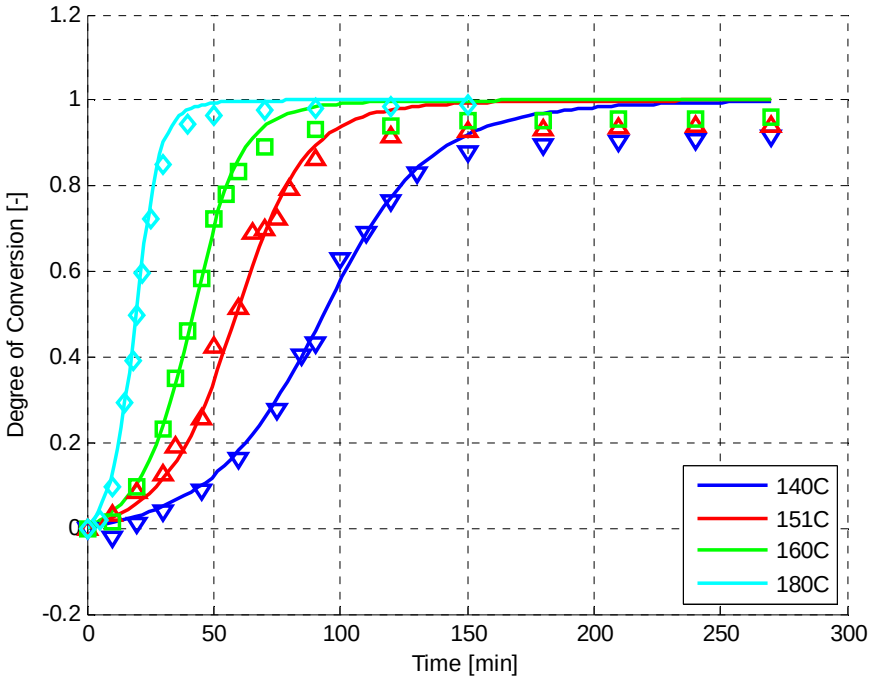

Equation. 46

Model 3 TUD DATA: On that case, Kamal-Sourour equation needs to be extended in order to include the diffusion-controlled region. The model that has been used for the monocomponent RTM 6 resin system will also is used in this case. That is:

Modified Kamal-Sourour:

$$\frac{d\alpha}{dt} = (\frac{K_1 K_d}{K_1 + K_d} + \frac{K_2 K_d}{K_2 + K_d}\alpha^m)(1-\alpha)^n$$

Equation. 47

In which:

$$K_i = A_i \exp(\frac{-E_i}{RT}) \qquad \text{for } i = 1,2$$

Equation. 48

And:

$$K_d = A_d \exp(\frac{-E_d}{RT}) \exp(\frac{-b}{0.00048(T - T_g) + 0.025})$$

Equation. 49

Some plots of experimental are done on each experiment:

- Figure 2: Model 2: reaction rate vs. time
- Figure 3: Model 3: degree of conversion vs. time
- Figure 4: Model 2: reaction rate vs. degree of conversion

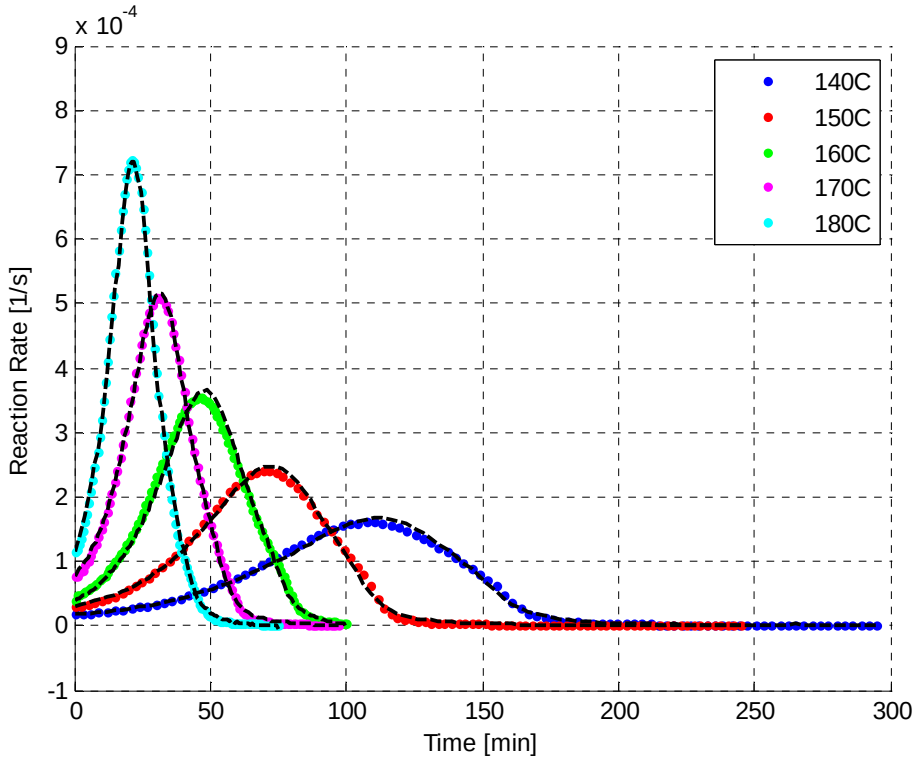
x 10^-4
Reaction Rate [1/s]
Time [min]
140C
150C
160C
170C
180C

Fig. 36

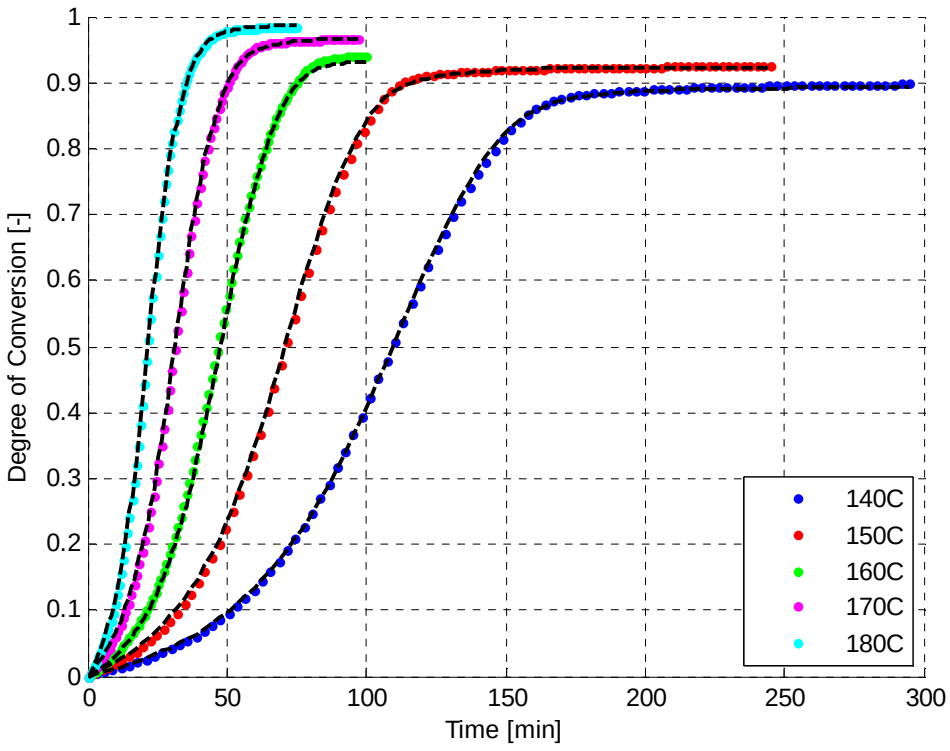
Degree of Conversion [-]
Time [min]
140C
150C
160C
170C
180C

Fig. 37

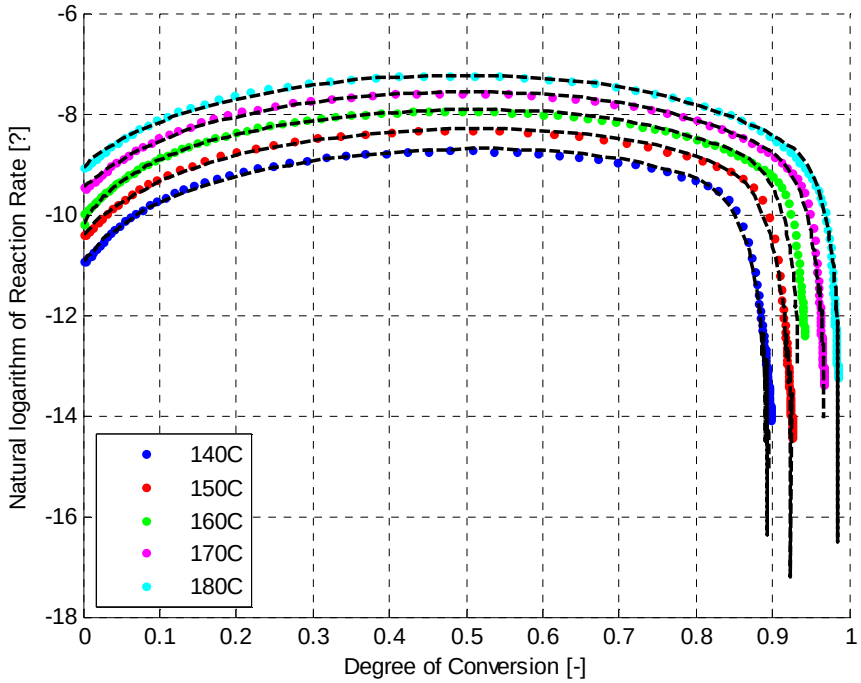

Fig. 38

Model 4 NRC DATA: The Kamal-Sourour equation needs to be extended in order to include the diffusion-controlled region. The model that as been used for the monocomponent RTM 6 resin system will also is used in this case. That is:

Modified Kamal-Sourour:

$$\frac{d\alpha}{dt} = \left(\frac{K_1 K_d}{K_1 + K_d} + \frac{K_2 K_d}{K_2 + K_d}\alpha^m\right)(1-\alpha)^n$$

Equation. 50

In which:

$$K_i = A_i \exp\left(\frac{-E_i}{RT}\right) \qquad \text{for } i = 1,2$$

Equation. 51

And:

$$K_d = A_d \exp\left(\frac{-E_d}{RT}\right)\exp\left(\frac{-b}{0.00048(T-T_g)+0.025}\right)$$

Equation. 52

A similar approach has been used: only the pre-exponential factor A_d was varied and not enough data points for proper fitting of the diffusion-controlled region.

The parameters for this model are listed below:

- Chemically-controlled region:

Parameters:	E_1	A_1	E_2	A_2	m	n	R
	[kJ/mol]	10^3 [1/s]	[kJ/mol]	10^3 [1/s]	[-]	[-]	[J/(mol-K)]
	73.26	36.05	57.49	17.63	1.1818	1.1886	8.314472

Table. 2

- Diffusion-controlled region:

Parameters:	E_d	A_d	b
	[kJ/mol]	10^{25} [1/s]	[°C]
	207.33	49.804	0.1622

Table. 3

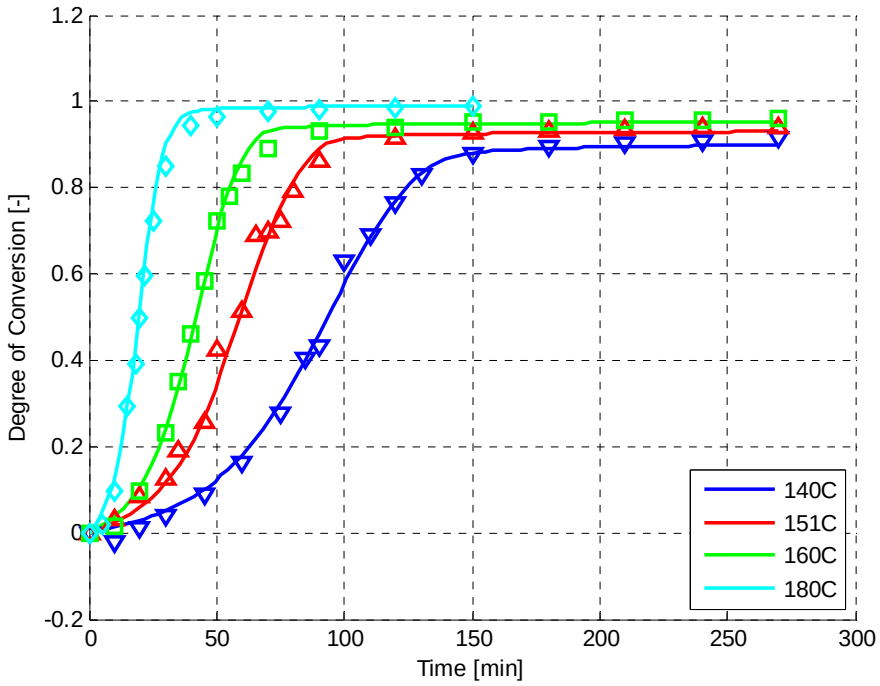

Fig. 39

3.2 The model in COMSOL Multiphysics

The model we are going to use for the COMSOL Multiphysics modelisations is implemented by two equations. First one is the equation for the heat transfer in conduction in transient analysis, which is given by:

$$\delta_{ts}\rho C_p \frac{\partial T}{\partial t} - \nabla(K\nabla T) = Q + h_{trans}(T_{ext} - T) + C_{trans}({T_{ambtrans}}^4 - T^4)$$

Equation. 53

Where:

δ_{ts} = Time-scaling coefficient

K = Thermal conductivity

ρ = Density

C_p = Heat capacity at constant pressure

Q = Heat source

h_{trans} = Convective heat transfer coefficient

T_{ext} = External temperature

C_{trans} = User-defined constant

$T_{ambtrans}$ = Ambient temperature

In order to obtain values of the thermo-physic parameters which belong to the resin, the rule of mixture can be used. Following equations belong to the rule of mixture:

$$\rho_c = V_f \rho_f + V_m \rho_m$$
$$C_{pc} = V_f C_{pf} + V_m C_{pm}$$

Equation. 54

This solution is not allowed to be used in order to calculate the resin thermal conductivity because K contact value can not be calculated in the border of fibres. Some experiments need to be run at the laboratory to calculate average values of thermal conductivity.

The equation we are going to use is the following one:

$$\rho_c C_{cp} \frac{dT}{dt} = \frac{d}{dz} K \frac{dT}{dz} + \rho_r V_r H_u \frac{d\alpha}{dt}$$

Equation. 55

Where:

ρ_c = Density of composite

C_{pc} = Specific heat capacity

K = Thermal conductivity

ρ_r = Density of resin

V_r = Resin volume

H_u = Heat of reaction

$\frac{d\alpha}{dt}$ = Cure rate

The other equation is a partial differential equation which is a model using a system of one or more time-dependent partial differential equations in coefficient form. This time-dependent coefficients are mass, diffusion or absorption coefficients.

$$e_a \partial^2 u / \partial t^2 + d_a \partial u / \partial t + \nabla(-c\nabla u - \alpha u + \gamma) + au + \beta\nabla u = f$$

Equation. 56

Where:

$c =$ diffusion coefficient

$a =$ absorption coefficient

$f =$ source term

$e_a =$ mass coefficient

$d_a =$ damping mass coefficient\

$\alpha =$ conservative flux convection coefficient

$\beta =$ convection coefficient

$\gamma =$ conservative flux source term

d_a is set to 1 and the source term value is related to the cure kinetics model function.

4 Experimental work

Experimental part of the work relates of acquiring data from the RTM experiments. The procedure followed at the laboratory explains how to work in order to obtain best results during the RTM processes. No detailed procedures can be found on this document, general explanation of the procedure is explained in an instruction manual placed in the laboratory.

The main target of the laboratory work is to run experiments on manufacturing composite plates of 25 mm thickness to acquire data of temperature in measurement points. Resin Transfer Moulding process is done in a mould made of two parts (top and bottom) with an inner cavity, where a vacuum is created and a resin is injected.

This part of the whole project was one of the most important on the schedule. High quality acquired data is a must to run good simulations and obtain remarkable results to give knowledge to go further in the science field. Two months and a half of laboratory work were necessary to run all the experiments firstly scheduled. Which means, the time spent at the laboratory was a hard time full of precise work and dedication.

For the experiments, it was decided to use RTM 6 as the thermosetting resin. RTM 6 is an epoxy/amine monocomponent system that is supplied by Hexcel Composites, France. It is specially developed to fulfill requirements of the aerospace industries in advanced RTM processes. The epoxy system is premixed and degassed and its service temperature ranges from -60 ºC up to 180 ºC. At 23 ºC the storage life of RTM 6 is 15 days, while it has a guaranteed storage life of nine months at -18 ºC [1]. For processing it needs to be preheated to 80 ºC, whereas the mould should be preheated to 120 ºC. The injection should take place under low pressure (1 to 3 bars). At 120 ºC the time to gel is more than 240 minutes. The MRCC recommends a cure in mould of 75 minutes at 160 ºC and a free-standing postcure of 120 minutes at 180 ºC with a ramp of 1 ºC/min.

Different values of heat rate and cure temperature were set to run the experiments. Based on the MRCC, some changes were introduced to estimate the influence of various heating rates or curing temperatures. Those values are going to be detailed in following main points.

HexFlow® RTM 6 is a resin already degassed, specifically developed to fulfill the requirements of the aerospace and space industries in advanced resin transfer moulding (RTM) process. At room temperature, it is a brown translucid paste but its viscosity decreases quickly by increasing the resin temperature.

Glass fibre used in the experiment is called Hexforce 7581. It is provided by Hexcel and is an hybrid fibre fabrics for use in advanced composites. The fabric dry weight is 303 g/m².

4.1 Preparation of the mould

Part of the laboratory work related to the mould preparation has an important influence on results. In order to obtain a correct data acquisition, some steps should be followed during the mould preparation. Correct processing is explained step by step in the testplanner for production of advanced composites with the RTM unit. Surfing treatments must be applied correctly and orderly to have a fitted surface for injection and vacuum without leakage.

Two sealing rings help to create a vacuum inside de mould correctly. Those rings can be reused if there is no influence in the leakage test. Endings need to be fixed with glue and be placed in the gap which is going to be filled with silicone.

The silicone assures the vacuum along the cavity where thermocouple wires are placed with the thermal expansion. It also creates a problem in the integrity of thermocouple wires, some of them can be broken by tensions created by thermal expansion. In order to solve this problem, wires integrity is protected by a metal mesh which assures the proper function of those devices. In addition, two small pieces of cured silicone are installed to create a limit of silicone expansion.

4.2 Layout of glass fibre layers and thermocouples

Sensors are used during the experiment to acquire data of temperature in different parts of the plate. Two measurement points are implemented, as can be seen in the figure below. It explains the implemented layout of the thermocouples:

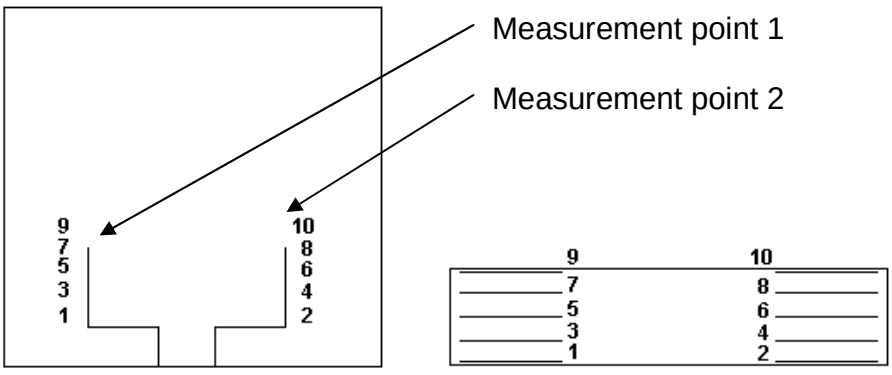

Fig. 40

Each measurement point is provided by 5 thermocouples placed along the through-thickness. There are 30 layers of glass fibre between each thermocouple. In all, 122 layers of glass fibre are placed one over the other to build the 25 mm thickness plate. First 61 layers have an orientation at 0°, and the other 61 are rotated 90°.

Bottom and top layers belongs are the initial and the end of the layout, and is the place where thermocouples no. 1, 2 and 3, 4 are installed respectively. With the purpose of obtaining a profile temperature along the thickness, thermocouples are placed in the bottom, in the first quarter, in the middle, in the three quarter and in the upper part.
Preparation of thermocouples consists of the correct union between the two inner wires, twisted and welded properly. The way to add the thermocouple and the layer is done with high temperature tape. In addition, a part of it (in contact with the metal mesh) needs to be stripped and covered.

4.3 Procedure

Inlet and outlet Teflon tubes are connected before applying the glass fibre layers, using special connections to assure the vacuum in the mould. Those tubes are going to be way to introduce the resin during the injection.

To close the mould, some guides are used to make the closing mould procedure easier. Bolts need to be tightened in order to make the union correctly and assure a satisfactory leakage test. It is going to be created through a vacuum pump.

An injection unit controller manages the injection procedure. And is done from the bottom to the upper part (against gravity), and in special conditions of temperature and pressure. Explanation in detail can be found in the laboratory instruction manual. The oil heating unit provides the profile temperature in the mould along the whole experiment.

In brief, three computers support the experiment. First one is programmed to manage the resin injection unit. Second one controls the oil heating unit. Third one is responsible for the temperature data acquisition measured by the sensors.

4.4 Density and volume fraction calculation

After its manufacturing, the study of density takes part of the main procedure. The plate needs to be cut in different pieces to study the volume fraction of each section of the plate and obtain average values. Slices of different representative parts of the plate are cut with help of a cutting machine. Taking in account dry spots, densities zones colored different created by non homogeneous curing

process, regions closed to the sensors, representative parts of the plate should be selected for the study in order to calculate an average value with good agreement.

The following description explains the samples obtained from a plate manufactured at the laboratory. The first 3 samples belong to the part closed to the measurement point number 1. Numbering goes from top part to the bottom, i.e. 1 belongs to top side (outlet), 2 belong to middle part and 3 belong to bottom part (inlet).

- Sample 1: 25x20x6.5 (mm)
- Sample 2: 25x20x6 (mm)
- Sample 3: 25x20x8 (mm)

The same goes with rest of samples, from number 4 to 6 the emplacement is from the top to the bottom.

- Sample 4: 25x20x6 (mm)
- Sample 5: 25x21x6 (mm)
- Sample 6: 25x21x6 (mm)

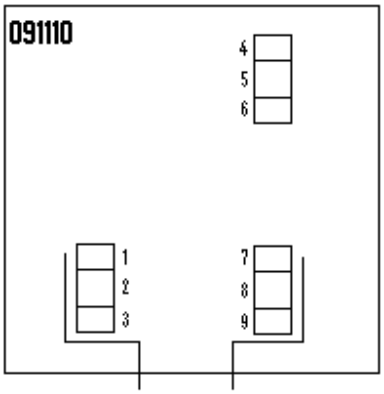

During the study of the plate, the upper right side had a different appearance related to resin density. As a result of this, this part was introduced on the volume fraction study.

Last part of the study was focused on the zone closed to the measurement point number 2.

- Sample 7: 25x20x6 (mm)
- Sample 8: 25x20x6 (mm)
- Sample 9: 25x20x6 (mm)

Continuing with the procedure, some measurements need to be done to calculate the volume fractions. Calculation of weights in different situations is carried out by a scale. Following procedure explains the way to measure an obtain results:

First of all, dry weight of each sample need to be calculated. Then, the wet weight is evaluated. After those steps, is necessary to measure crucible weights and the value obtained of measuring weight plus the sample.

With all of these values calculated, burn step of the samples can be done. Introducing each sample on the oven and heating up to 560˚ for a period of 45 min resin is burn and both materials can be separated. After burning period,

glass fiber is the only remaining material. Then, calculation of fibre weight can be done easily.

Having values of weights of fibre and resin separately, specimen values can be calculated using the following formula:

$$\rho = \frac{dry\ weight}{(dry\ weight - wet\ weight)}(water\ density - air\ density) + air\ density$$

Equation. 57

With the knowledge of all of these values, calculation of fibre and resin volume fraction can be done. The following sheet shows the average values obtained from each experiment:

EXPERIMENT	Fiber Density (Reinforcement)	Fiber Volume Fraction (Reinforcement)	Resin Density (Matrix)	Resin Volume Fraction (Matrix)
091104	2.56	56.75467	1.04	44.19951
091110	2.56	55.690380	1.04	42.84812
091202	2.56	57.58047	1.04	43.50448
100216	2.56	56.56591	1.04	44.01831
100223	2.56	55.44041	1.04	44.80622
Average	2.56	56.40637	1.04	43.87533
		0.56406		0.43875
UNITS	10E3 kg/m3	%	10E3 kg/m3	%

Table. 4

Bottom row gives an average value, which is going to be used on following simulations.

5 Simulation of the RTM curing process and its results

5.1 Parameters settings and equations

At summary, a number of experiments were run at the laboratory. Those experiments are named according with the date where were run:

- 090717 (2009, 17th of July)
- 091029 (2009, 29th of October)
- 091104 (2009, 4th of November)
- 091110 (2009, 10th of November)
- 091202 (2009, 2nd of December)
- 100210 (2010, 10th of February)
- 100216 (2010, 16th of February)
- 100223 (2010, 23rd of February)

The main purpose of these simulations is to obtain the most accurate value of thermal diffusivity which gives the best agreement between model solution and experimental work.

Before obtaining the thermal conductivity value, a calculation of thermal diffusivity is necessary. Matlab program MainFileFIT.m makes a calculation of thermal diffusivity values for each region along the experiment. These regions are injection, cure and cool down. Then, there are three different values that can be obtained. The values obtained running the simulation give the value with the minimum SSE (Sum of Square Error), which is calculated with the following equation:

```
Errorvector_2   = MOD.T{2} - EXP.T{2}';
Errorvector_3   = MOD.T{3} - EXP.T{3}';
Errorvector_4   = MOD.T{4} - EXP.T{4}';
SSE{m}(j) = sum(Errorvector_2.^2) + sum(Errorvector_3.^2) +
sum(Errorvector_4.^2);
```

It makes a calculation with the subtraction in thermocouples 2, 3 and 4 of values obtained from model calculation and the values obtained from the interpolation of experimental data. Adding all the error, the sum of errors can be obtained. The minimum error, matches the most accurate value of thermal diffusivity. This way of calculate the accuracy between solutions from modeling and experimental work was seen in literature and has been used in some researching works.

As has been explained, values of thermal diffusivity α, can be calculated with the help of the program. In order to obtain values of thermal conductivity, a relation between α and K needs to be implemented.

The equation which is going to be used appears below:

$$\rho_c C_{cp} \frac{dT}{dt} = \frac{d}{dz} K \frac{dT}{dz} + \rho_r V_r H_u \frac{d\alpha}{dt}$$

Equation. 58

As it has been explained, we obtain 3 different values of thermal diffusivity belonging to three different sections of the experiment. During the first part of the experiment there is no exothermic reaction:

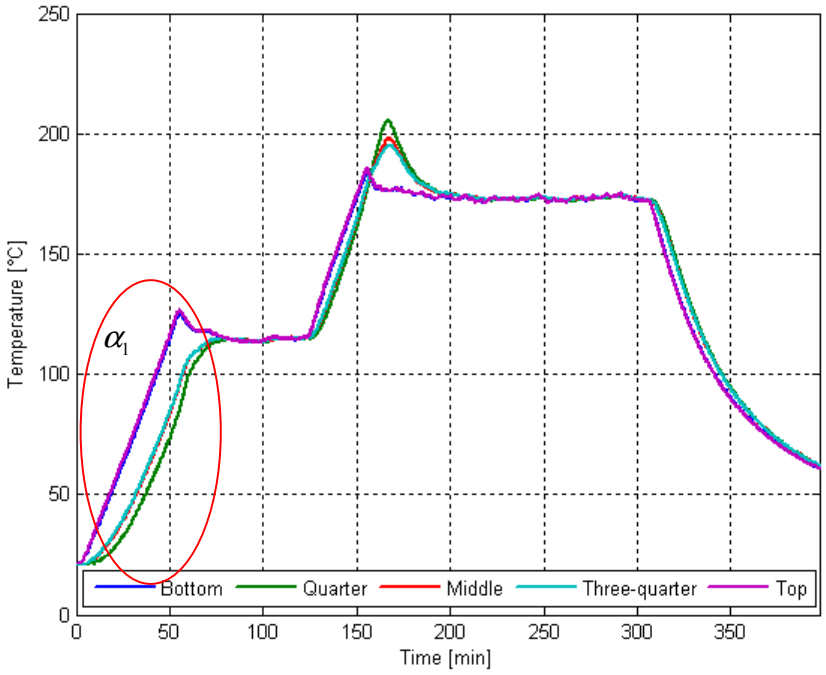

Fig. 41

Can be seen that there is no heat of reaction, actually is equalized to zero. So, the equation is simplified as follows:

$$\rho_c C_{pc} \frac{dT}{dt} = \frac{d}{dz} K \frac{dT}{dz}$$

Equation. 59

Values of density and specific heat capacity belong to the composite material, and need to be calculated by the rule of mixture. Firstly, are going to be set to 1, to relate thermal diffusivity and thermal conductivity. The equation that relates both coefficients is the following:

$$\alpha = \frac{K}{\rho_c C_{pc}}$$

Equation. 60

Taking into account the initial values of density and specific heat capacity, we can say:

$$\alpha = K$$

Equation. 61

Thermal diffusivity and thermal conductivity have the same value. Then, going back to the primary equation, we can say:

$$\rho_c C_{pc} \frac{dT}{dt} = \frac{d}{dz} \alpha \frac{dT}{dz}$$

Equation. 62

Continuing with the study along the profile temperature, thermal diffusivity during the cure period (α_2) gives a value according to the lowest error between model solution and experimental results. Here, exothermic reaction takes part and error between the two solutions can be seen in following experiments. Evaluation of thermal conductivity value needs to be carried in order to find the most accurate solution. Increasing the thermal conductivity the model solution gives higher peaks of temperature.

The third thermal diffusivity value belongs to the cool down region. On the following figure can be seen both regions where thermal conductivity values number 2 and 3 are calculated.

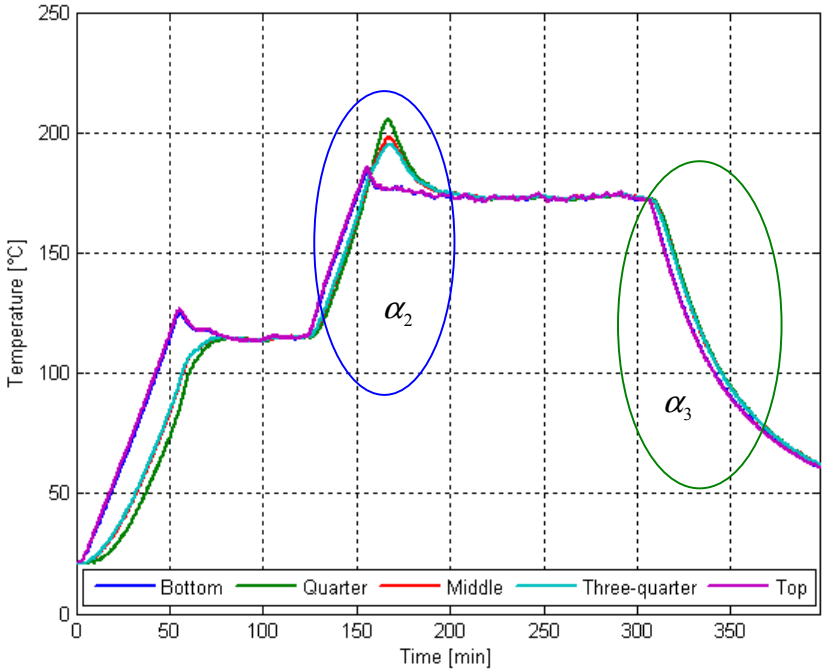

Fig. 42

In the region where exothermic reaction appears, resin is liquid, and α_2 can reach high values because of the difference between solutions. Something similar happens along the cool down region, but resin is in solid state. A value of thermal diffusivity for both regions is generated on each simulation. Next explanation extends the information about the calculation on this part of the work. Results were obtained from an experiment carried out on 23rd of February in 2010. The experiment has the following characteristics: The heat rate after the starting point of heating for curing is 1˚C/min, the curing temperature is set to 160˚C and there is no post-curing period.

5.2 Calculation of the SSE and thermal diffusivity

The following figure shows the profile temperature along the whole experiment. The five lines belong to the same measurement point, which can be chosen in the Matlab program. It can be seen that the top and bottom have the same temperature along the experiment less part before reaching 120˚C. The top part reaches set temperature imposed by oil heating unit a little bit faster than bottom, and at the end of the initial slope the thermal inertia of top part gives a low peak. That is not really important, because profiles are exactly the same along the rest of the experiment, it means, during the exothermic reaction, along the curing period and later in the cool down.

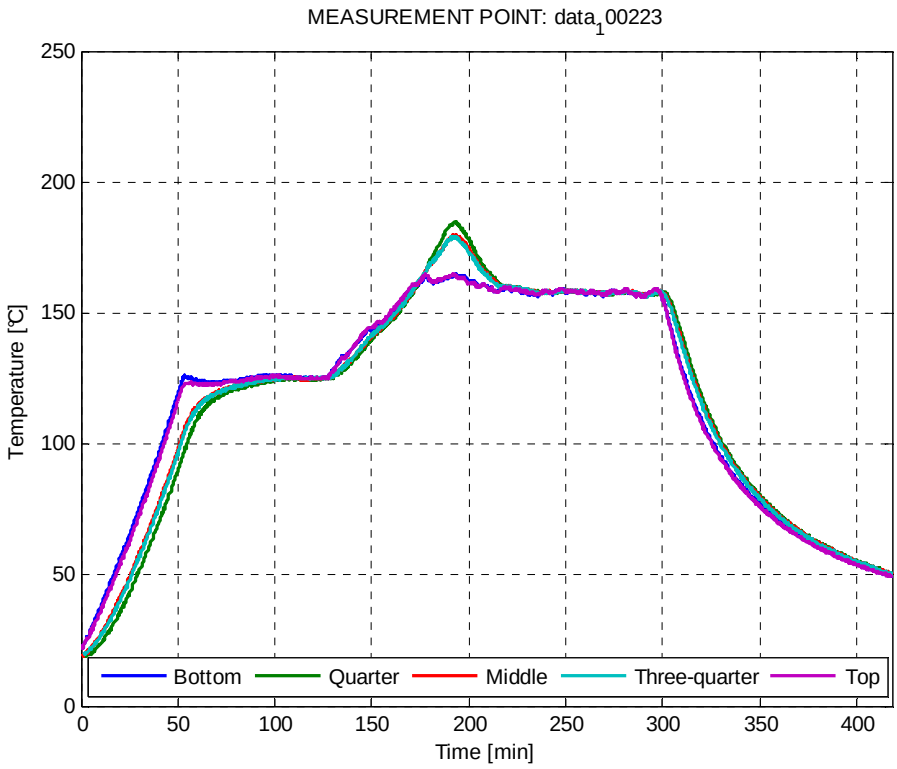

Fig. 43

Studying this profile temperature time values can be calculated easily. Start point heating of curing is exactly when second slope starts, been aware that the heat rate is 1˚C/min, the start heating point is minutes before the start of the slope. Start point curing is the point where lines of non top and bottom differ in parallelism. It means that exothermic reaction starts and temperatures increases start to be different. Following figures show how those points were calculated:

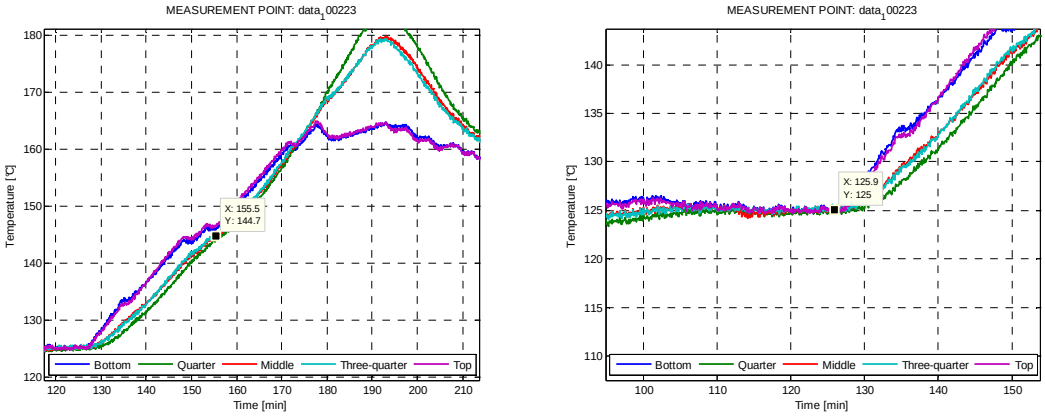

Fig. 44

Start Point Heating for curing: 126 min Start Point Curing: 155 min

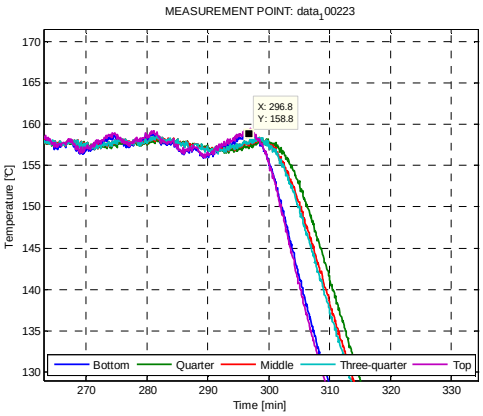

Fig. 45

End point of curing gives the time value when cool down regions starts. It happens at minute 296. Cool down period start just after the curing region because no post-curing region was configured to take part on that experiment. Otherwise, a third slope should appear after cure period to reach 180˚C.

The program gives a solution for the curing period, which is plotted below.

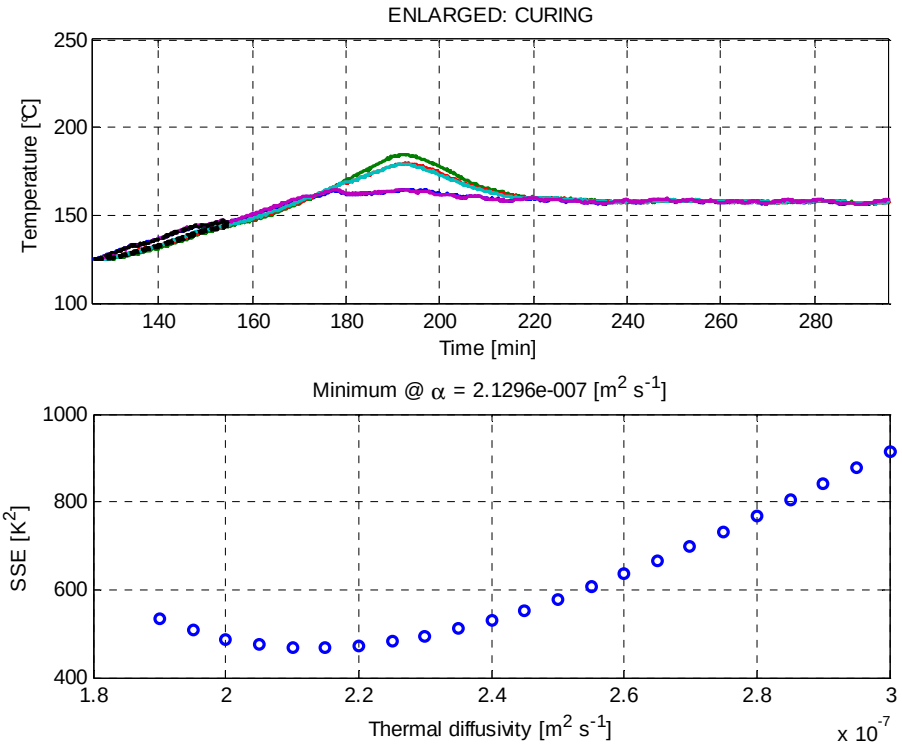

Fig. 46

Here, can be seen that the value of sum of square error reach the minimum between 1.8E-07 and 3.0E-07. These boundaries need to be changed in order to calculate the minimum value of SSE (Sum of Square Error), most accurate solution. The minimum value of α which makes the lowest SSE is:

$$\alpha = 2.1296e-007\ [\mathrm{m^2 s^{-1}}]$$

Equation. 63

Also, during the cool down period boundaries need to be set in order to find the minimum value of SSE. This time boundaries are 1.6E-07 and 3.0E-07. Below appears the curve of different values of SSE:

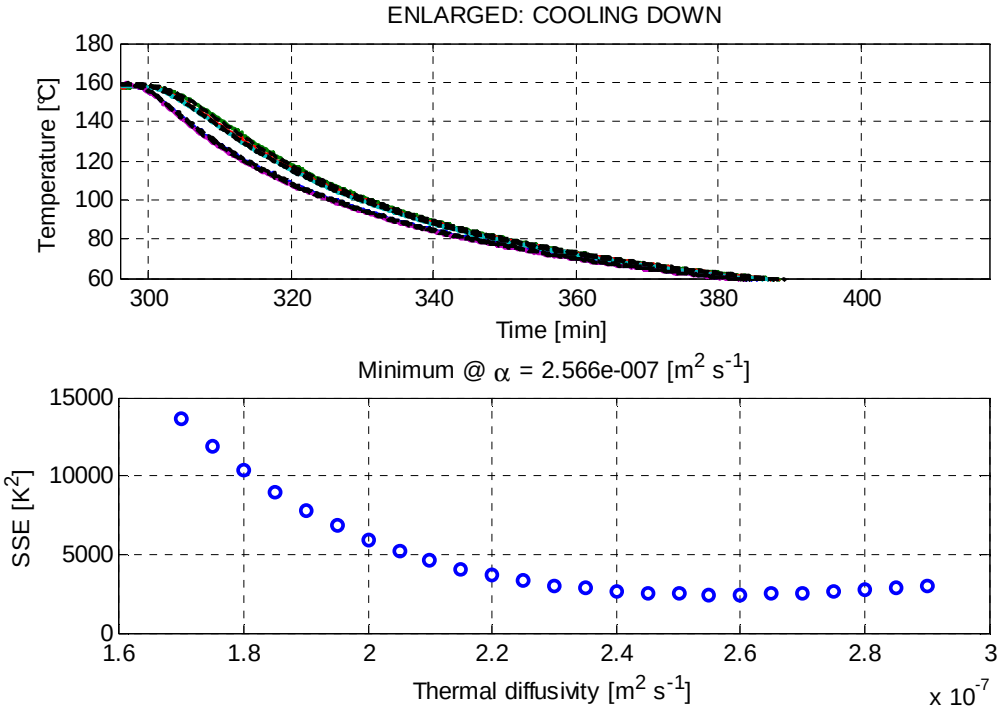

Fig. 47

The minimum value of α which makes the lowest SSE is:

$$\alpha = 2.566e-007\ [\mathrm{m^2 s^{-1}}]$$

Equation. 64

To set the boundaries of calculation for thermal diffusivity, need to be considered how the model is working. If the model line shows an increase of temperature slower than the experimental line, it means that thermal diffusivity needs to be higher. So, the value of α that gives the minimum SSE is going to be in a region of higher values of thermal diffusivity.

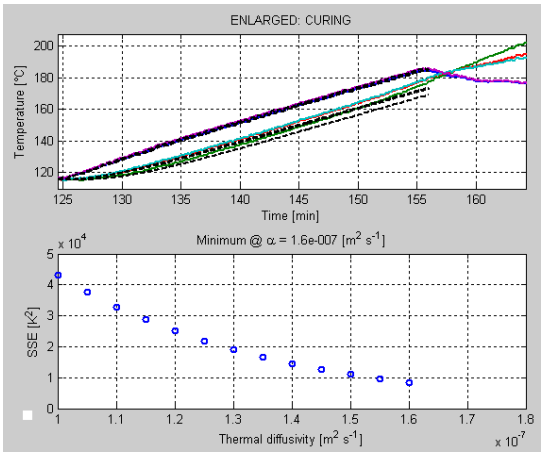

Fig. 48

The following figure shows the situation explained above. Here, can be seen that the model curve is under the experimental curve, it is predicting a slower increase of temperature. Boundaries of calculation were changed in order to find a better agreement between the two solutions.

After calculation of the two values of thermal diffusivity, the procedure continues obtaining thermal conductivity values of the two regions. Those values can be calculated using the following equation that relates thermo-physical properties:

$$K = \alpha \rho_c C_{pc}$$

Equation. 65

Values of density and specific heat capacity belong to composite material. The rule of mixture which is explained below is used to calculate these values:

$$\rho_c = V_f \rho_f + V_m \rho_m$$
$$C_{pc} = V_f C_{pf} + V_m C_{pm}$$

Equation. 66

Specific heat capacity value of the fibre is related with temperature, it means that a fixed value should be chosen in order to run simulations along the work. Making an interpolation from the curve provided from the original manufacturer, a value for 160˚C can be obtained. On the side of bi-component RTM-6, two curves of specific heat capacity belonging to unreacted resin or fully cured sample can be plotted depending on the resin sample. The value of liquid state at 160˚C is the one chosen to set this thermo-physical parameter.

$$C_{pf} = 830\ [J/kg.K]$$
$$C_{pm} = 2200\ [J/kg.K]$$

Equation. 67

In case of the density, these are the values for resin at 160˚C and glass fibre:

$$\rho_f = 2560\ [kg/m^3]$$

$$\rho_m = 1040\ [kg/m^3]$$

Equation. 68

With those values, thermal conductivity can be generated. The following sheet shows the values obtained on each experiment and the average values of thermal diffusivity and thermal conductivity.

EXPERIMENT N. 1	α1	α2	α3		Kii	Kiii
090717	not interested	1.7016E-07	1.5567E-07		4.6351E-01	4.2404E-01
091029	not interested	1.9894E-07	3.2139E-07		5.4190E-01	8.7545E-01
091104	not interested	2.1843E-07	2.7225E-07		5.9499E-01	7.4160E-01
091110	not interested	2.2319E-07	2.7498E-07	K=α*ρc*Cpc	6.0796E-01	7.4903E-01
091202	not interested	1.2259E-07	2.6772E-07		3.3393E-01	7.2926E-01
102010	not interested	2.5679E-07	1.9659E-07		6.9948E-01	5.3550E-01
100216	not interested	2.4824E-07	2.3645E-07		6.7619E-01	6.4408E-01
100223	not interested	2.1296E-07	2.5666E-07		5.8009E-01	6.9913E-01
Average		2.0641E-07	2.4771E-07	Average	5.5971E-01	6.7128E-01
UNITS	m2/s	m2/s	m2/s		[W/mK]	[W/mK]

Table. 5

Same procedure was followed to obtain α values with the other experiments. Results of the other experiments are shown in Appendix 1.

5.3 Calculation of thermal conductivity

With those K average values, simulations with MainFileFITCURE.m can be run. This program makes a comparison at the start of heating for curing to the end of curing period between experimental results and the model chosen. To start studying the agreement of the solution, values of K_2 (cure period) and K_3 (cool down period) were introduced in the program. The obtained solutions are going to be explained below:

The simulation, continuing with the same experiment, is going to be done with data corresponding to the experiment run in the laboratory on the 23rd of February in 2010. The model used to run the simulations were the one provided by NRC number 2. Thermo-physical parameters are to:

$$\rho_c = 1900\ [kg/m^3]$$
$$Cp_c = 1430\ [J/kg.K]$$

Equation. 69

The first figure shows the simulation corresponding to the value of thermal conductivity which belongs to curing period, $K = 0.58\ [\mathrm{w/m.K}]$.

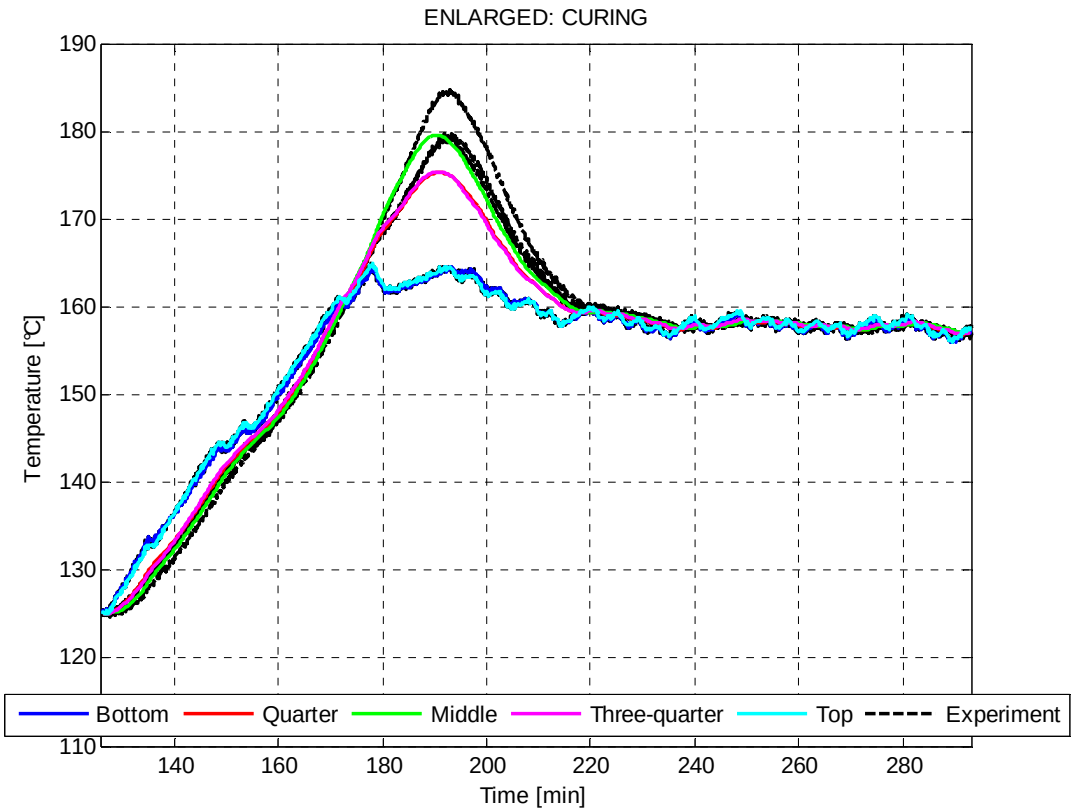

Fig. 49

As can be seen, first solution given by Matlab does not generate a well accurate solution. Peak temperature of model solution differ almost 5˚C by the experimental curve. Making the comparison with $K = 0.69\ [\mathrm{w/m.K}]$, the solution obtained appears below:

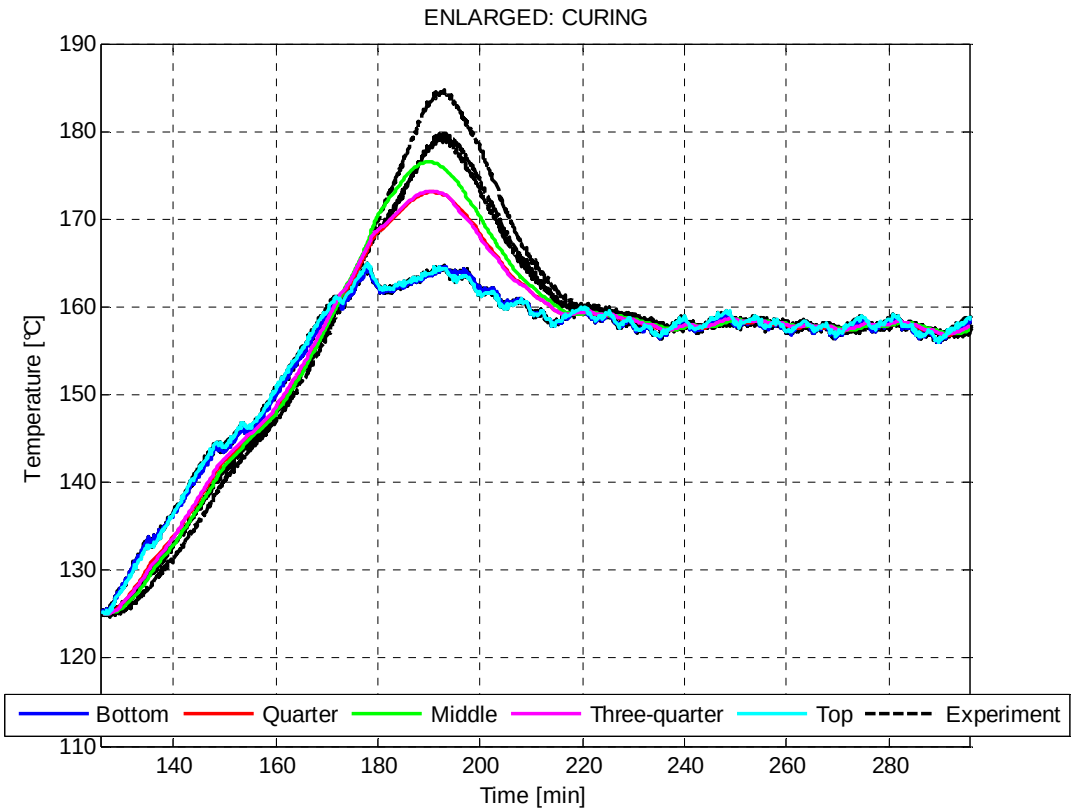

Fig. 50

Can be seen the non accurate result, obtaining a gap of 8.5˚C, which is none allowed difference for a correct simulation. With this thermal conductivity value, solution is still not well accurate. In order to find the best solution and generate the thermal conductivity value corresponding to the most accurate solution, a Matlab program was done to solve this problem. It is called MainFileFITCURE_FITK.m and makes a calculation between two thermal conductivity boundaries. Those boundaries are values obtained for curing and cool down regions. If solution does not match properly, it means that the optimum is out of those boundaries. Therefore, fittest thermal conductivity value should be evaluated along the possible range [0.4-0.7] with a gap of 0.01. Thirty points were used to make the approximation by cubic splines, and 6 time step per minute were evaluated during the calculation. For the first experiment, result appears below:

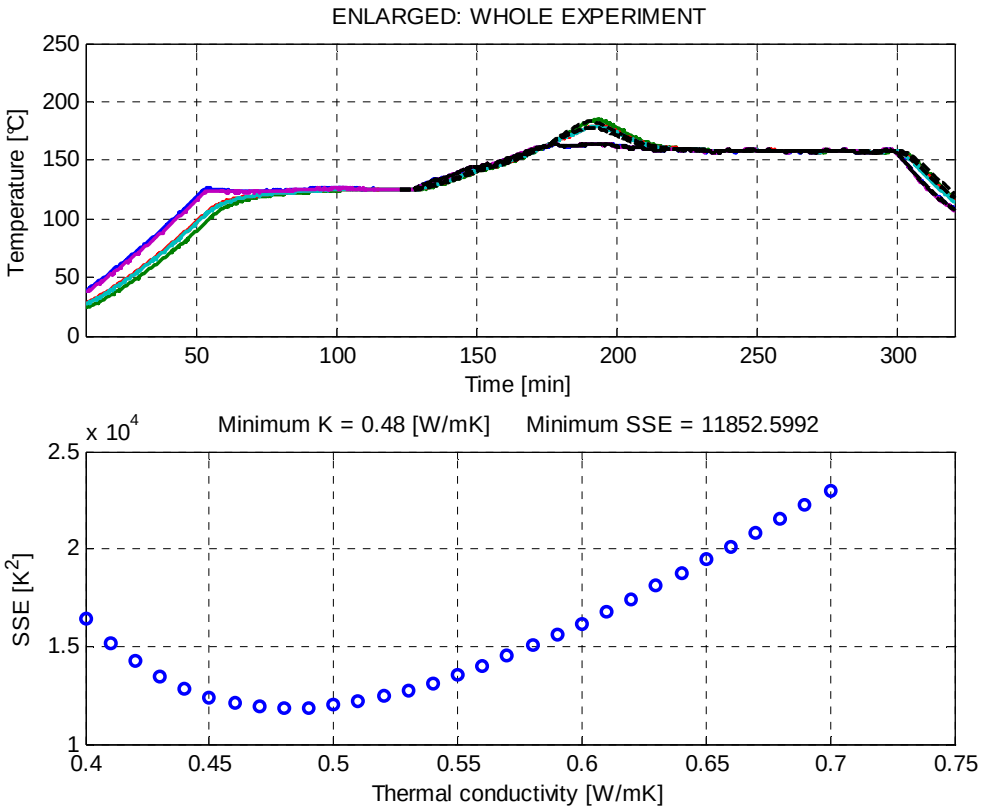

Fig. 51

Curve of error values given by the program shows the calculus of minimum value of SSE, set to 11852.5992. If we make a calculation of time steps used to obtain that result, the range of error can be evaluated. Bounds of time are 122 and 320, what is 198 minutes. Multiplied by 6 steps per minute, we obtain 1188 step times along the calculation. It can be said that there is a gap error of 1.82˚C between experimental and model curve. The thermal conductivity value is 0.48 W/mK, which is out of bounds. If the program MainFileFITCURE.m is run again with the thermal conductivity value obtained by the other one, best agreement is obtained in the solution.

Continuing with the fittest solution, following figure shows the evolution of degree of conversion along the time. The slope starts at 165 min, which correspond with the initial of curing period starts at zero, that initial value is not real and will be changed to a more accurate value in the following Matlab file.

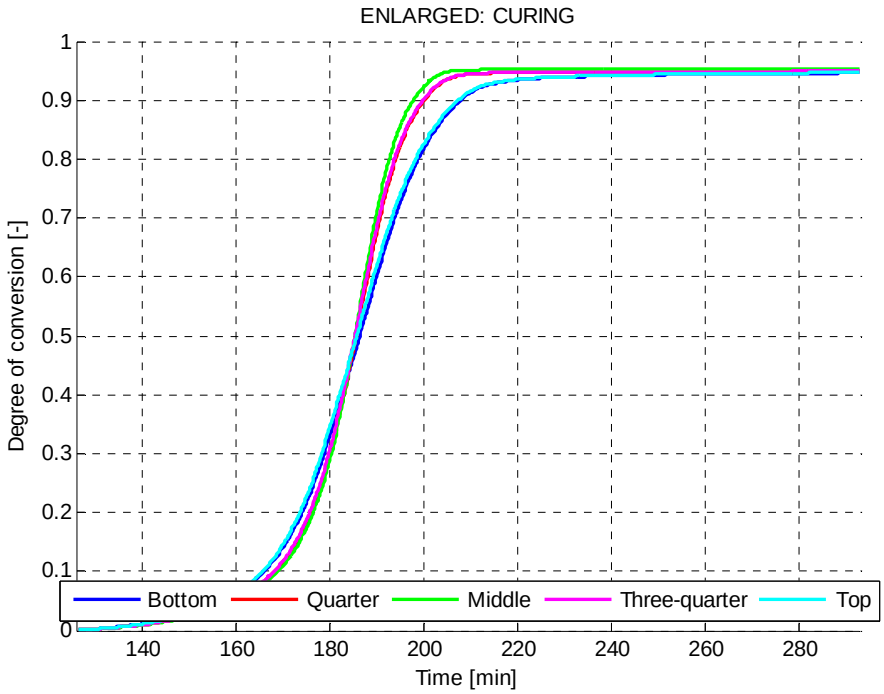

Fig. 52

On the following picture the evolution of degree of conversion along the time can be seen. It starts at zero, that initial value is not real and will be changed to a more accurate value in the following Matlab file.

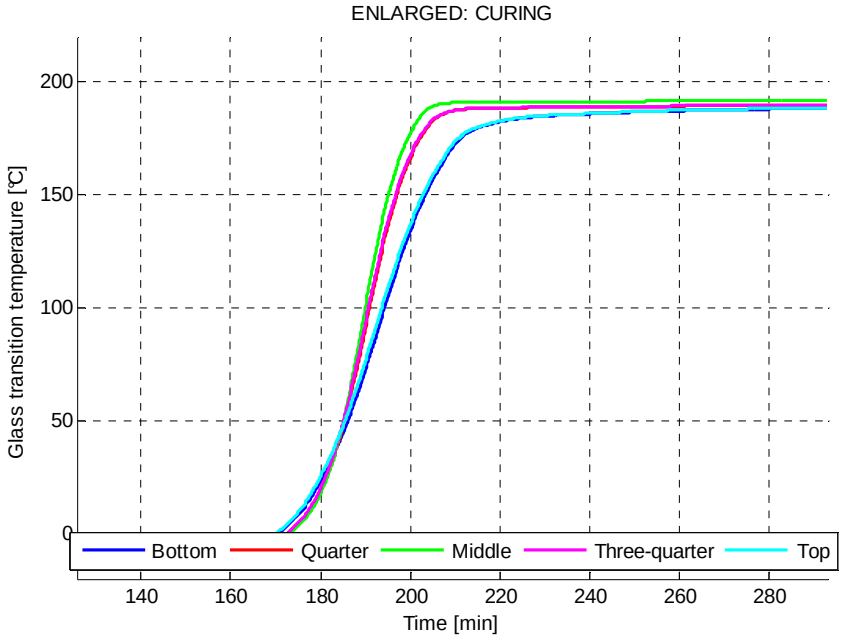

Fig. 53

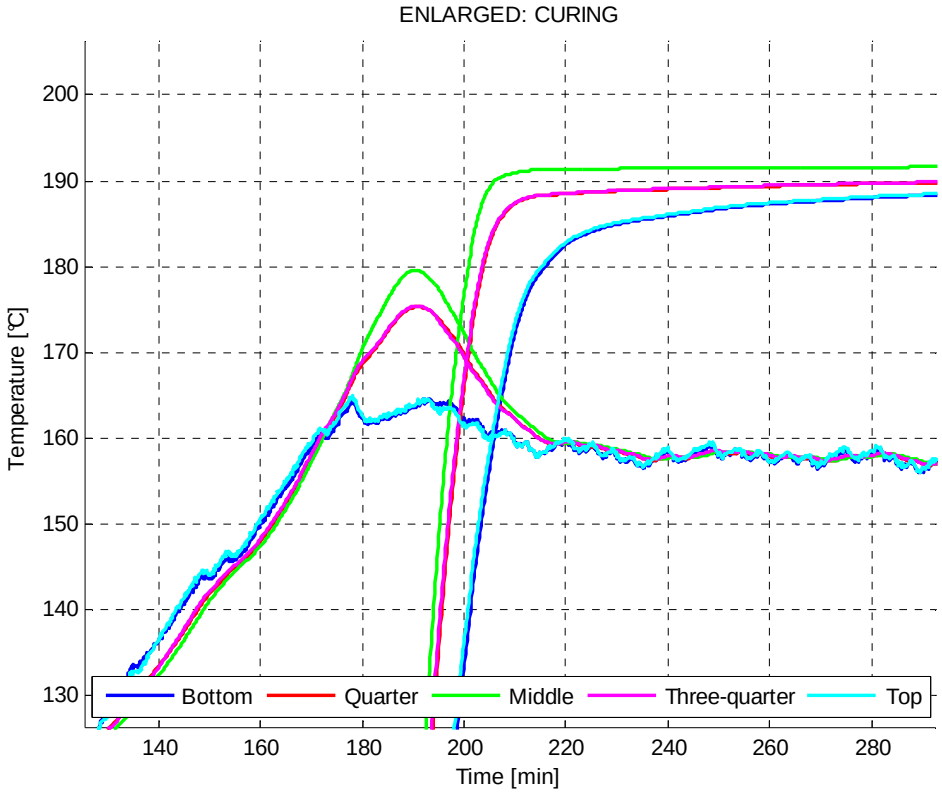

Fig. 54

Same procedure was followed to obtain fittest K values on each experiment. Results of the other experiments are shown in Appendix 2.

The following table collects thermal conductivity values obtained in all the experiments after its evaluation with the Matlab program MainFileFITCURE_FITK.m:

Experiment	Fittest K	Minimum SSE	Start point of calculation	End point of calculation	Cure Temperature
090717	0.4	15641.0702	86	338	160
091029	0.5	14510.6747	132	620	160
091104	0.52	22309.5979	120	332	180
091110	0.63	11067.3135	150	478	140
091202	0.31	14238.5947	100	377	140
100210	0.46	3368.8942	135	463	160
100216	0.47	8104.3006	184	376	160
100223	0.48	11852.5992	122	320	160

Table. 6. Fittest thermal conductivity of the composite.

The average obtained to find the most accurate thermal conductivity K value is $K=0.47125\ [W/mK]$, and its standard deviation is 0.092340596. The majority of those values are in a range of values between 0.4 and 0.5, only 2 are out of these boundaries.

5.4 Effect of Cure Cycle in thermal conductivity calculation

The Manufacturer's Recommended Cure Cycle (MRCC) corresponds to the following temperature and time values: It starts at 120 ℃, there is a ramp with positive slope which belongs to the heating up step. Temperature reaches 160 ℃ and holds for a plateau of 75 minutes. Then, the cool down starts to reach 120 ℃ again. The following figure shows the profile te mperature explained before:

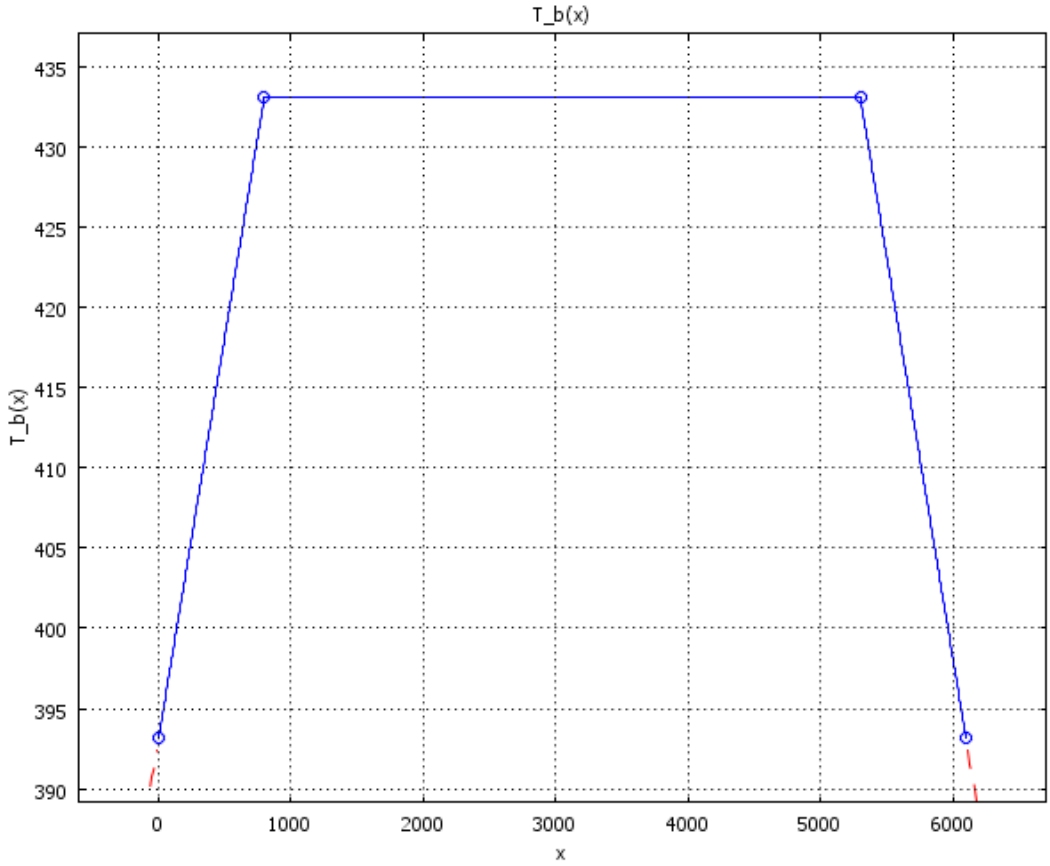

Fig. 55. Manufacturer Recommended Cure Cycle (MRCC)

The following figures gives the main points of the configuration of each experiment run at the laboratory:

Experiment	Start point of calculation	End point of calculation	Cure Temperature [˚C]	Heat Rate [˚C/min]	Post Curing	K (curing period) [W/mK]	K (cool down period) [W/mK]
090717	86	338	160	3	YES	0.46	0.42
091029	132	620	160	3	YES	0.54	0.87
091104	120	332	180	1	YES	0.59	0.74
091110	150	478	140	3	YES	0.61	0.75
091202	100	377	140	3	YES	0.33	0.73
100210	135	463	160	1	YES	0.69	0.54
100216	184	376	160	1	NO	0.68	0.64
100223	122	320	160	1	NO	0.58	0.69

Table. 7. Cure Cycles.

In order to verify obtained values for the thermal conductivity of the composite and the study of the effect of cure cycle on its calculation, the following figure shows the thermal conductivity values distribution related to the cure cycle used to run the experiment:

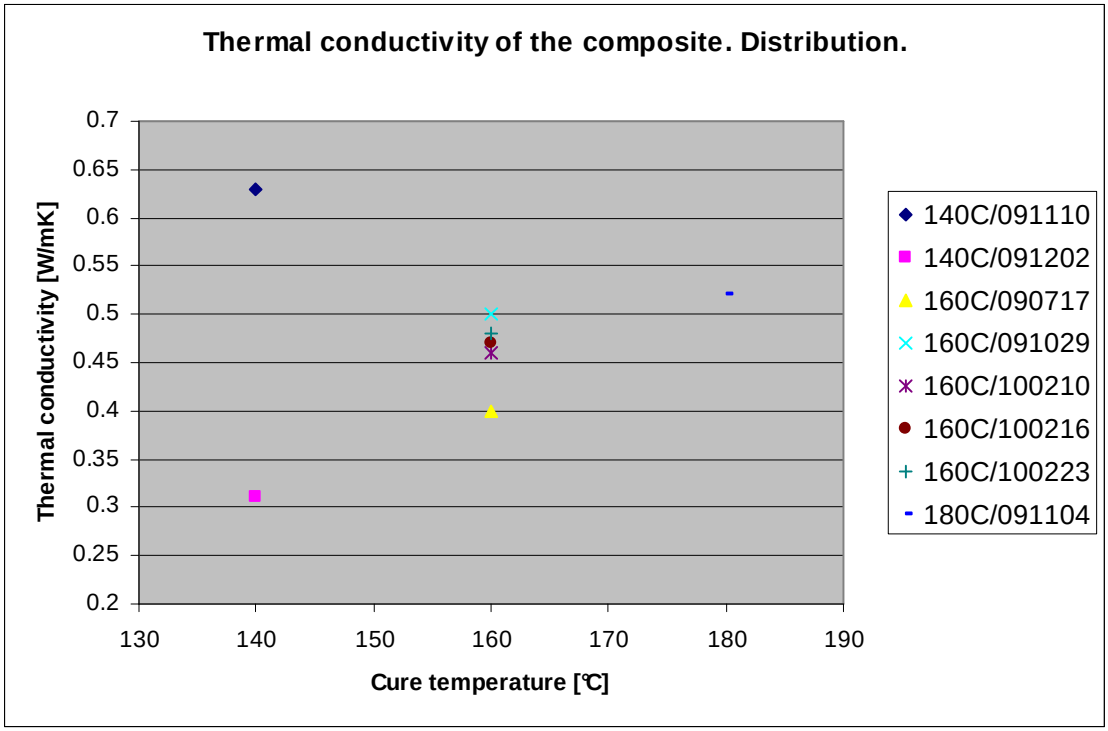

Fig. 56. Distribution of thermal conductivity values for composite material.

It can be seen that, values of thermal conductivity obtained in experiment with cure temperatures of 160℃ yields values between an acceptable ranges (0.4-0.5).

Excluding the value obtained on the experiment 091110, thermal conductivity value tends to increase with the increment of cure temperature. Therefore, it can

be said that the thermal conductivity calculated has higher values with higher temperatures in the flat part of the mould profile temperature.

6 Modelisation and its results

Software COMSOL Multiphysics gives the platform to create models to simulate the RTM manufacturing process. Introducing the model and the equations for the resin kinetics and the curing process, a solution can be obtained.

6.1 One dimension (1D)

The study of simulation starts with the one dimension model. Here, the thickness can be evaluated in an infinite beam. Thermo physical parameters need to be introduced as values by the program. The following table shows those values:

rho_f	2560	Fibre density [kg/m3]
cp_f	830	Fibre heat capacity [kg/m3]
FVF	0.56406	Fibre Volume Fraction []
rho_m	1040	Matrix density [kg/m3]
cp_m	2200	Matrix heat capacity [kg/m3]
MVF	(1-FVF)	Matrix Volume Fraction
k_c	0.47125	Composite thermal conductivity
Hu	4.29E+05	Heat of reaction

Table. 8

For the 1D model, the influence of the variation of matrix volume fraction (MVF) and thickness wants to be evaluated.

6.1.1 Influence of MVF

To study the influence of MVF in the profile temperature along the thickness of the plate, correct thermo physical parameters need to be obtained. MVF value is related to the thermal conductivity of the composite material; therefore, a non-fixed k_c is necessary to study the process for different MVF. As can be seen in literature review, some models were used by other researchers to obtain the thermal conductivity value of the composite. To obtain the target value, a simplex series conduction model is applied:

$$\frac{1}{k_c} = \frac{FVF}{k_f} + \frac{MVF}{k_m}$$

Equation. 70

Firstly, the program needs to calculate the thermal conductivity of the resin, k_m. Those values are introduced to obtain k_m:

$$k_f = 1.04\ [\frac{W}{mK}]$$
$$k_c = 0.47125\ [\frac{W}{mK}]$$
$$MVF = 0.43473\ [\frac{W}{mK}]$$
$$FVF = (1 - MVF)$$

Equation. 71

Value of thermal conductivity of the fibre is set comparing with other values obtained in literature review. Those were used by other research at work with glass fibre. On the other hand, thermal conductivity of the composite was obtained by experimental work at the laboratory, as well as initial MVF.

When target value is obtained, all the thermo physical parameters are set. Then, series conduction model can be applied to obtain values of thermal conductivity related to the MVF. The evaluation of MVF is in a range of fractional values between 0.3 and 0.7. The following figure shows the profile temperatures in the middle part for each values of MVF. It increases each 0.01:

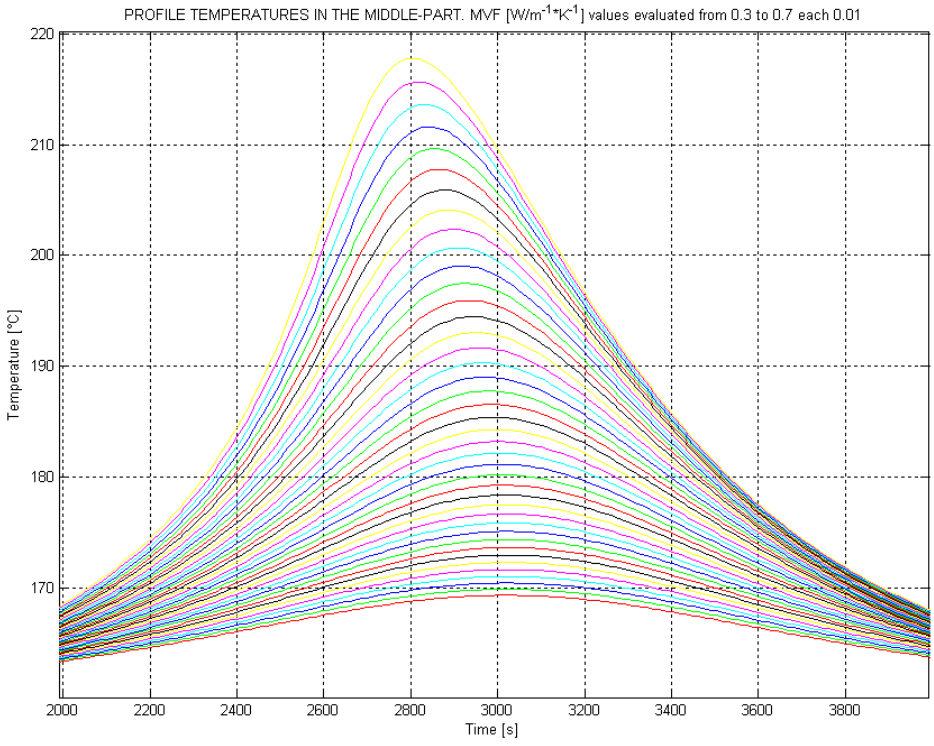

Fig. 57. Temperature overshoot during reaction.

The program calculates the peak temperature value obtained in the middle part of the thickness for a wide range of MVF values.

MVF values calculated starts at 0.3 and increases each 0.01 step to 0.7, in fractional values. Also, peak temperatures values at the time when is reached were calculated. The following table shows those values:

MVF: 0.31, $Peak_{temp}$: 169.8473°C, Time: 3030 s	MVF: 0.51, $Peak_{temp}$: 186.551°C, Time: 2990 s
MVF: 0.32, $Peak_{temp}$: 170.4148°C, Time: 3030 s	MVF: 0.52, $Peak_{temp}$: 187.7588°C, Time: 2990 s
MVF: 0.33, $Peak_{temp}$: 171.0076°C, Time: 3030 s	MVF: 0.53, $Peak_{temp}$: 189.0061°C, Time: 2980 s
MVF: 0.34, $Peak_{temp}$: 171.6248°C, Time: 3030 s	MVF: 0.54, $Peak_{temp}$: 190.2927°C, Time: 2980 s
MVF: 0.35, $Peak_{temp}$: 172.2664°C, Time: 3030 s	MVF: 0.55, $Peak_{temp}$: 191.6342°C, Time: 2970 s
MVF: 0.36, $Peak_{temp}$: 172.9324°C, Time: 3030 s	MVF: 0.56, $Peak_{temp}$: 193.0226°C, Time: 2960 s
MVF: 0.37, $Peak_{temp}$: 173.623°C, Time: 3030 s	MVF: 0.57, $Peak_{temp}$: 194.4542°C, Time: 2950 s
MVF: 0.38, $Peak_{temp}$: 174.3381°C, Time: 3030 s	MVF: 0.58, $Peak_{temp}$: 195.9327°C, Time: 2950 s
MVF: 0.39, $Peak_{temp}$: 175.0781°C, Time: 3030 s	MVF: 0.59, $Peak_{temp}$: 197.4703°C, Time: 2940 s
MVF: 0.40, $Peak_{temp}$: 175.8497°C, Time: 3030 s	MVF: 0.60, $Peak_{temp}$: 199.0557°C, Time: 2930 s
MVF: 0.41, $Peak_{temp}$: 176.6538°C, Time: 3030 s	MVF: 0.61, $Peak_{temp}$: 200.6881°C, Time: 2920 s
MVF: 0.42, $Peak_{temp}$: 177.4892°C, Time: 3030 s	MVF: 0.62, $Peak_{temp}$: 202.3794°C, Time: 2910 s
MVF: 0.43, $Peak_{temp}$: 178.3548°C, Time: 3030 s	MVF: 0.63, $Peak_{temp}$: 204.1211°C, Time: 2900 s
MVF: 0.44, $Peak_{temp}$: 179.2517°C, Time: 3020 s	MVF: 0.64, $Peak_{temp}$: 205.9116°C, Time: 2890 s
MVF: 0.45, $Peak_{temp}$: 180.1792°C, Time: 3020 s	MVF: 0.65, $Peak_{temp}$: 207.7615°C, Time: 2880 s
MVF: 0.46, $Peak_{temp}$: 181.1457°C, Time: 3020 s	MVF: 0.66, $Peak_{temp}$: 209.6625°C, Time: 2860 s
MVF: 0.47, $Peak_{temp}$: 182.1515°C, Time: 3010 s	MVF: 0.67, $Peak_{temp}$: 211.6217°C, Time: 2850 s
MVF: 0.48, $Peak_{temp}$: 183.1951°C, Time: 3010 s	MVF: 0.68, $Peak_{temp}$: 213.6368°C, Time: 2840 s
MVF: 0.49, $Peak_{temp}$: 184.2728°C, Time: 3000 s	MVF: 0.69, $Peak_{temp}$: 215.697°C, Time: 2830 s
MVF: 0.50, $Peak_{temp}$: 185.3895°C, Time: 3000 s	MVF: 0.70, $Peak_{temp}$: 217.8121°C, Time: 2810 s

Table. 9

Can be easily seen the increase of the peak temperature related to the increase of MVF value. Those increments are higher when the MVF is high. The gap starts at 0.546˚C, but can be higher than 2˚C if we compare at a MVF value of 0.69. Non-uniform increment was found on the simulation.

Maximum peak temperature is set to 217.8121˚C, which is under to overshoot limit of 220˚C. Over that limit, mould can be damaged. In that, an optimisation to reduce temperature overshoot should be necessary.

Also, the time to reach the peak temperature value becomes lower with the increase of the MVF. Reaction runs before and the maximum difference obtained is 20 seconds for each 0.01 MVF increment.

6.1.2 Influence of the thickness

For that study, the influence of the variation of thickness is going to be studied in order to find a relationship between it and peak temperatures.

Thermo physical values were introduced exactly as was explained for the previous study. The simplex series conduction model was used to obtain the thermal conductivity value of the composite material. Those values are fixed in that case, because thickness is not related to them. The following table shows the peak temperature value obtained for each simulation. The program gives a solution of the profile temperature in the middle part of the thickness, evaluated from 0.01 m to 0.1 m each 0.005 m. Maximum peak temperature overshoot was imposed at 220˚C, which is reached at 0.01 m thickness.

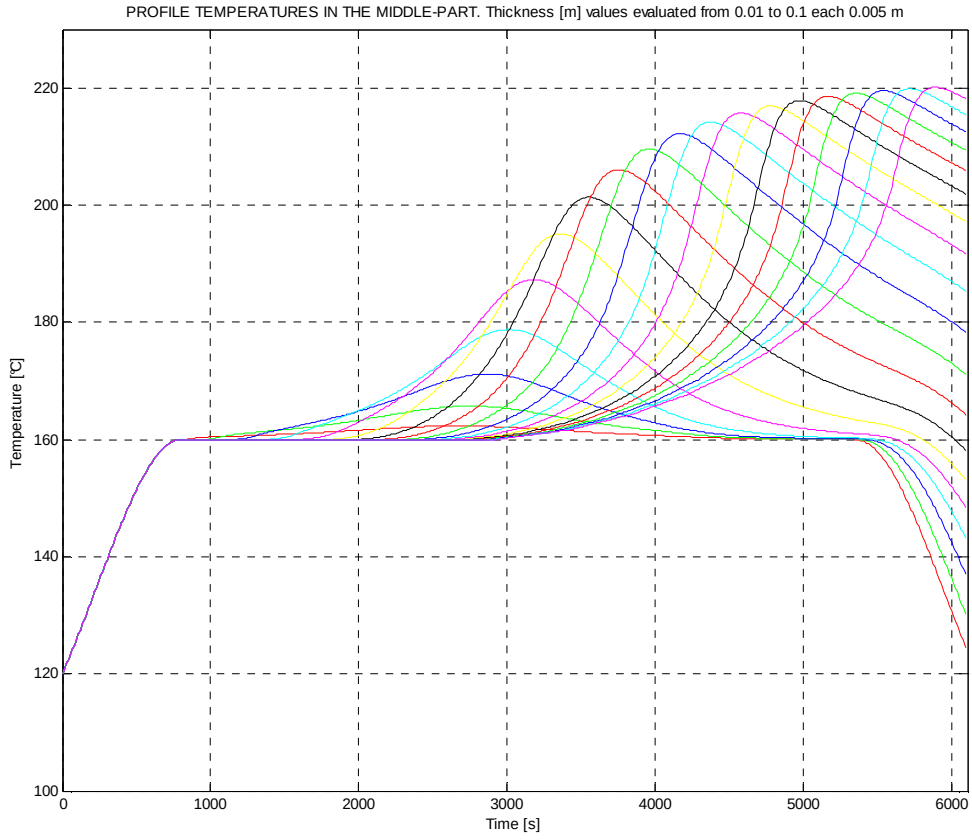

Fig. 58. Temperature overshoot during reaction.

More interesting data are given by the figure above. The peak temperature during the curing reaction is reached later when the thickness is increased. The higher the thickness, the longer the time to reach peak temperature will be. Following table shows the legend, where can be seen the peak temperature for each value and the time at maximum temperature is reached.

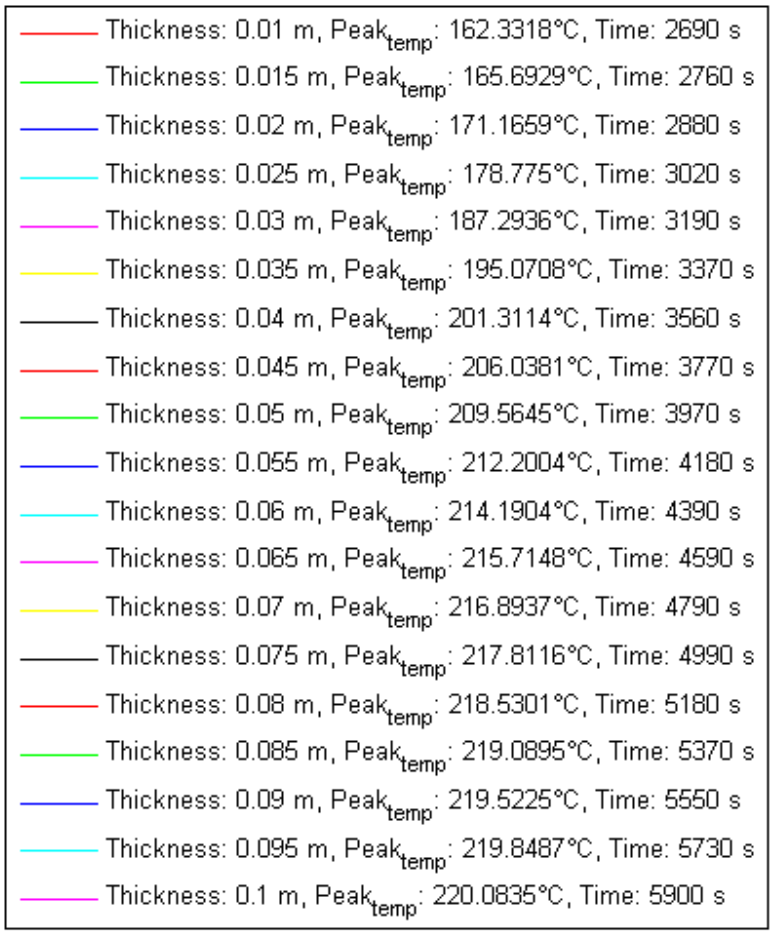

Table. 10

Making a comparison between reach times, time increases a 50% between boundary values of thickness. It means that, manufacturing time becomes longer depending on the thickness. And it is an important goal for optimisation to reduce this value.

6.2 Two dimensions (2D)

Introducing the second dimension, a cross-section of a plate can be drawn. Width and length are dimensions that take part in the study. The standard plate size is 0.3 x 0.025 [m]. Simulations were run with that size plate.

The following figure shows the appearance of the plate after its simulation in COMSOL Multiphysics.

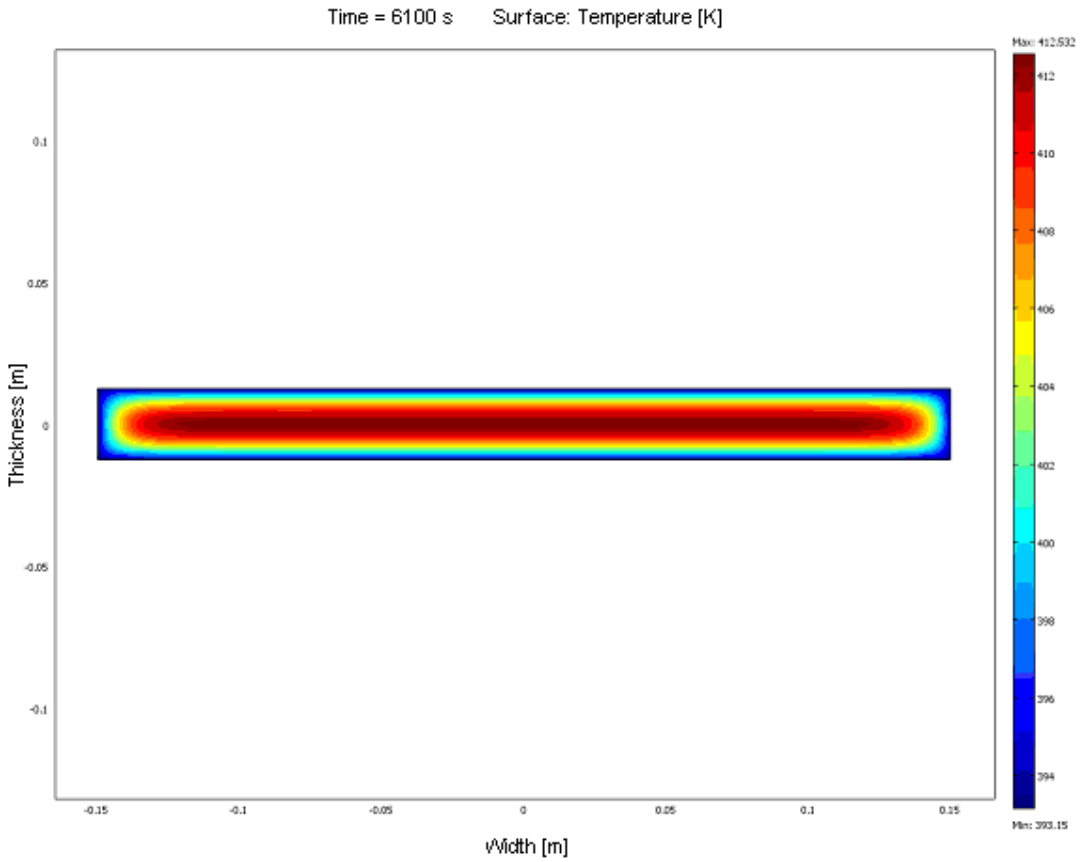

Fig. 59. COMSOL Multiphysics solution for 2D standard plate.

The color bar shows the temperature difference along the thickness. Solution at 6100 s is plotted, which is the end of the simulation. It can be seen that in the centre of the plate, maximum temperatures are registered. In the middle part of the thickness, peak temperatures are also measured.

Edge effect appears in parts closed to both limits of the plate in x axis. Temperature distributions are different depending on the distance along the x axis. Phenomena of non-uniform consolidation and temperature along the thickness need to be studied. Its relation with the thickness and curvature of the plate will be tackled.

6.2.1 Influence of edge effect

Different thicknesses are going to be evaluated to calculate edge effect distances for each plate. Its effect is going to appear and a relation between thickness and distance effect is going to be obtained, which is the target of the study.
Firstly, the calculation of it effect is focused on the comparison of the through-thickness temperatures along the x axis. The program, which calculates thermo physical parameters with the same procedure as the ones used in the one dimensional modelisations, yields the figure 16 where maximum temperature difference is 1℃.

The model used for the calculation of thermal conductivity of the composite was a parallel distribution conduction model, given by the following equation:

$$k_c = (k_{fL} * FVF) + (k_m * MVF)$$

Equation. **72**

Where k_{fL} is longitudinal thermal conductivity of the fibre. It is comparable with the simplex rule of mixture, and is going to generate higher values of peak temperature. The series conduction model is used to find the lower limit to start the calculation of the educated value.

This boundary gives the start of the edge effect, where one dimensional solution can not be extrapolated to the 2 dimensional plates.

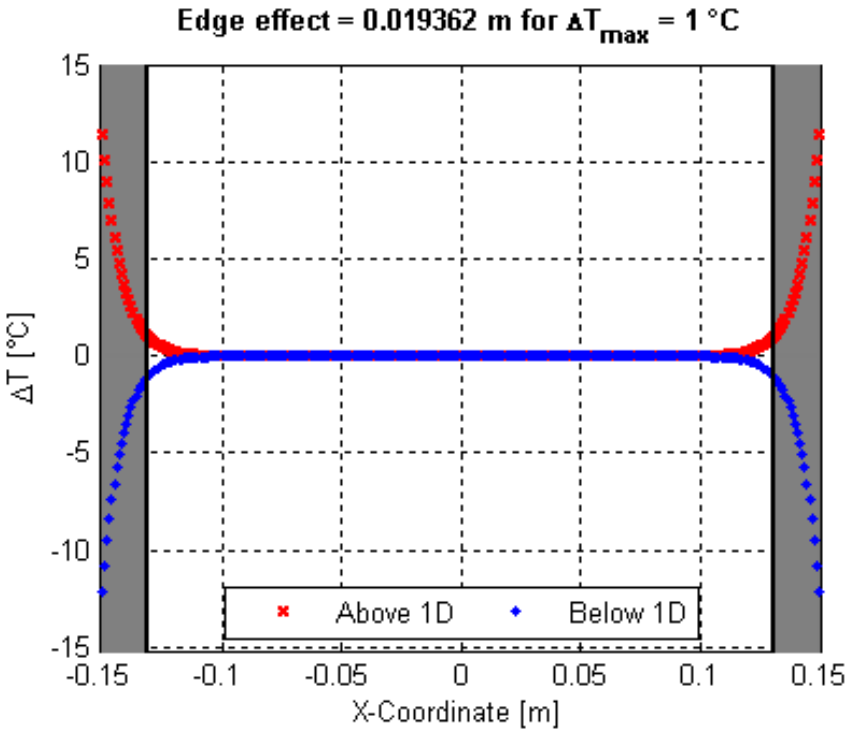

Fig. 60. Bandwidth analysis.

Those 2 lines give the temperatures of the 2 dimensional solutions compared with the one dimensional. Depending on the step of the profile temperature, 2 dimensional temperatures can be above or below one dimensional profile. The biggest difference gives the point at the effect starts. This solution is for a standard 25 mm thickness plate. Also, maximum temperature appears at the centre of the plate. That phenomenon can be seen in the following figure, where X mark shows exactly the point where maximum temperature is registered.

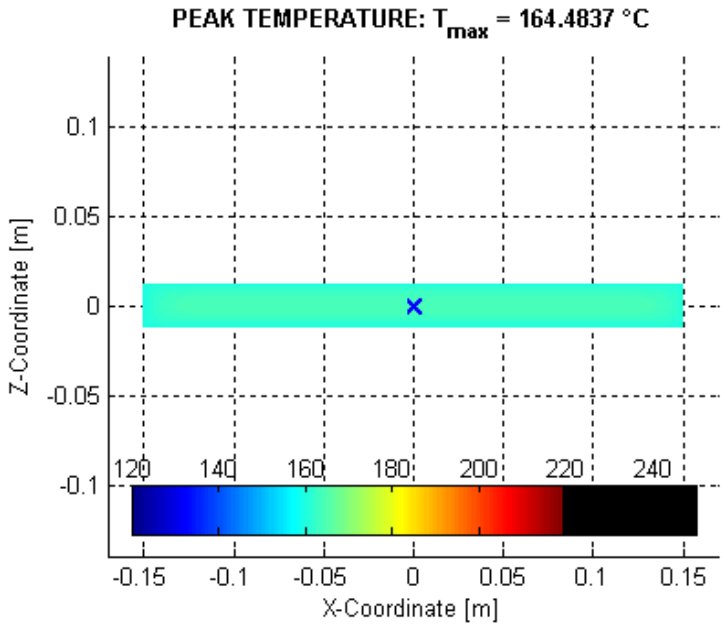

Fig. 61. Peak temperature.

For a range of thickness values from 0.01 m to 0.1 m each 0.01 m, edge effect was studied in order to obtain the relation between thickness and distance of influence.

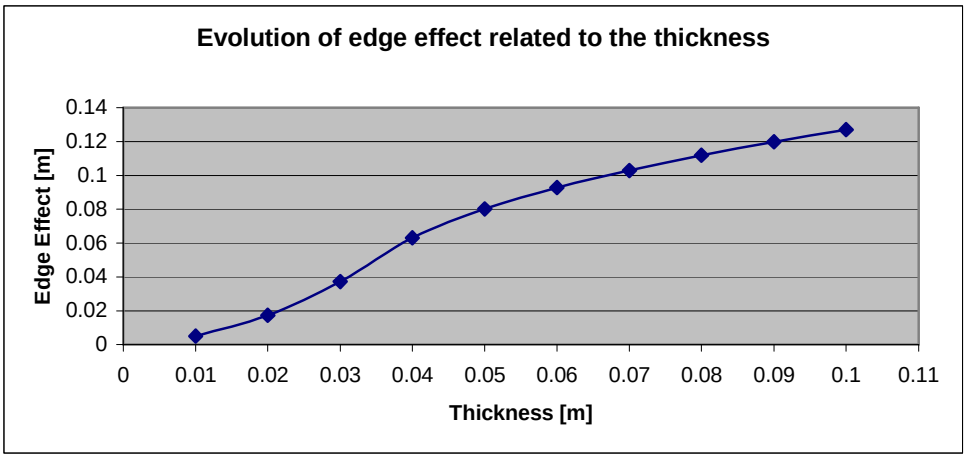

Fig. 62

And the table of values appears below:

Edge Effect [m]	Thickness [m]
0.0050014	0.01
0.017351	0.02
0.037317	0.03
0.06313	0.04
0.080199	0.05
0.092707	0.06
0.10301	0.07
0.11193	0.08
0.11981	0.09
0.12701	0.1

Table. 11

The increment in the plate thickness maximizes the edge effect, it means, the distance at its effect starts is higher. This increment is related to the temperature overshoot measured during the process. In the following table appear the values of peak temperatures registered on each simulation. Those can be compared with the ones obtained during the one dimensional model study, where a different equation where used to calculate the thermal conductivity of the composite. Here, $k_m = 0.2834\ [\frac{W}{mK}]$ and $k_c = 0.71\ [\frac{W}{mK}]$.

Peak Temperature [°C]	Thickness [m]
162.2796	0.01
170.888	0.02
186.872	0.03
201.6508	0.04
211.0877	0.05
216.8091	0.06
220.3601	0.07
222.6141	0.08
224.0316	0.09
224.8814	0.1

Table. 12

6.2.2 Influence of curvature

In order to obtain the influence of curvature in the manufacturing process of the plate, a range of different values of radius were studied and its effect. To tackle the problem, the cross-section of a circular plate was modeled with an axis of symmetry. The width, height and radius are input parameters. A range of values for radius were evaluated to calculate the peak temperature. Calculations where done with the standard size plate 0.3 x 0.025 [m], starting with a radius value of 0.01 m to 0.95 m each 0.05 m. The following table shows the peak temperature values obtained on each simulation in the middle part of the curved plate. Maximum temperature difference registered is under 1℃.

Peak Temperature [°C]	Radius [m]	Peak Temperature [°C]	Radius [m]
179.5818	0.01	178.7694	0.5
178.821	0.05	178.7692	0.55
178.7866	0.1	178.691	0.6
178.7775	0.15	178.69	0.65
178.7739	0.2	178.7689	0.7
178.772	0.25	178.7688	0.75
178.771	0.3	178.7688	0.8
178.7704	0.35	178.7687	0.85
178.7669	0.4	178.7687	0.9
178.7696	0.45	178.7687	0.95

Table. 13

Making a comparison of the boundary values of radius, for a value of 0.01 m, which is the lowest value evaluated, a big difference between one dimensional model and two dimensional curved model can be found. The following figure compares values obtained for both simulation and plots it along the through-thickness.

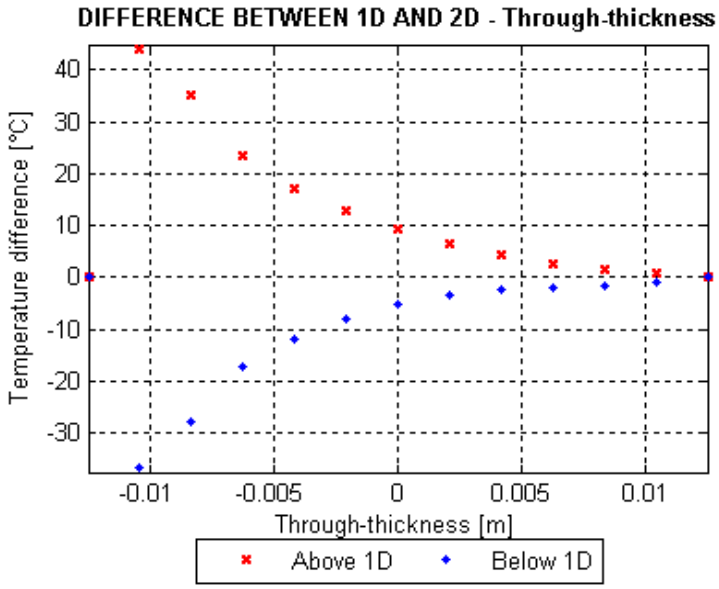

Fig. 63

Evaluating from the inner part to the outer wall of the ring, the difference becomes lower. In the internal wall of the ring the most difference can be found. On the other hand, evaluating the biggest radius, the following figure shows that in the parts closed to the boundaries there is no big difference. Temperature variation appears in the middle part. Simulations were run in a standard plate 0.3 x 0.025 [m].

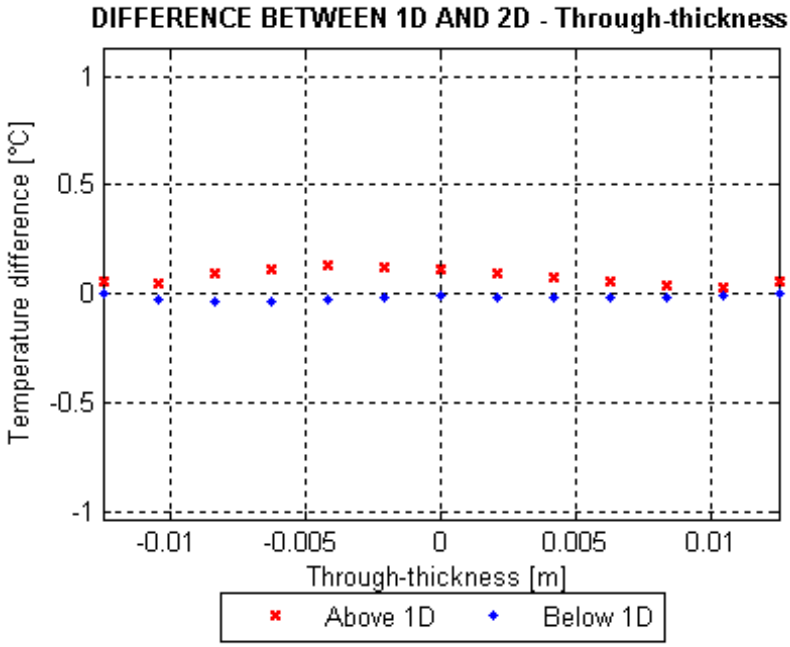

Fig. 64

6.2.3 Influence of edge effect in curved parts

Last part of the study for the two dimensional case is focused on the study of the edge effect plus the curvature. For that case, a different procedure was followed to study the edge effect in boundaries. Because of the plate which is focus of study is an infinite plate, boundaries do not show edge effect. Therefore, is not possible to study comparing profile temperature along the through-thickness in the x axis of the two dimensional solution.

The focus of the comparison is the peak temperature distribution in the through-thickness along the experiment. It can be seen how maximum values are reached before or after in comparison with the one dimensional solution. The procedure is going to be explained: For the one dimensional solution, peak temperatures were recorder along the thickness line. The following figure shows the 15 measurement points distribution:

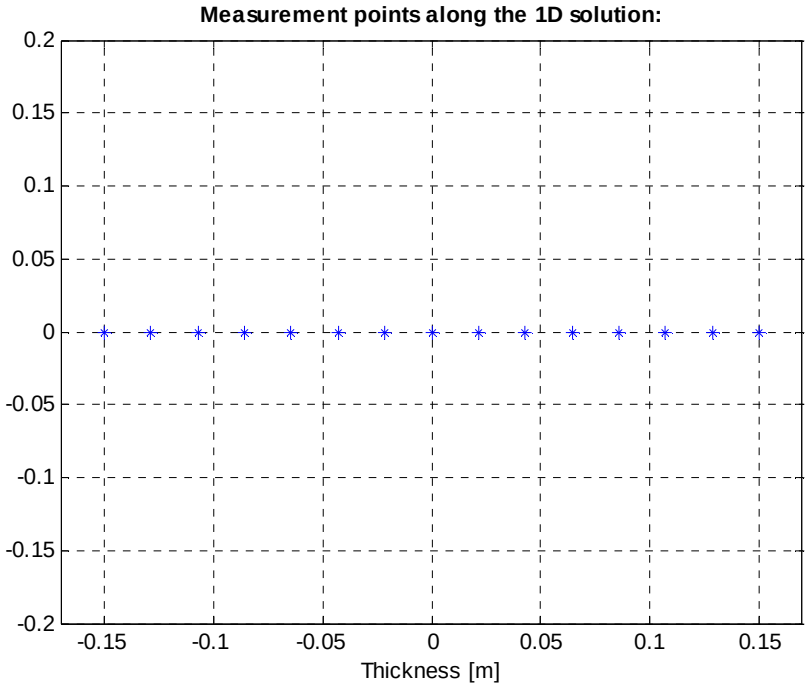

Fig. 65

The one dimensional symmetrically profile temperature differ with the two dimensional distribution. For the two dimensional solution, the measurement points are placed along its through-thickness.

The width, height and radius are input parameters. A range of values for radius were evaluated to calculate the peak temperature. Calculations where done with

the standard size plate 0.3 x 0.025 [m], starting with a radius value of 0.01 m to 0.95 m each 0.05 m.

The model used for the calculation of thermal conductivity of the composite was a parallel distribution conduction model, given by the following equation:

$$k_c = (k_{fL} * FVF) + (k_m * MVF)$$

Equation. 73

Where k_{fL} is longitudinal thermal conductivity of the fibre. It is comparable with the simplex rule of mixture. The other thermo physical parameters were calculated at the start of the program on the same procedure as the ones used in the one dimensional modelisations.

The next figure shows the temperature distribution for the one dimensional solution and the two dimensional solution for a radius value of 0.05 m. The lower the radius, the larger the difference.

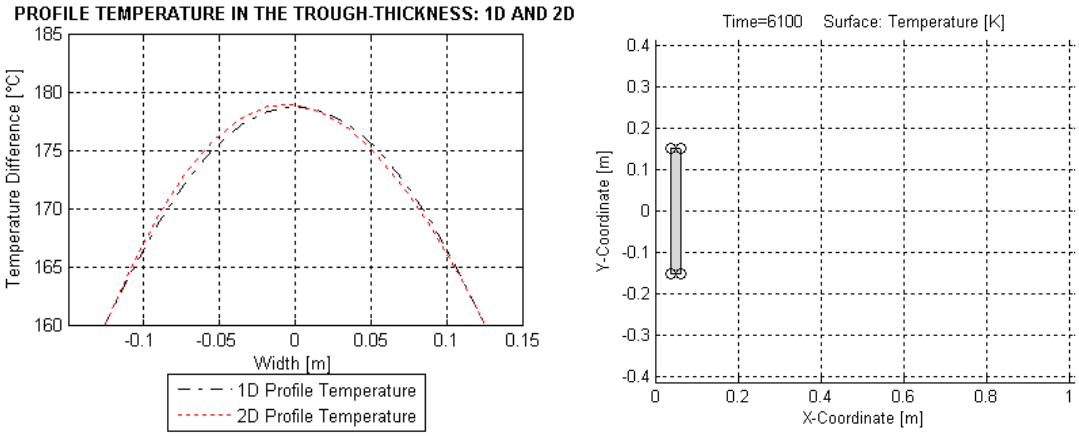

Fig. 66

Can be seen, that on the left side of the thickness (inner radius side of the curved part), profile temperatures that belong to the two dimensional solution are higher than in the one dimensional distribution. If the evaluation moves along the through-thickness to the outer radius, one dimensional temperature distributions become higher than the two dimensional temperatures. The evaluated shape is figured on the right. The following figure shows the difference on each measurement points along the through thickness:

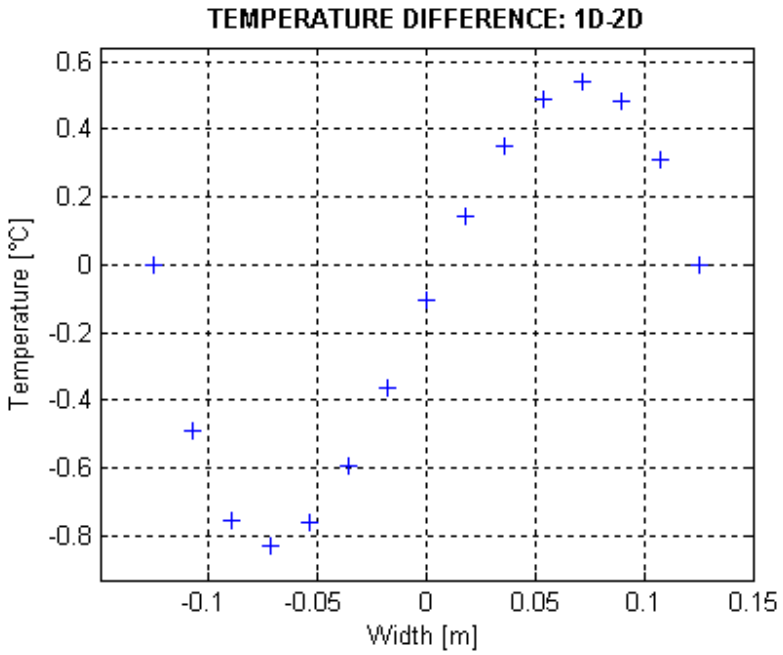

Fig. 67

Those points are the difference the two solutions, one and two dimensional simulations. The following vector yields the values in ℃:

X-axis [m]	-0.0125	-0.0107	-0.0089	-0.0071	-0.0054	-0.0036	-0.0018	0.0000
Temperature difference [℃]	0.0000	-0.4900	-0.7541	-0.8299	-0.7625	-0.5938	-0.3624	-0.1057
X-axis [m]	0.0018	0.0036	0.0054	0.0071	0.0089	0.0107	0.0125	
Temperature difference [℃]	0.1407	0.3483	0.4886	0.5413	0.4823	0.3076	0.0000	

Table. 14

To show the influence of increasing the radius in the temperature difference, some solutions of different comparison are going to be simulated:

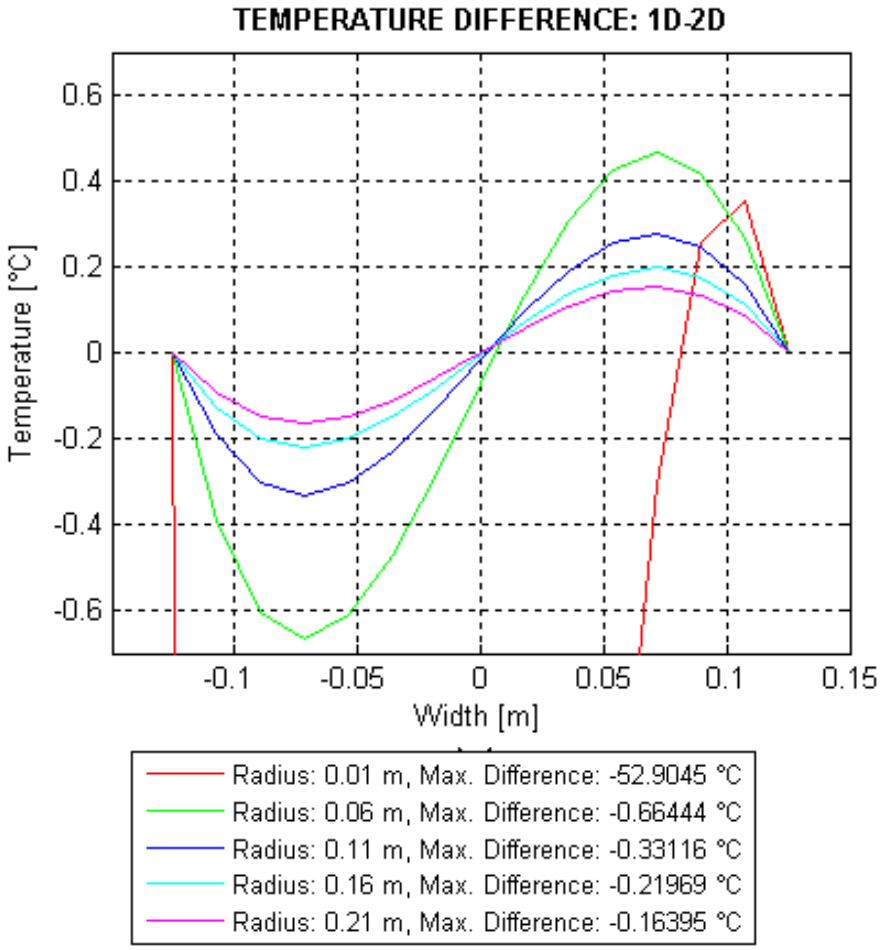

Fig. 68. Temperature difference for values between 0.01 to 0.21 [m] each 0.05 [m]

Temperature differences decrease when the plate reduces its curvature, cause becomes more similar to a flat plate. Red line belongs to a radius value of 0.01, which a maximum difference of 52.9045℃. We are eva luating a disc with an inner diameter of 0.02 m, which is significantly small. Next radius values have quite lower differences, for example, from 0.06 to 0.21 m.

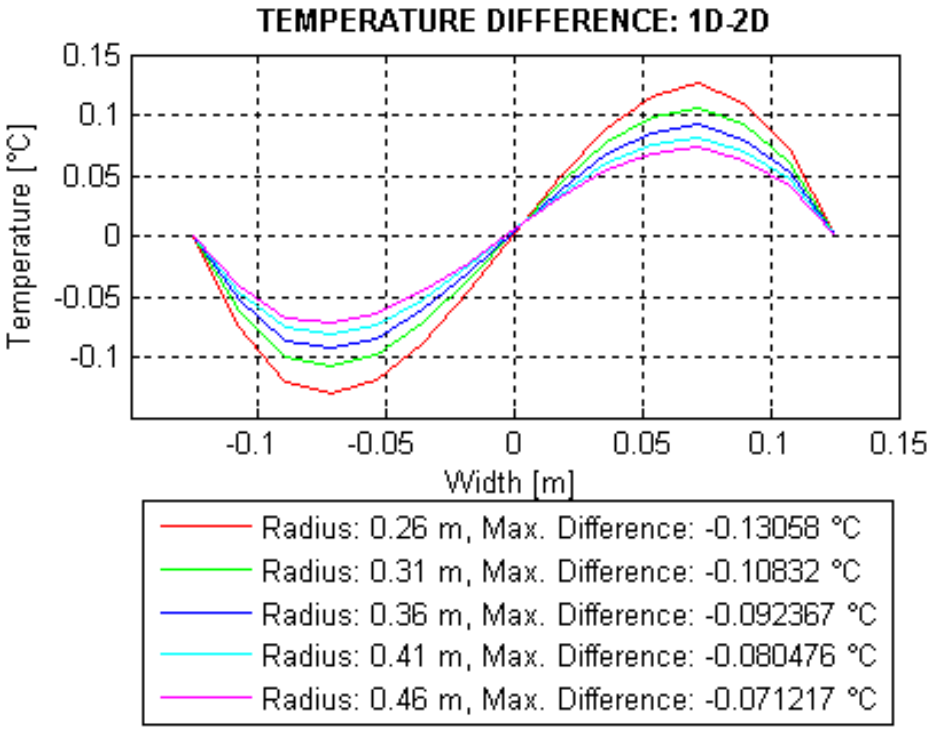

Fig. 69. Temperature difference for values between 0.26 to 0.46 [m] each 0.05 [m]

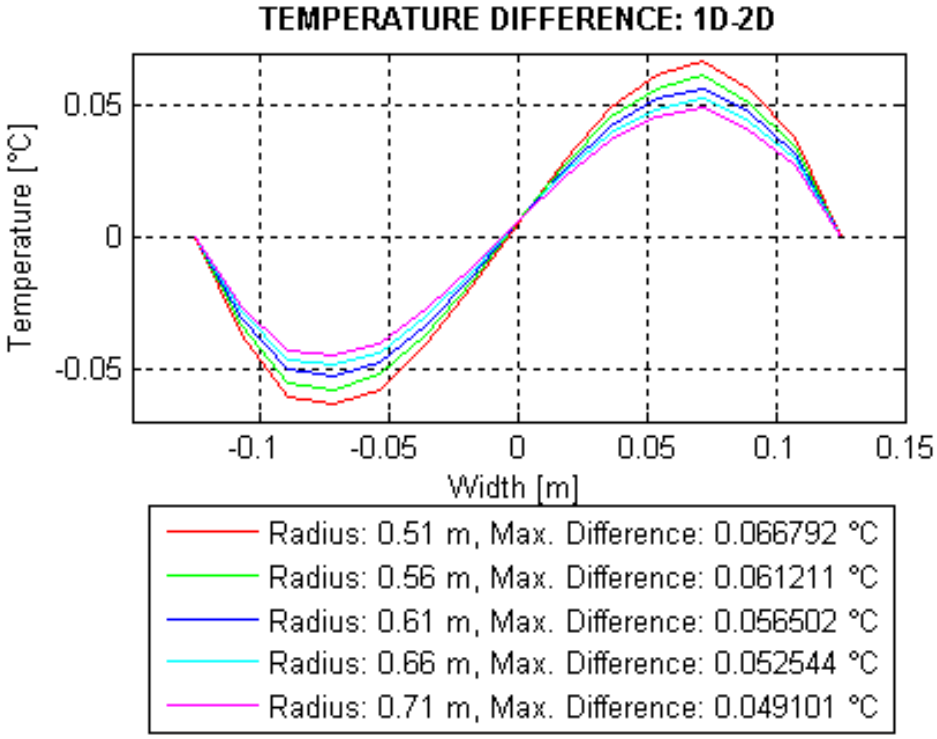

Fig. 70. Temperature difference for values between 0.51 to 0.71 [m] each 0.05 [m]

As it can be seen, maximum difference values now appear closed to the outer radius.

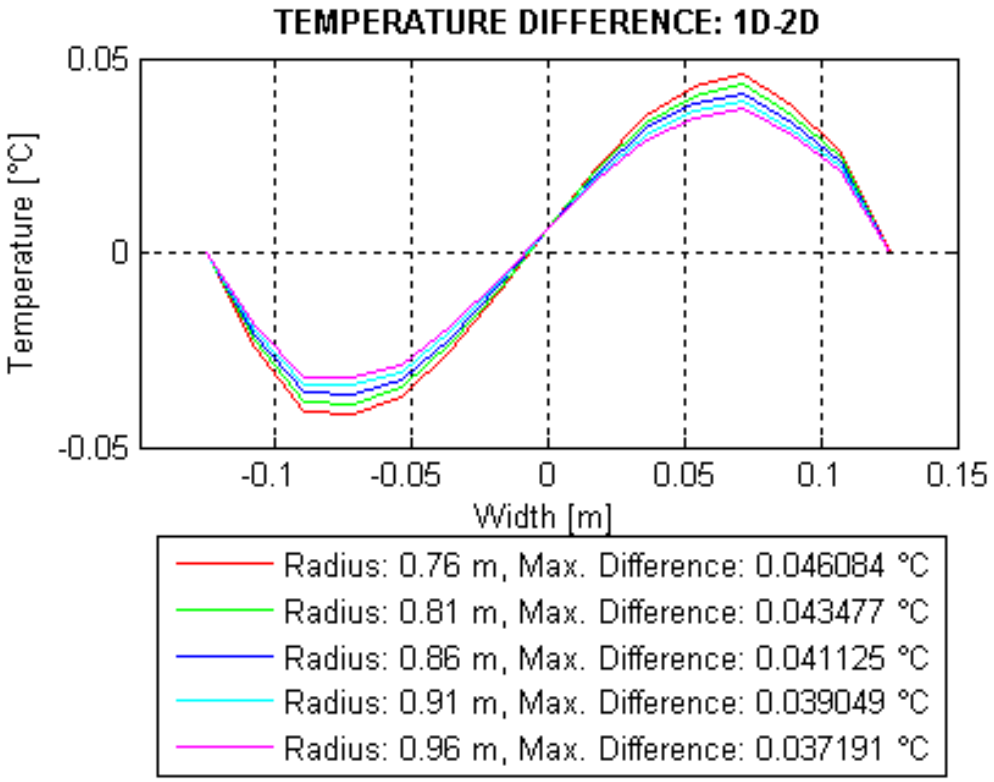

Fig. 71. Temperature difference for values between 0.76 to 0.96 [m] each 0.05 [m

6.2.4 Influence of cure cycle

Simulations run before were done under manufacturer recommended cure cycle. In order to study the influence of the cure cycle used on the experiment, some experiments were run with different cure cycles. The implemented cycles are the followings:

- varying the slope: 1℃/min, 3℃/min and 10℃/min.
- varying the cure temperature: at 140℃, 160℃ and 180℃.

Introducing a variation in the first slope of the profile temperature, the following results are obtained. The values of heat rate used for those experiments are: 1, 3, 5, 8 and 10℃.

Peak temperatures and edge effects distances were compared for each value of heat rate. The following figure shows the values of the peak temperature related to the range of slope values:

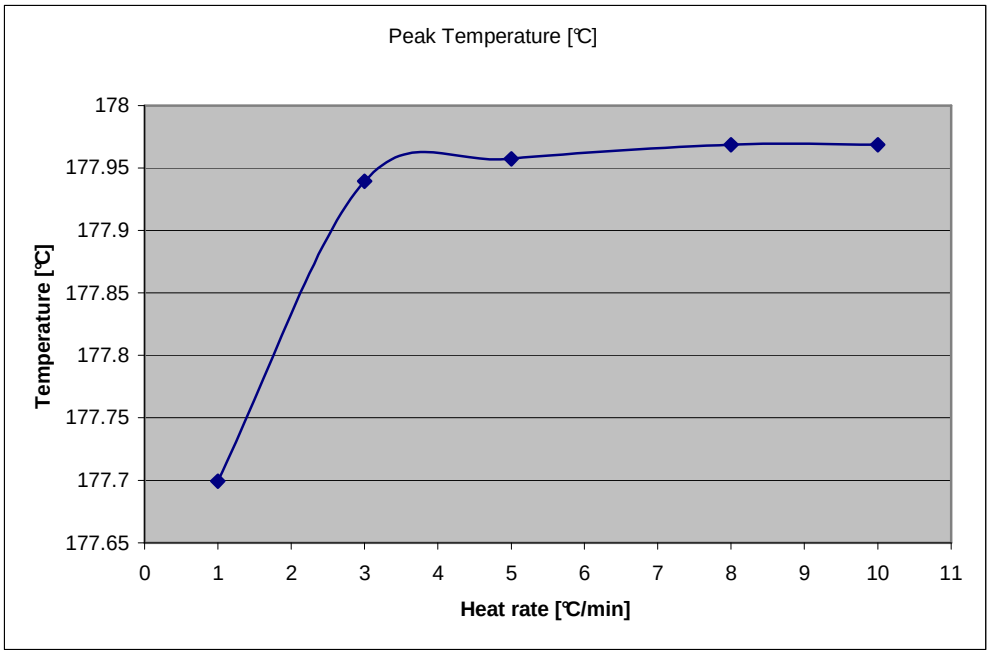

Fig. 72. Peak temperature values with heat rate variation

There is no big variation in peak temperature; the maximal difference between maximum and minimum value is around 0.2℃. Peak tem perature is the overshoot increases with the increment of the heat rate.

The following figure shows the variation in the edge effect:

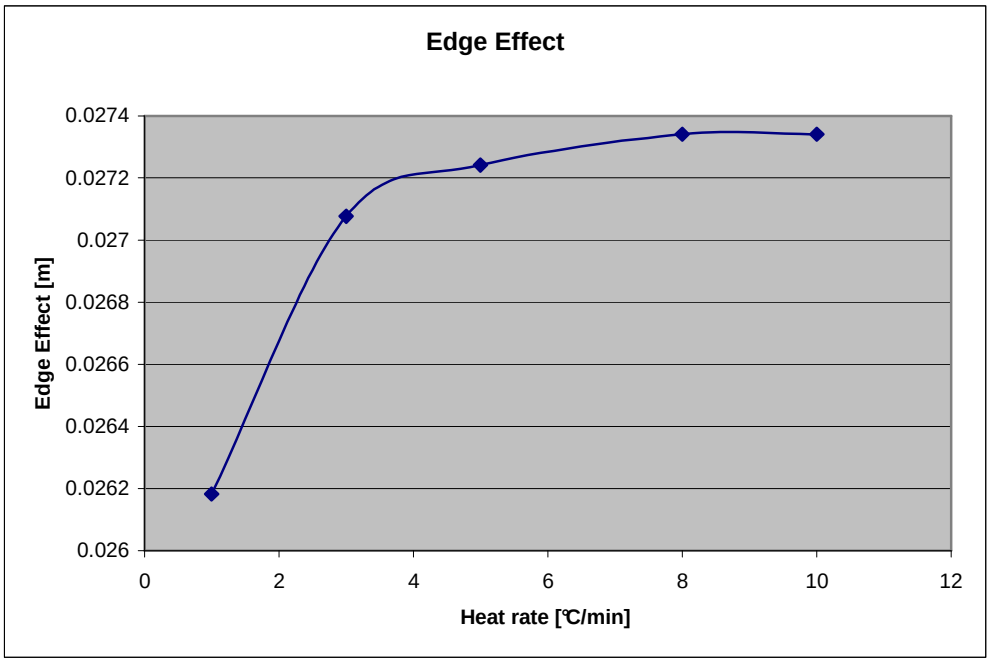

Fig. 73. Edge effect values with heat rate variation

On the figure above, a similar variation can be seen. Edge effect distance increases with the heat rate applied on the experiment. For maximal values of heat rate, highest values of edge effect are registered.

To study the variations related to the cure temperature. Some simulations were run. The temperature values used to run it are: 140, 150, 160, 170 and 180℃. The following figure shows how the peak temperature increases:

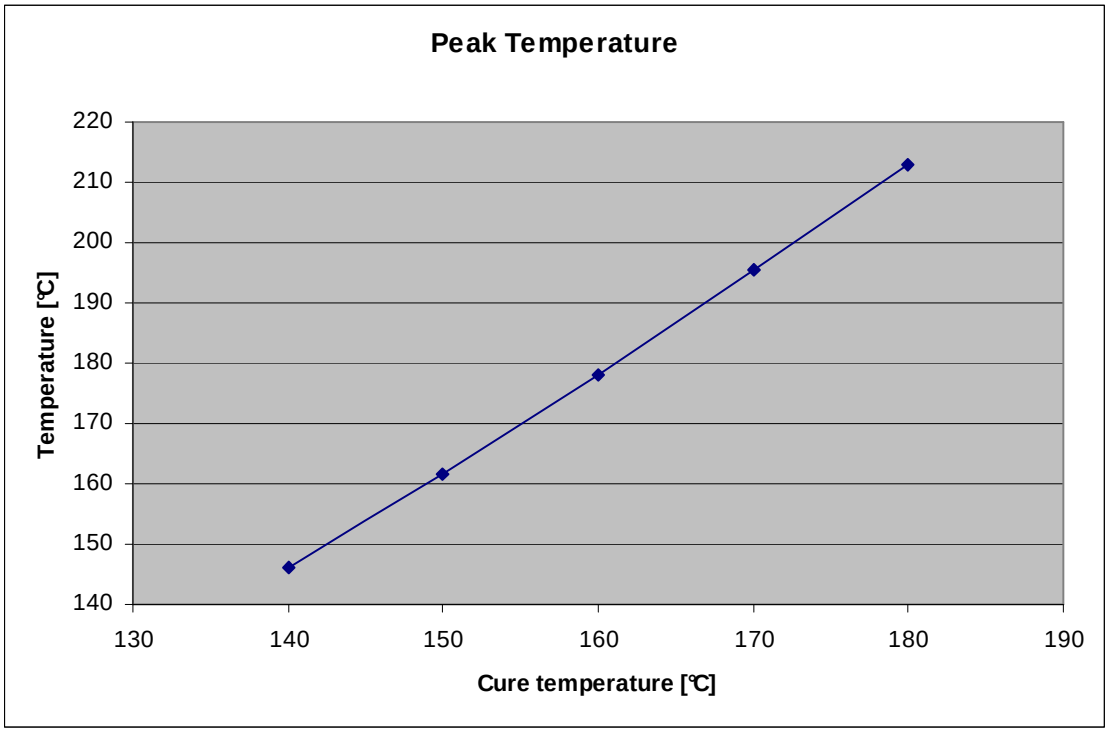

Fig. 74. Peak temperature values with cure temperature variation

The figure shows how the peak temperature increases related to the cure temperature variation. Highest values are obtained at 180℃ cure temperature.

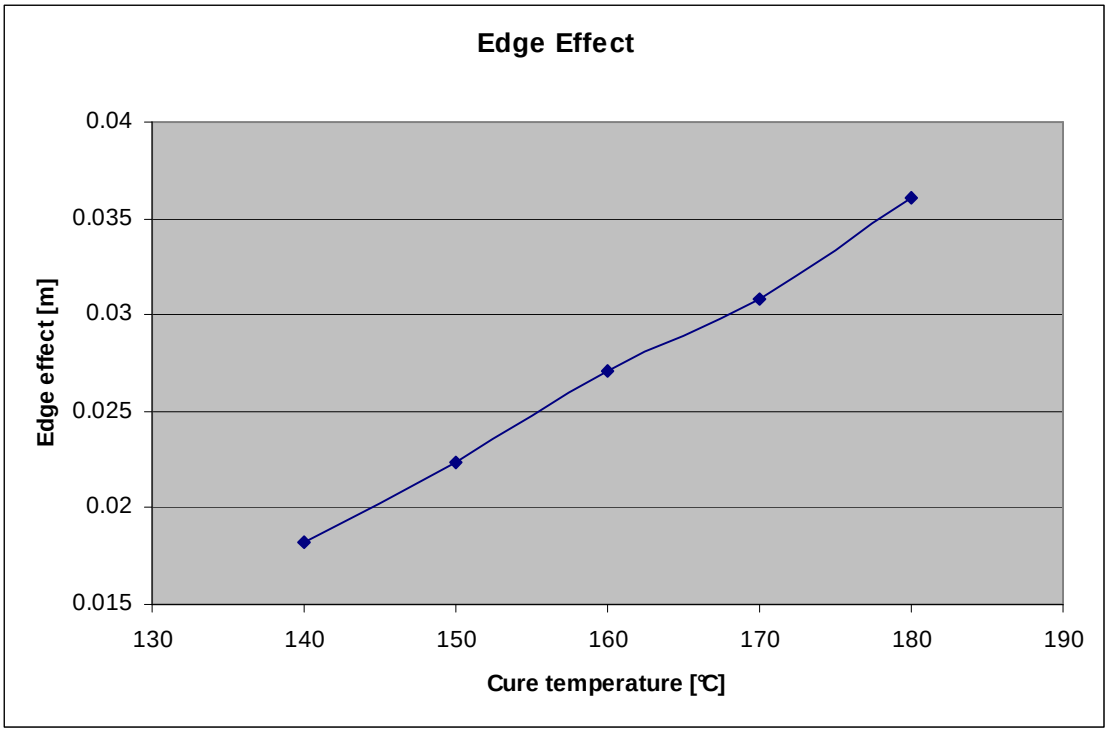

Fig. 75. Edge effect values with cure temperature variation

As was seen in the previous figure, a linear increment of edge effect can be seen on that experiment. Maximum values of edge effect appear on experiment run at 180℃ cure temperature.

6.2.5 Influence of thermal conductivity ratio

As it was explained in previous chapters, there is no isotropic thermal conductivity in a composite part. This assumption should be taken in account in order to calculate correctly the heat transfer along the through-thickness or along the x axis. The following equation relates transverse thermal conductivity and longitudinal thermal conductivity, and gives a value. This ratio is going to be studied in a range of values to obtain knowledge about the influence in edge effect and peak temperature.

Range of values starts at 0.1 to ∞. Maximum value of ratio was set helped by the limit 0.035 $[W/mK]$ obtained in literatures, which is 0.052 $[W/mK]$ corresponding to a ratio of 20. The following figure shows how the edge effect distance increases with the ratio. It means that, transverse thermal conductivity decreases:

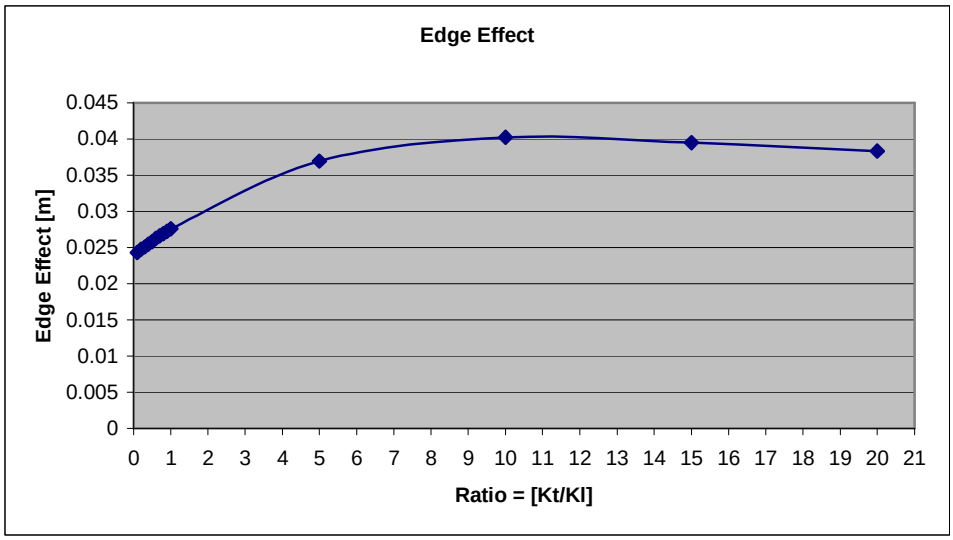

Fig. 76. Edge effect variation with the thermal conductivity ratio

For a range of ratio values between 0 and 1, the study was carried out with a calculation step of 0.1. As can be seen, there are no big differences in edge effect values. It tends to increase in short steps. Rest of the study is run for values from 1 to 20. At a ratio of 10, which means $0.104\ [W/mK]$, edge effect reaches its maximum value. After that point, if transverse value continues going down, edge effect starts to decrease.

The following figure shows values of peak temperatures obtained along this experiment:

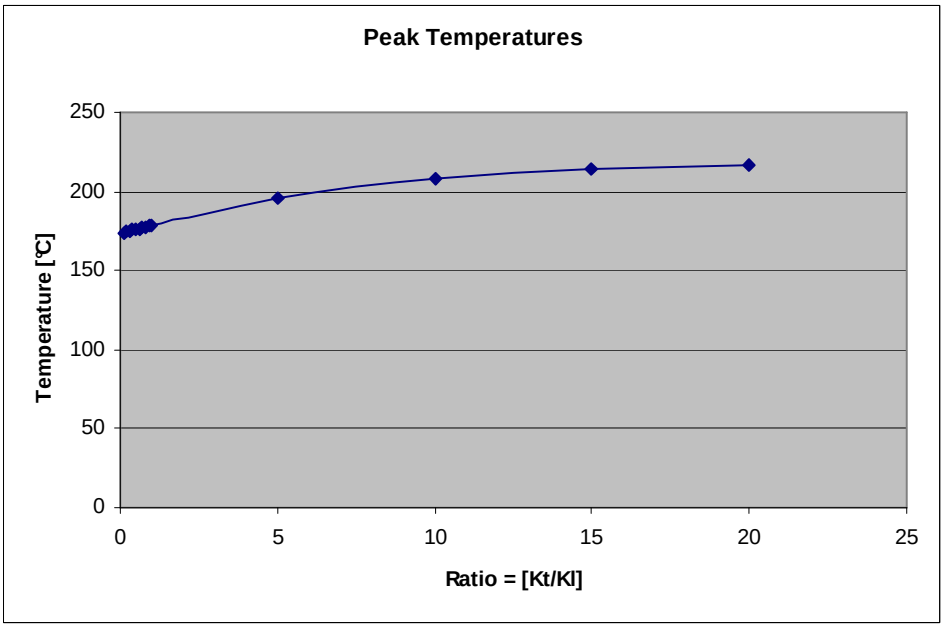

Fig. 77. Peak temperature variation with the thermal conductivity ratio

We can observe the increment of the peak temperature during the overshoot. This values increases when transverse thermal conductivity decreases.

6.3 Two dimensions (2D). T-joint.

T-shaped structures are widely used in industry, they can be found in many applications. It is important to know how a t-joint structure deals during the simulation of the resin transfer moulding process. The study of t-shaped structure is focus on the peak temperatures registered during the process and the influence of edge effect.

The shape which is used on the simulations has the standard size: Thickness: 0.025 m, Length of each arm: 0.15 m. Standard cure cycle is also implemented for the experiment.

The following figure shows the solution given by COMSOL Multiphysics:

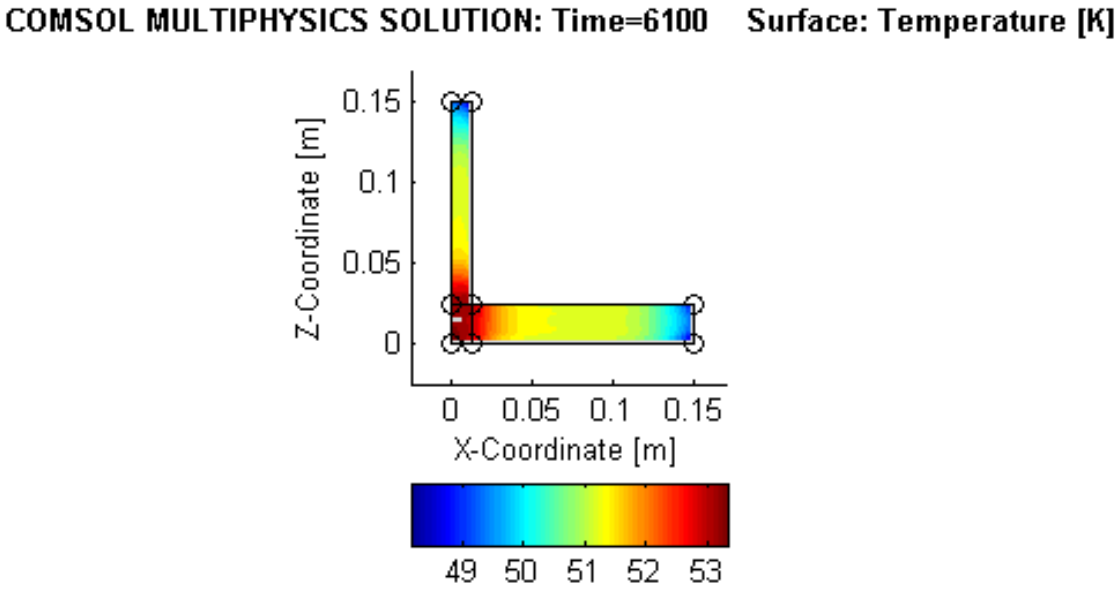

Fig. 78. T-shaped structure.

Axis of symmetry Y is placed on the left side of the half t-shape. As can be seen, maximum temperature appears in the centre of the T-joint. Maximum temperature is 188.3341˚C and is reached at minute 83. The following figures shows the solutions given by the program, which calculates those values:

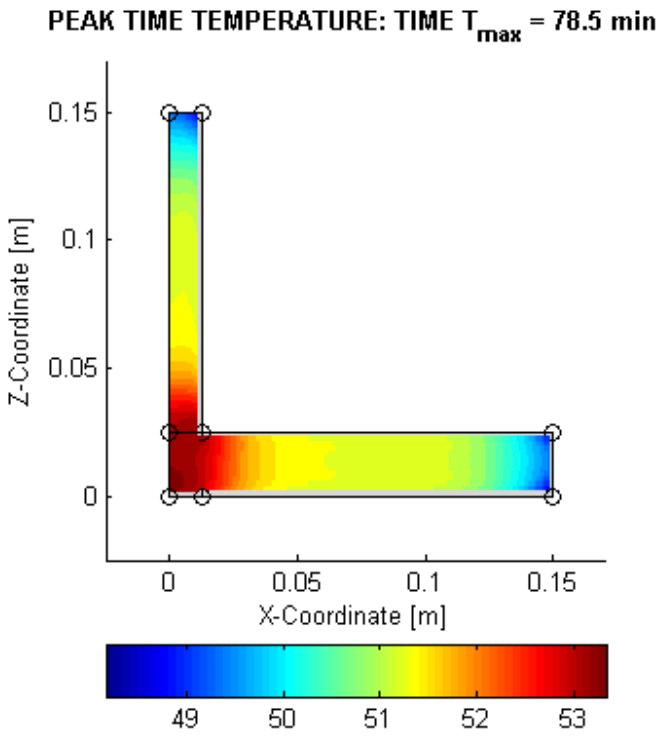

Fig. 79. Maximum temperature reach time.

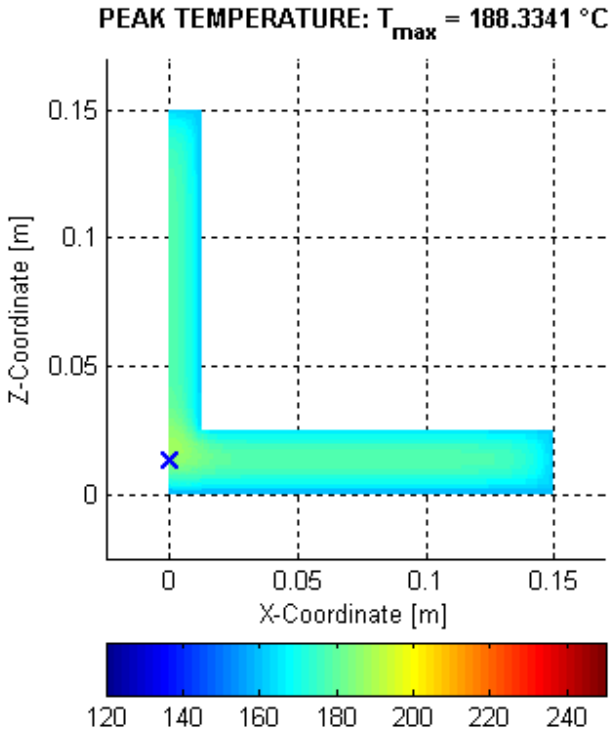

Fig. 80. Maximum temperature.

Peak temperatures are registered at the centre of the t-joint.

For the edge effect calculation, the following figure shows this effect in one of the 3 arm of the t-joint:

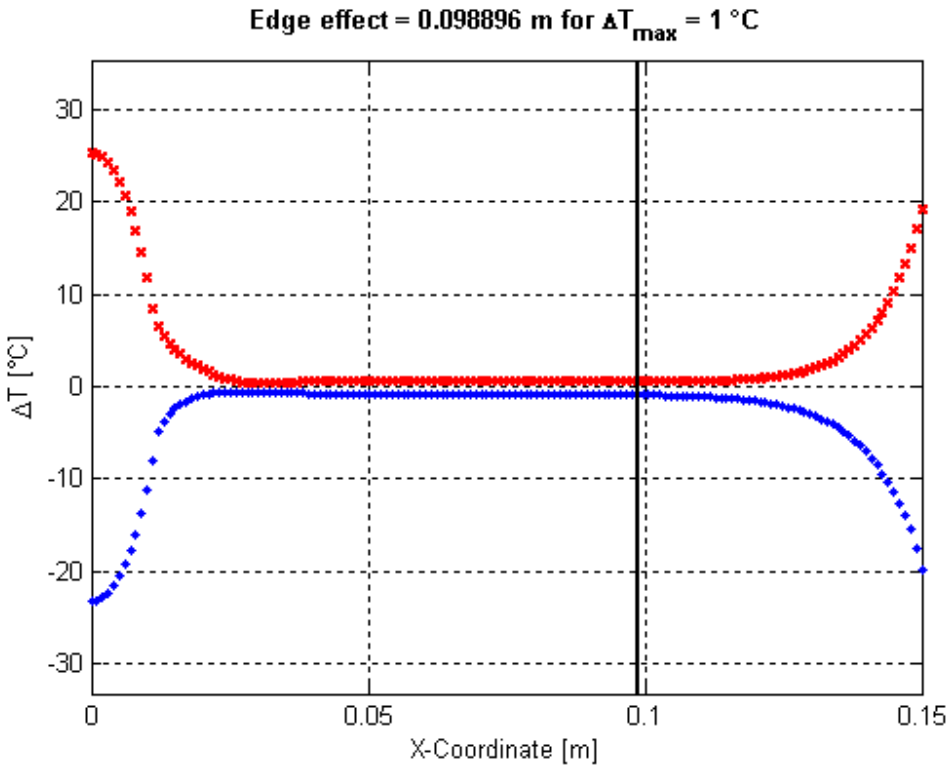

Fig. 81. Edge effect in t-shaped structure.

To continue with the study of t-shaped structures, different widths are going to be evaluated in order to acquire knowledge about the influence in the edge effect phenomenon.

6.4 Three dimensions (3D)

This chapter is focused in the study of three dimensional parts. The block object of study has the following shape: a square base of 0.3 m width and a thickness of 0.025 m. Solve this three dimensional matrix of dots, takes a long time because of the calculation of the big amount of temperature data. In order to reduce this calculation time, the evaluation of the plate can be optimized. 1/8 of the block was extracted and evaluated separately. The dimensions of the new block are: a square base of 0.15 m width and a thickness of 0.0125 m. The following figure shows both plates and its dimensions:

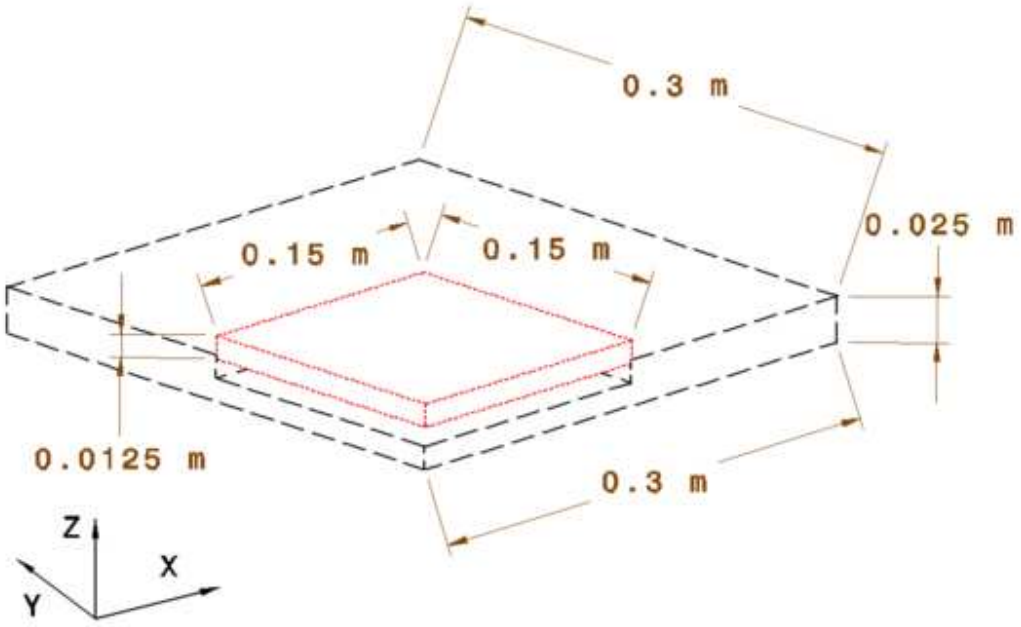

Fig. 82. Dimensions of the 3D model

The red block is object of calculation. The mesh created for calculation of the temperature matrix has 30 x 30 x 7 dots of calculation, which means 6300 values.

Evaluating only this part of the whole block, knowledge of the behavior of the three dimensional model can be obtained. Because there are axes of symmetry and the behavior of the other 1/8 parts of the plate is the same. COMSOL Multiphysics solver was programmed taking into account this assumption, and some border surface were set to thermal insulation heat transfer as boundary settings.

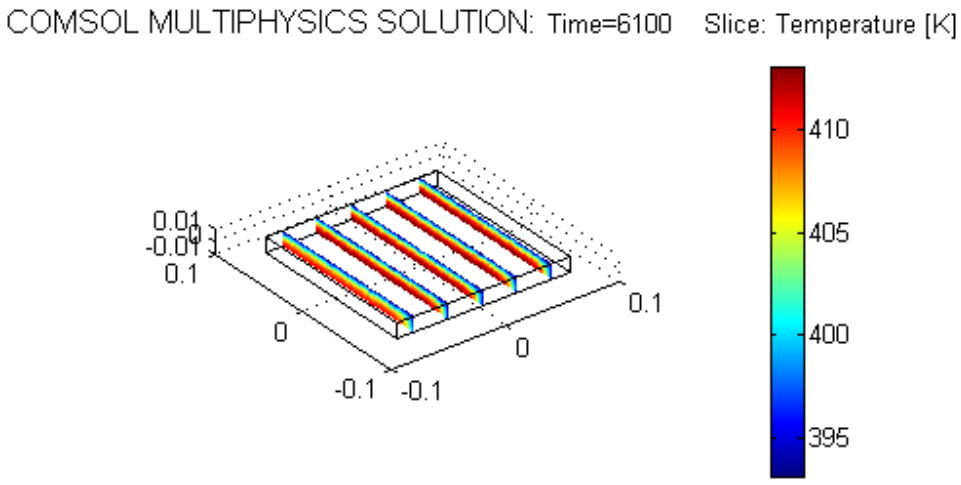

Fig. 83. COMSOL MULTIPHYSICS SOLUTION.

6.4.1 Influence of edge effect

Previously, it was proved the influence of edge effect in infinite beams for a two dimensional model. In this study, a third dimension has been introduced, which means that the beam can be transformed into a finite beam.

It is expected that edge effect phenomenon appears closed to the borders of the plate, but it is necessary to evaluate it to obtain knowledge about this phenomena in a finite beam.

The following figure shows the influence of edge effect along the X axis. It can be seen that edge effect starts at 0.1275 m, which means that there is an edge effect of 0.0525 m. Maximum temperature difference between one dimensional model and three dimensional model is set to 1℃. On e dimensional solution can be extended to the region of the plate which is none affected by the edge effect phenomenon. The width of the plate which is placed on the left of the boundary black line can be compared with one dimensional temperature distribution. Part of the thick which is on the right side, is affected by edge effect phenomena.

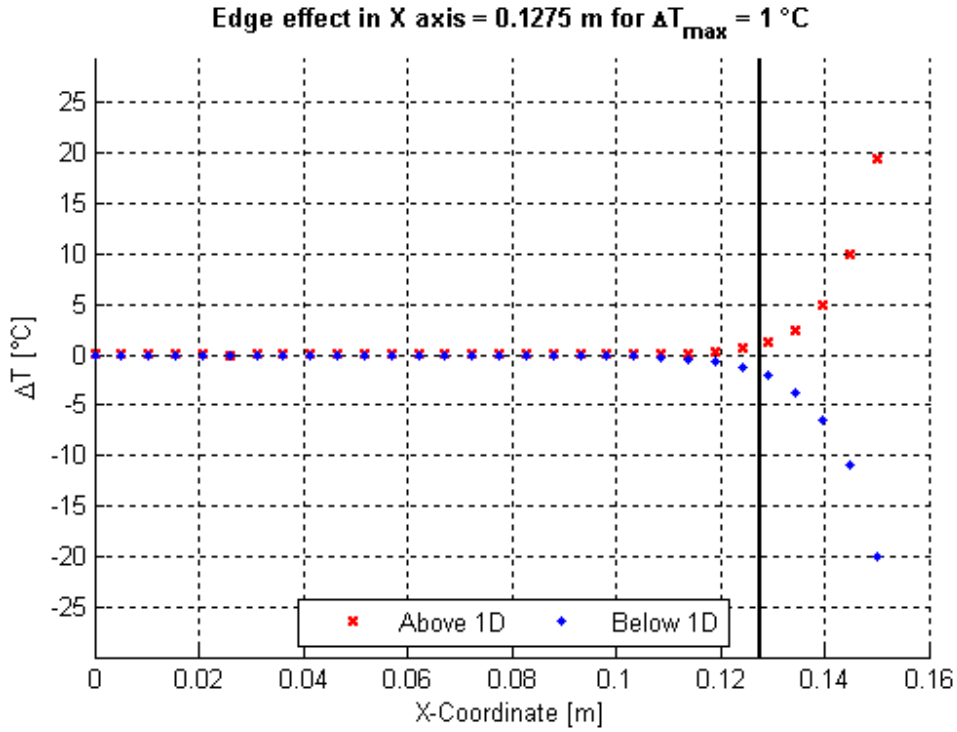

Fig. 84. Edge effect in X axis of the 3D model

The following figure represents the same result with the same orientation of the X axis:

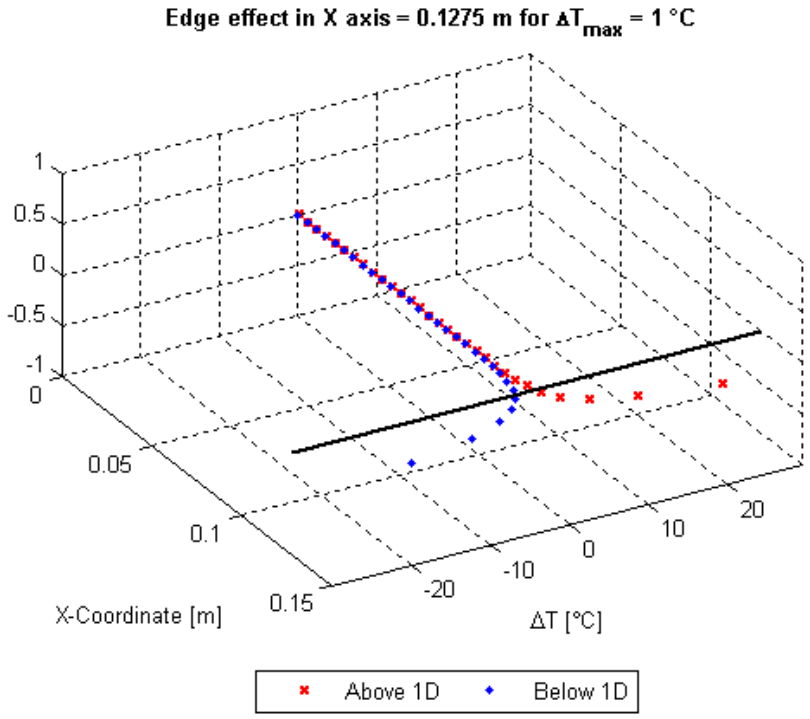

Fig. 85. Edge effect in X axis of the 3D model

Moreover, the same procedure was followed to check edge effect phenomena along the Y axis:

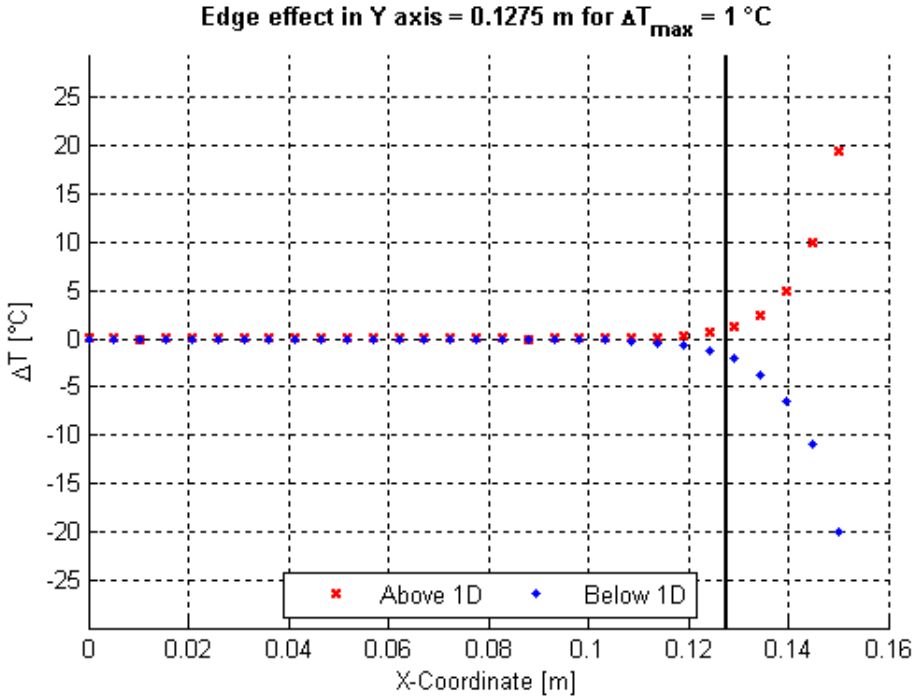

Fig. 86. Edge effect in Y axis of the 3D model

The following figure represents the same result with the same orientation of the X axis:

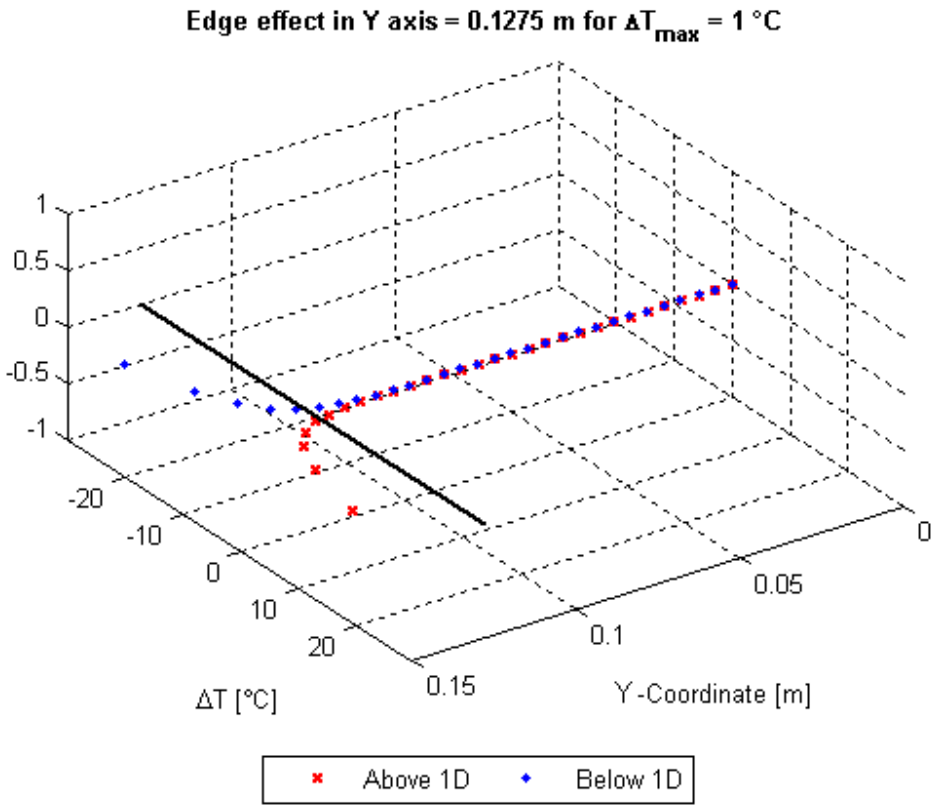

Fig. 87. Edge effect in Y axis of the 3D model

The same edge effect distance is registered along the Y axis, 0.0525 m. Therefore, behavior of the plate along the two axes is the same. One dimensional solution can be extended to the region of the plate which is none affected by the edge effect phenomenon, which is the region on the left side of the boundary (black line).

Then, the diagonal line which goes from the centre of the plate to one corner was also evaluated, in order to know edge effect influence in the region closed to the corner. As it was seen in axes X and Y, edge effect boundaries of both axes should cross in a point of the plate.

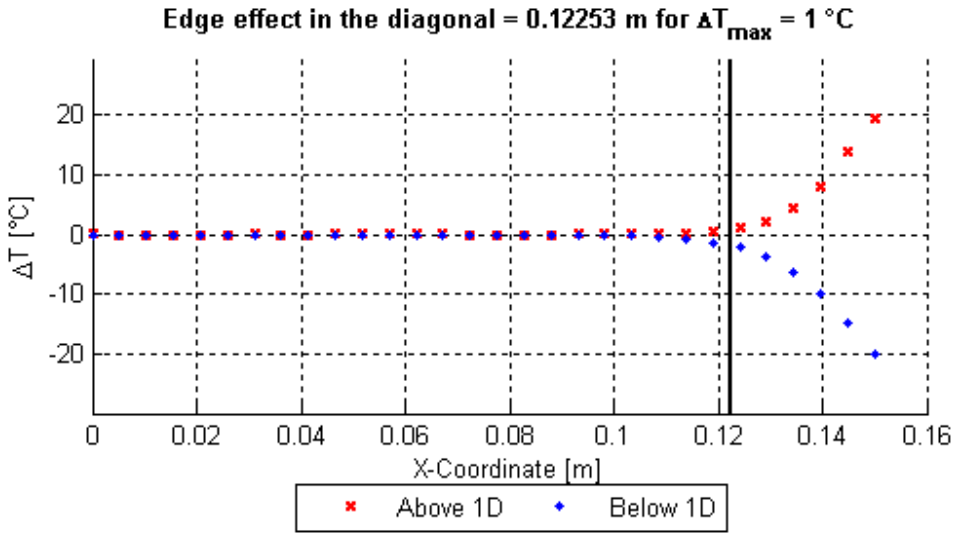

Fig. 88. Edge effect in the diagonal of the 3D model

As can be seen, width of edge effect phenomenon is larger than in X or Y axis, which means that in the region closed to the corner edge effect appears in a wider range of values.

The following figure gives a vertical view of the plate were can be seen the influence of edge effect.

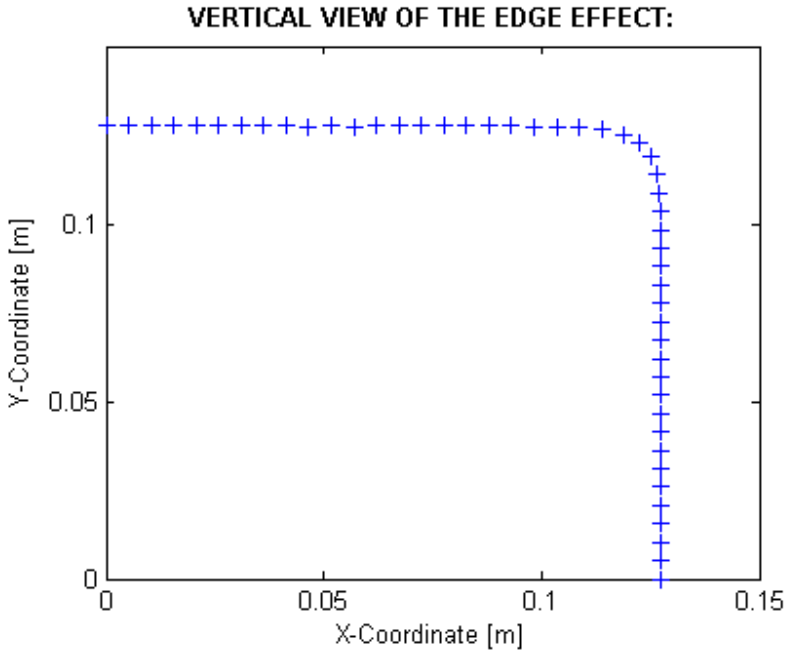

Fig. 89. Vertical view of the edge effect

As it can be seen, the effect of the finite beam in the region closed to the corner is notorious. It can be noticed that the curved distribution of boundary dots of edge effect phenomenon is related to the increased edge effect in the diagonal. It value is set at 0.12253 m. This plot is made by the evaluation of 49 dots along the two axes. The Y vector is formed by the first 24 values of edge effect distances along the Y axis in the plate until the maximum temperature difference in the diagonal, which is dot number 25. Rest of the values is related to the calculation step along the X axis. The X vector is formed by the first 24 values related to the calculation step along the Y axis until the X coordinate of the boundary limit in the diagonal line. Rest of the values is related to the edge effect distances along the X axis.

7 Conclusions

Manufacturing of thick-walled is complex procedure where different keys should be taken into account. The highest quality of the manufactured part needs to be achieved. A fully cured resin plate and homogeneous values should be achieved in order to go further on this research.

Seven experiments were run at the laboratory and good results were obtained with a low deviation, only two of them are out of bounds. The program MainFileFITCURE_FITK.m gives a correct agreement between experimental and model solution, which means that is a valid value. The average value of thermal conductivity has a low standard deviation and compared with results obtained by other researchers in different research programs, is comparable.

Because of this value is not fixed during the whole experiment, some models were used to evaluate this value. On each MATLAB program, a new calculation of the thermo physical parameters is done, taking into account values of transverse and longitudinal thermal conductivity. All these variations are taken into account before running the simulations, which means that results with good agreement are obtained.

The effect of the cure cycle in the calculation of thermal conductivity was studied in main point 3.4, where can be seen that high values of cure temperatures along the plateau in the profile yield high values of thermal conductivity.

Solutions obtained by the process of modelisation with COMSOL Multiphysics, gives some conclusions about the influence of different design parameters. For the one dimensional model, the MVF increment yields values of higher peak temperature during the overshoot related to the exothermic reaction. Taking into account maximum available values for the mould, the maximum MVF for a standard 25 mm thickness plate can be obtained, which is 0.7. Should by noted that possible range of values for the MVF is between 0.3 and 0.7.

The increase of the thickness plate shows and increment on the peak temperature during curing reaction and also in the time to reach this maximum temperature, which makes the manufacturing time longer.

Edge effect phenomenon is evaluated in the two and three dimensional models. It increases its influence with the thickness of the plate for a flat shaped part.

Evaluating the curvature of the plate and its influence in the design parameters, some relations where found with the peak temperature. It increases with the minimum radius. The temperature difference between the one dimensional model and the curved shape depends on the evaluated part of the thickness. On the left side of the thickness (inner radius side of the curved part), profile temperatures

that belong to the two dimensional solution are higher than in the one dimensional distribution. If the evaluation moves along the through-thickness to the outer radius, one dimensional temperature distributions become higher than the two dimensional temperatures.

For the 2 dimensional solution, the variation of the heat rate in the applied cure cycle introduces a small variation in the peak temperature. Edge effect increases with the increment of the initial heat rate.

For the study of the influence of cure temperature, a big variation in the peak temperature is obtained, as it happened for the one dimensional model. The same phenomenon happens with the edge effect.

The simulations for different thermal conductivity ratio $\frac{K_t}{K_l}$ values were carried out to generate knowledge of its influence in the manufacturing process. If transverse thermal conductivity decreases edge effect tends to increase, but no big differences can be obtained. Therefore, peak temperature increases also in short steps.

For T-shaped structures, the evaluation of peak temperatures during its manufacturing process is one of the most important objects of study. The centre of the T-joint, where the 3 beams and linked, is where maximum temperatures values are registered. Values of higher temperatures around 10°C more are measured at the centre of the T-shaped. As well, edge effect influence starts before for the same thickness than in a flat infinite plate.

Having a look into the solutions given by the COMSOL Solver, a “complex” color barcode appears at the centre region, this is the critical part of the T-joint body.

For the three dimensional model, influence of edge effect was evaluated along the whole plate in X and Y axis. This phenomenon appears in both axes with the same width, which is wider than in the flat shape. The diagonal gives values of edge effect influence closer to the centre point, which means that there is a curvature in the edge effect boundary line in the corners. This phenomena should be taken into account because affects to the integrity of the plate and its final quality.

Resin transfer moulding manufacturing process for thick-walled composites can generate high quality parts, taking into account restrictions as cure cycle, cure temperature, MVF and thickness of the manufactured part.

8 Future work

The future of composites in industry is infinite. On these days, composites are widely used in several fields, especially in automotive and aerospace industry.

9 Appendix 1. SSE and thermal diffusivity calculation

On this chapter, the simulations run with Matlab program to obtain the minimum value of Sum of Square Error and its related thermal diffusivity value are going to be showed.

9.1 Simulation 090717

Time boundaries are explained below:

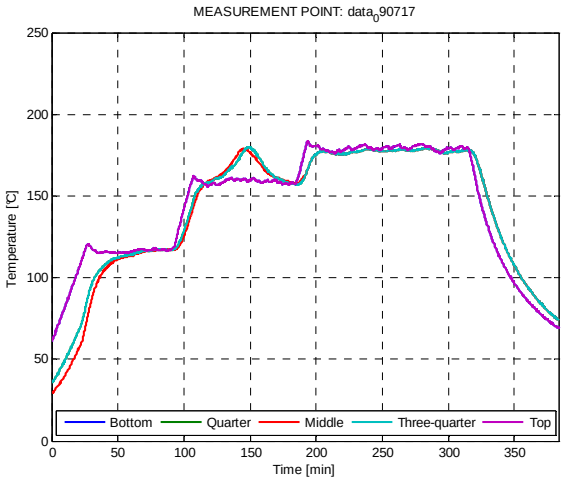

Fig. 90

- Start Point Heating for curing: 90 min
- Start Point Curing: 107 min
- End Point Curing: 183 min

Program is calculating the SEE for the three different regions. With those time values, region bounds are set.

The curve of SSE values obtained along the curing period is the following:

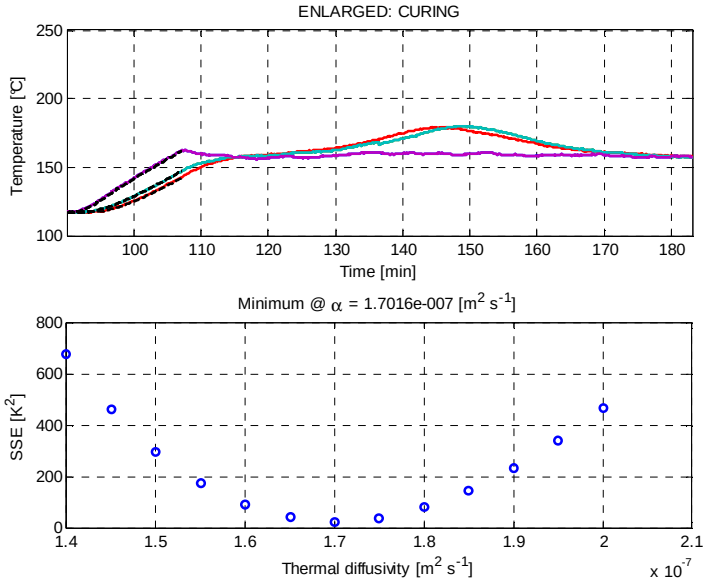

Fig. 91

The minimum value of α is obtained at:

$$\alpha = 1.7016e-007\ [m^2 s^{-1}]$$

Also, a SSE curve was obtained during the cool down. Thermal diffusivity value is a little bit lower, $\alpha = 1.5567e-007\ [m^2 s^{-1}]$:

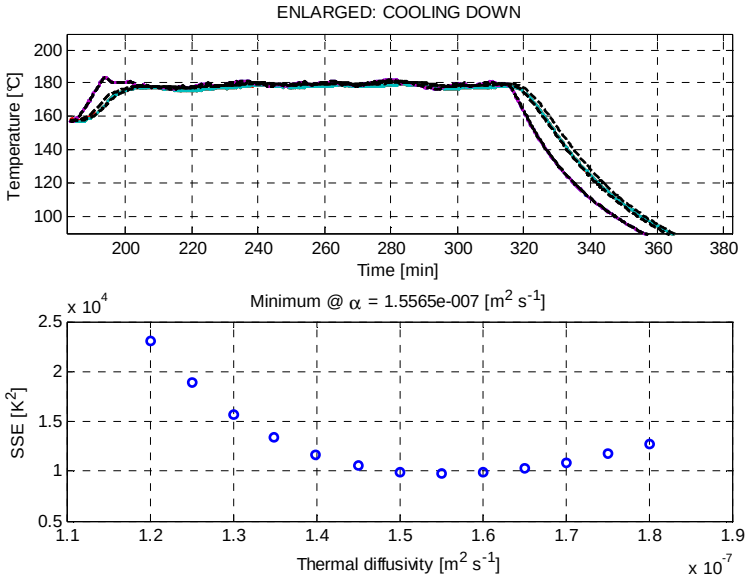

Fig. 92

9.2 Simulation 091029

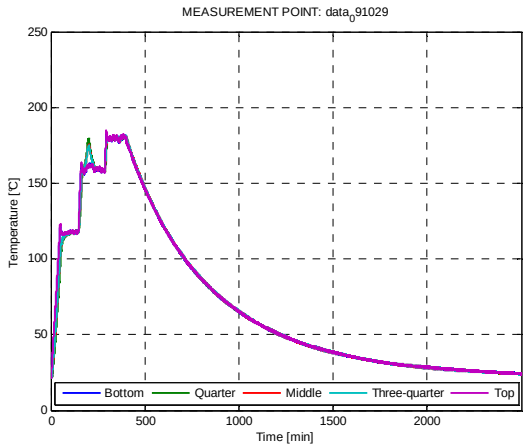

Fig. 93

Simulation run on the 29th of October in 2009 gives the following results:

- Start Point Heating for curing: 140min
- Start Point Curing: 164 min
- End Point Curing: 283 min

The study of curing region gives a value of thermal diffusivity for the minimum SSE of $\alpha = 1.9894e-007\ [m^2 s^{-1}]$. Following figure shows the curve of SSE values:

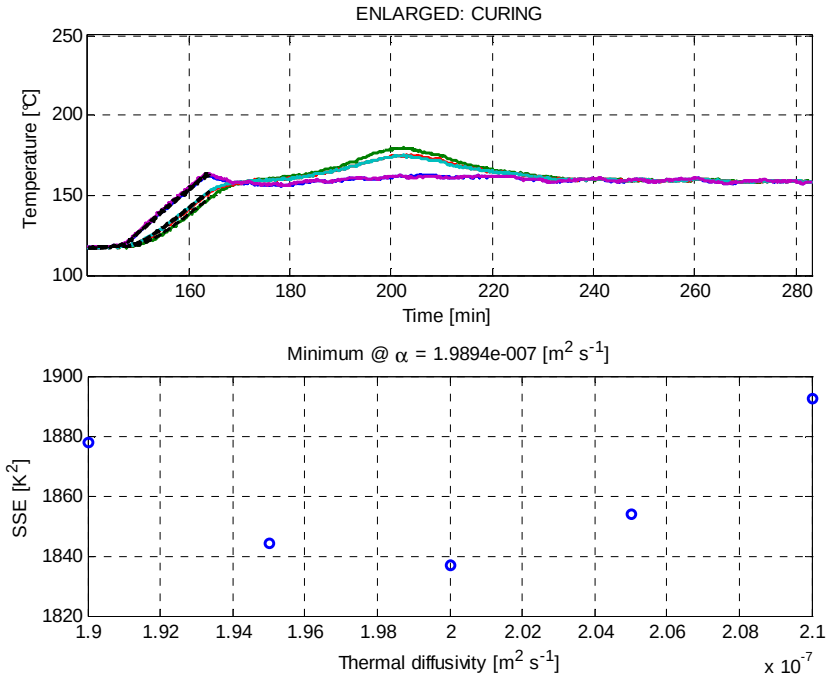

Fig. 94

Also, for the cool down region, the solution has this appearance:

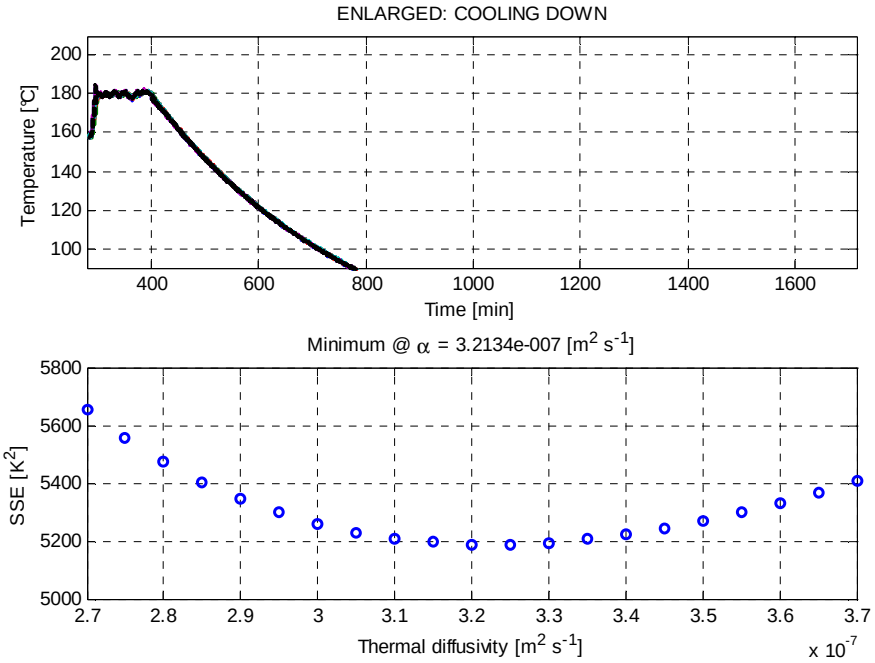

Fig. 95

Calculation of thermal diffusivity related to the minimum value of SSE gives the following result:

$$\alpha = 3.2134e-007\ [m^2 s^{-1}]$$

9.3 Simulation 091104

Below appears the profile temperature implement during the experiment run at the laboratory on 4th of November in 2009.

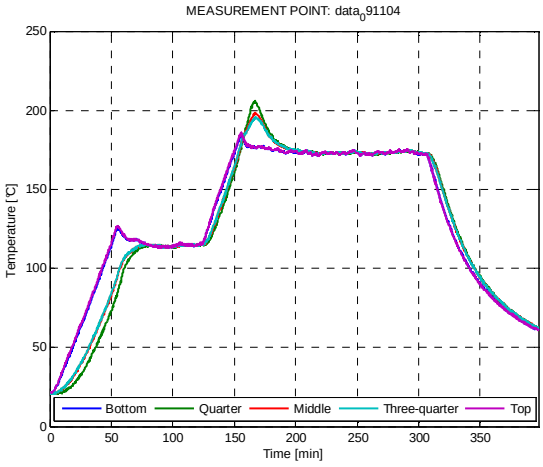

Fig. 96

- Start Point Heating for curing: 121 min
- Start Point Curing: 156 min
- End Point Curing: 305 min

The curve obtained during the curing period is displayed below:

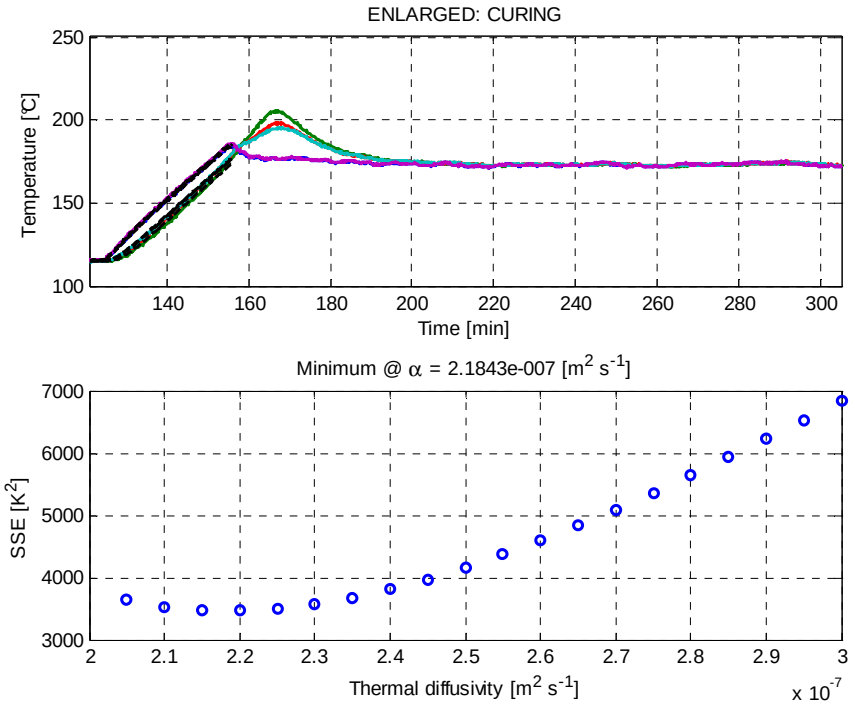

Fig. 97

The cubic spine calculation gives a value for the thermal diffusivity of $\alpha = 2.1843e-007\ [\mathrm{m^2 s^{-1}}]$.

Related to the cool down region of the experiment, the thermal diffusivity value generated is: $\alpha = 2.7225e-007\ [m^2 s^{-1}]$

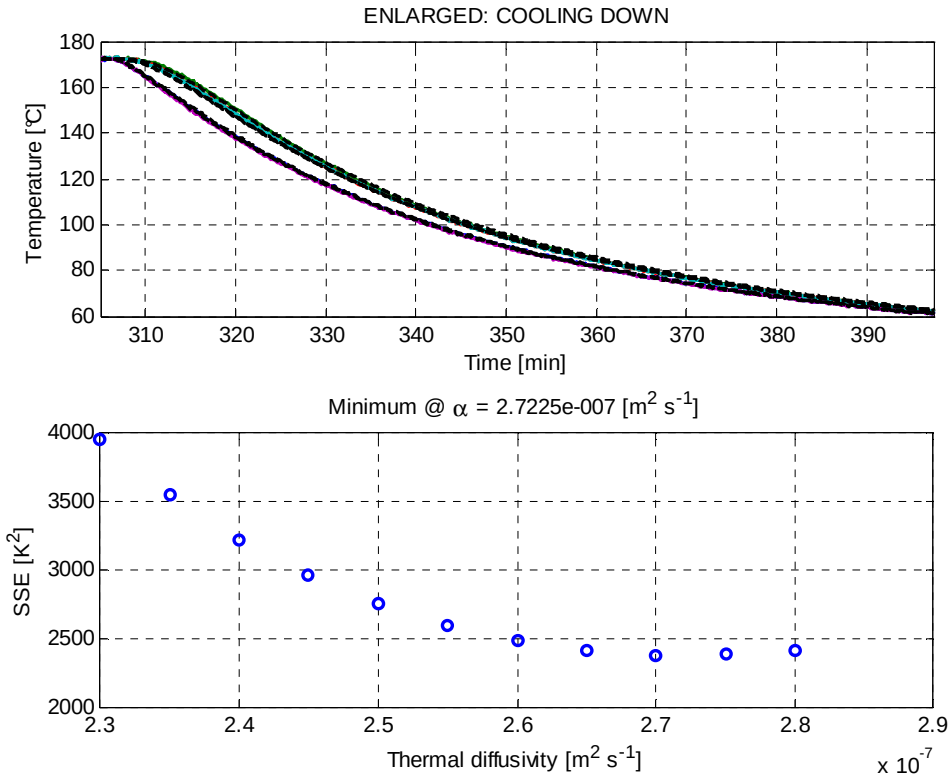

Fig. 98

9.4 Simulation 091110

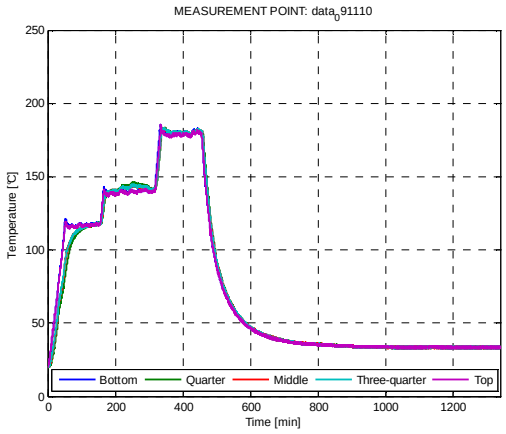

On this experiment, the profile experiment is as follows:

- Start Point Heating for curing: 150 min
- Start Point Curing: 167 min
- End Point Curing: 313 min

Fig. 99

As usual, two values for curing and cool down region were obtained. These figures show the results generated solving the program:

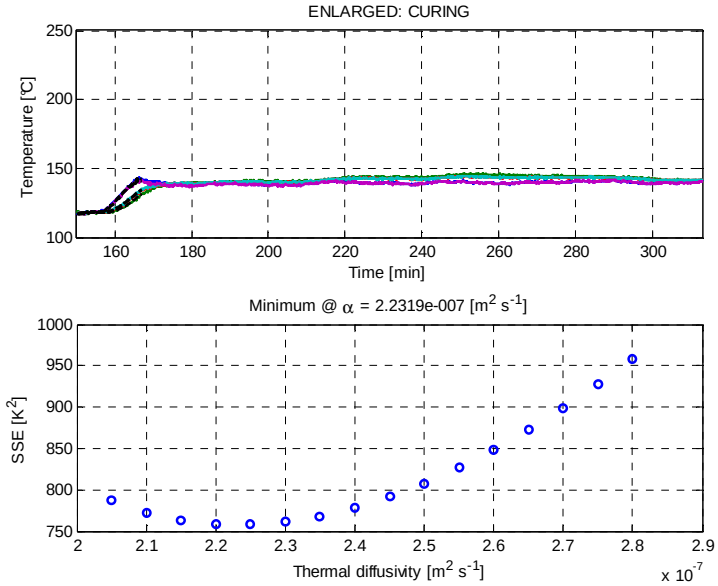

Fig. 100

The value of thermal diffusivity during curing α related to the lowest Sum of Square Error is:

$$\alpha = 2.2319e-007\ [m^2 s^{-1}]$$

Also, the calculation for the cool down period gives a value of thermal diffusivity of: $\alpha = 2.7498e-007\ [m^2 s^{-1}]$

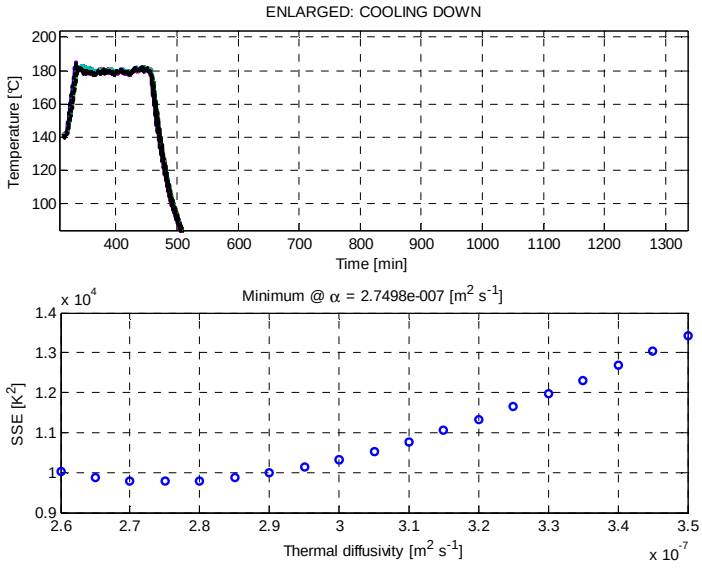

Fig. 101

9.5 Simulation 091202

For the experiment run on 2nd of December in 2009, the following figure shows the profile temperature:

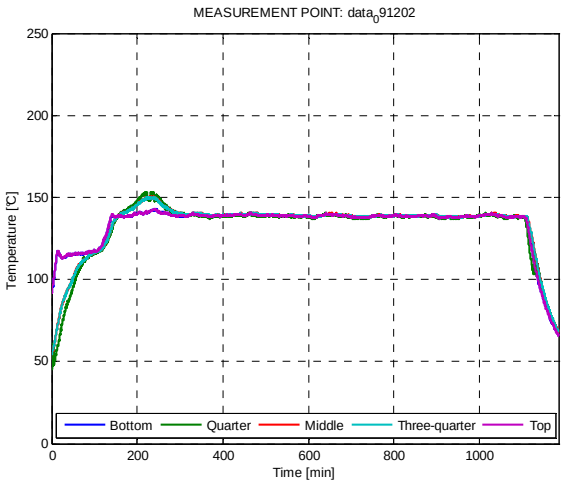

- Start Point Heating for curing: 98 min
- Start Point Curing: 142 min
- End Point Curing: 1105 min

Fig. 102

The value of thermal diffusivity is: $\alpha = 1.2259e-007\ [m^2 s^{-1}]$

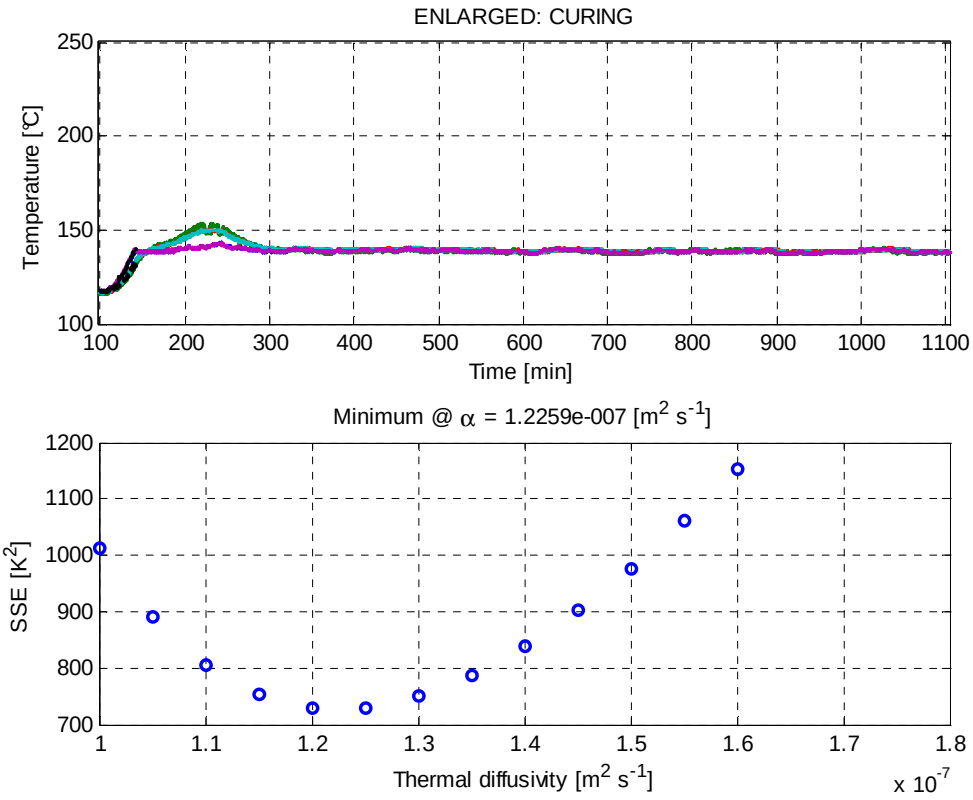

Fig. 103

The curve related to the cool down for the SSE is displayed below:

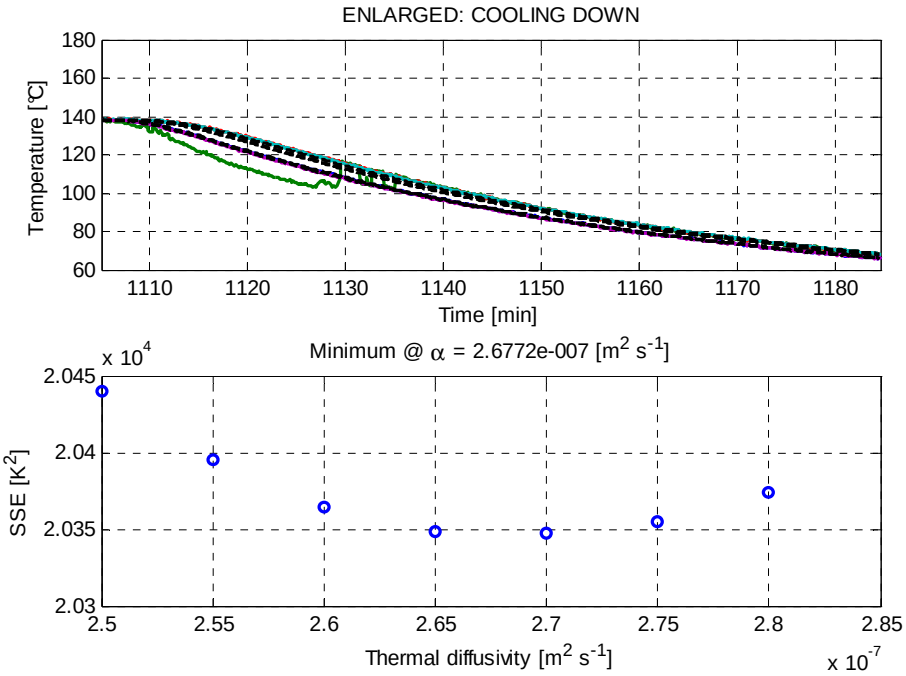

Fig. 104

Its thermal diffusivity value is: $\alpha = 2.6772e-007\ [m^2 s^{-1}]$

9.6 Simulation 100216

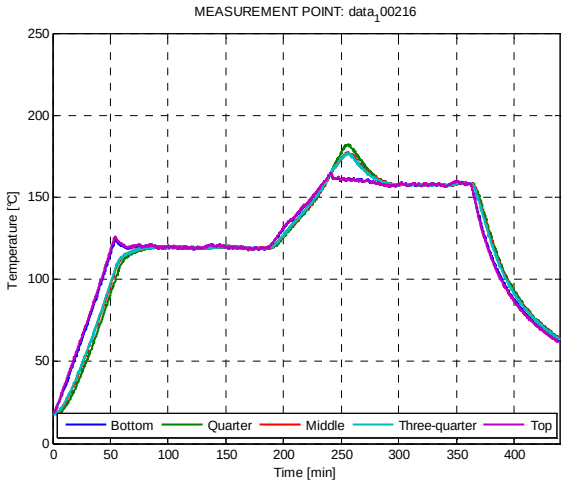

Fig. 105

Profile temperature of this experiment has the following calculation bounds:

- Start Point Heating for curing: 183 min
- Start Point Curing: 237 min
- End Point Curing: 361 min

No post-curing region can be found on that experiment.

The calculation along the curing region gives the following results:

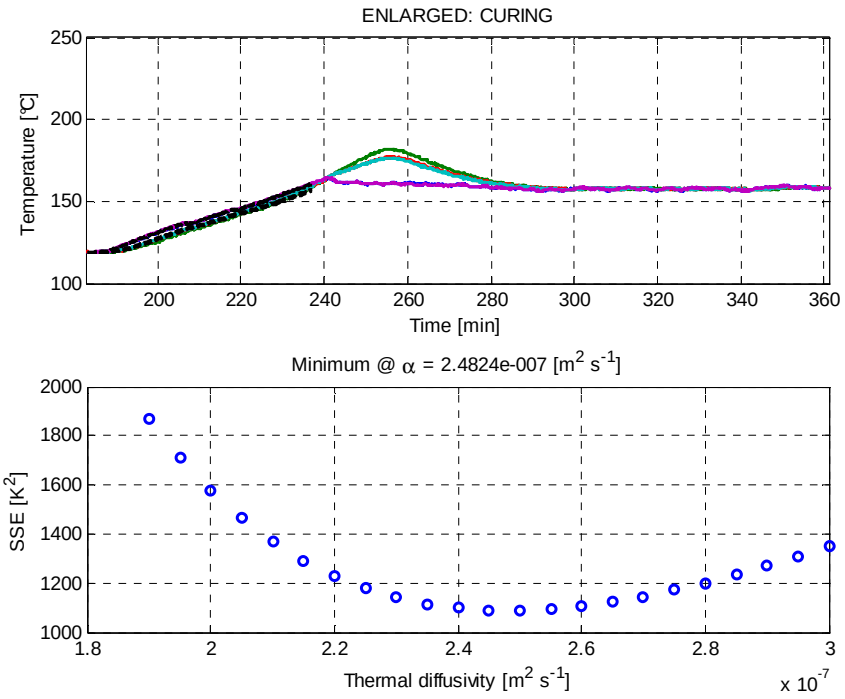

Fig. 106

The value of thermal diffusivity is: $\alpha = 2.4824e-007\ [\mathrm{m^2 s^{-1}}]$

The curve obtained during the cooling down period is the following:

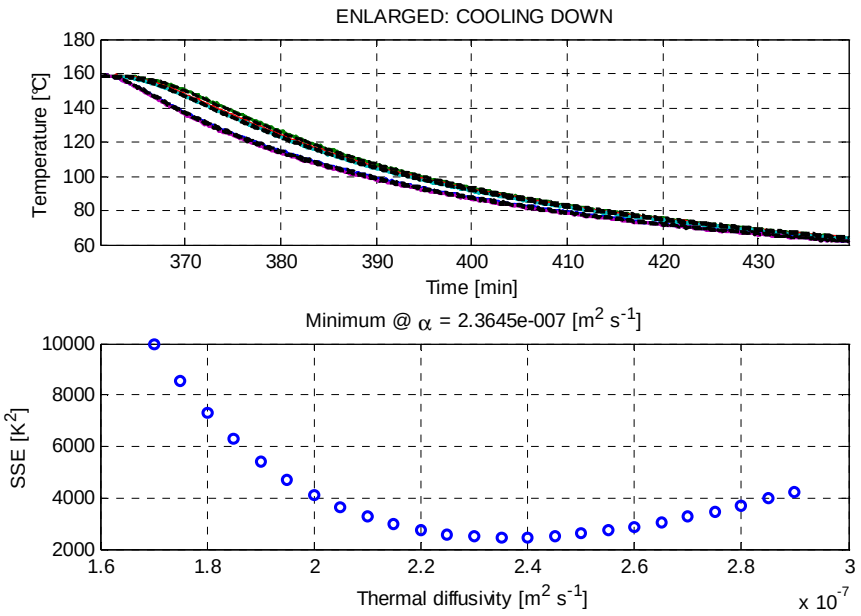

Fig. 107

The minimum value of α which makes the lowest error is:

$$\alpha = 2.3645e-007\ [\mathrm{m^2 s^{-1}}]$$

9.7 Simulation 100223

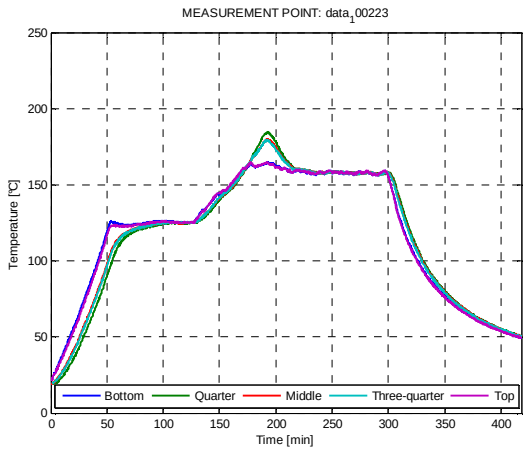

- Start Point Heating for curing: 126 min
- Start Point Curing: 155 min
- End Point Curing: 296 min

Fig. 108

The curve obtained during the curing period is the following:

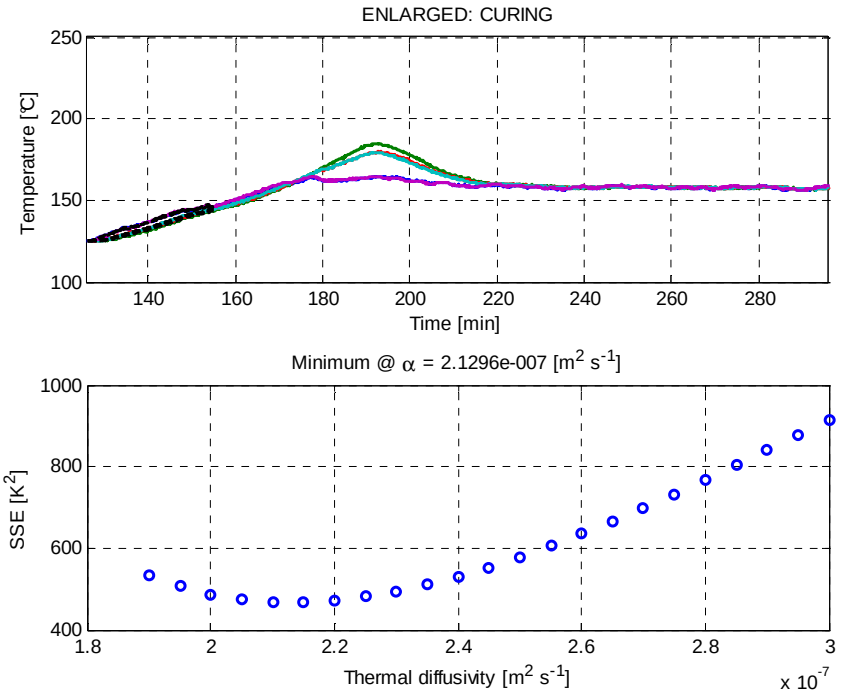

Fig. 109

The minimum value of α which makes the lowest error is:

$$\alpha = 2.1296e-007\ [\mathrm{m^2 s^{-1}}]$$

The curve obtained during the cooling down period is the following:

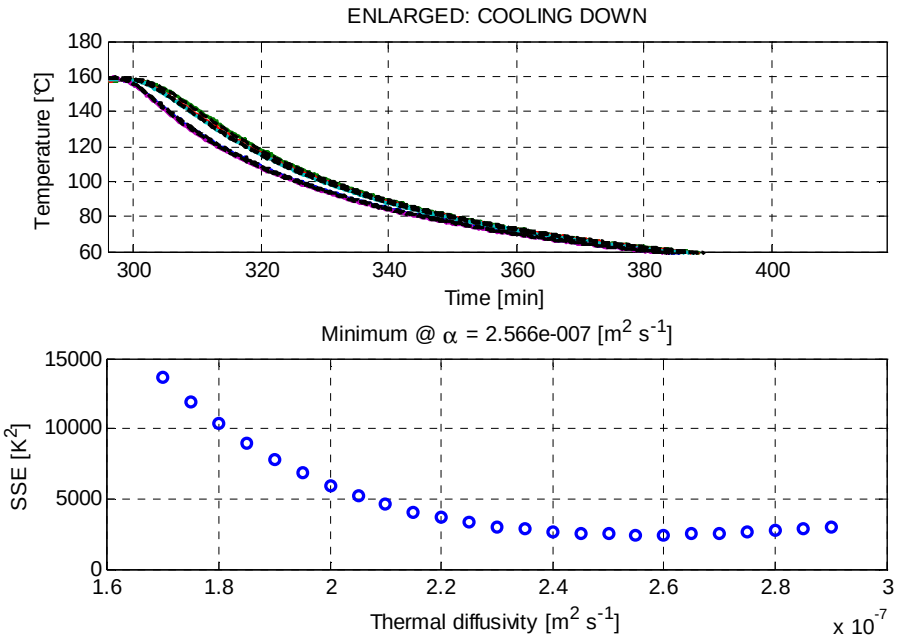

Fig. 110

The minimum value of α which makes the lowest error is:

$$\alpha = 2.566e-007\ [\mathrm{m^2 s^{-1}}]$$

9.8 Simulation 100210:

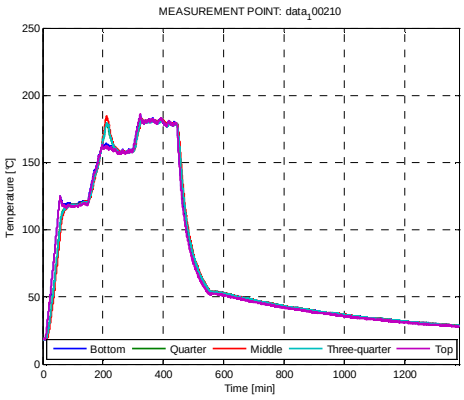

Fig. 111

- Start Point Heating for curing: 146 min
- Start Point Curing: 195 min
- End Point Curing: 299 min

The curve obtained during the curing period is the following:

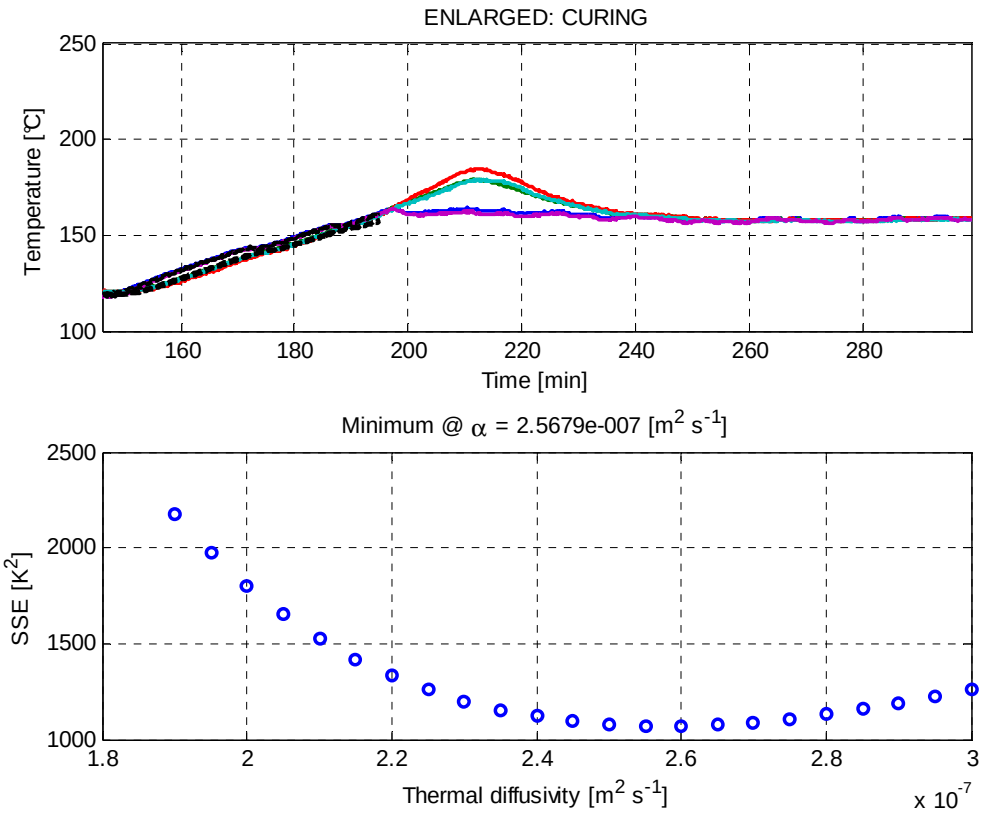

Fig. 112

The minimum value of α which makes the lowest error is:

$$\alpha = 2.5679e-007\ [\mathrm{m^2 s^{-1}}]$$

The curve obtained during the cooling down period is the following:

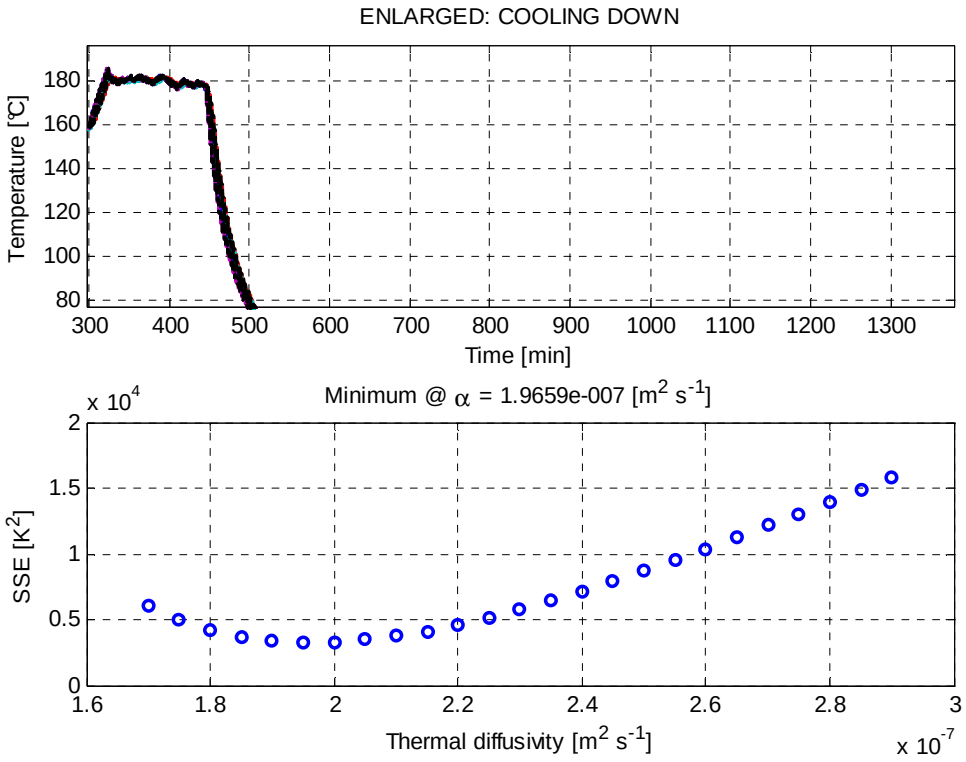

Fig. 113

The minimum value of α which makes the lowest error is:

$$\alpha = 1.9659e-007[m^2 s^{-1}]$$

10 Appendix 2. Calculation of the fittest thermal conductivity

On this appendix there is going to appear solutions given by the simulation with the program MainFileFITCURE_FITK.m, which is going to calculate the optimal thermal conductivity value of the composite material for each experiment run at the laboratory. Fittest K value is related to the minimum value of temperature difference between the model solution and the experimental solution. The range of temperature values evaluated along the profile temperature comprises almost the whole experiment, which means that the solution given has good approximation.

10.1 Simulation 090717:

Result obtained for the experiment 090717 is displayed below:

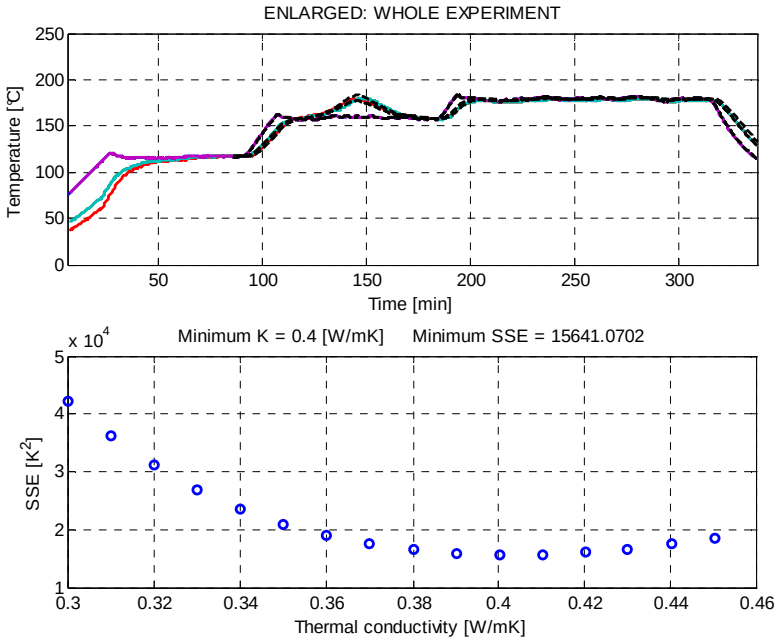

Fig. 114

The optimal thermal conductivity value is $0.4\ [W/mK]$ and its error is 15641.0702.

10.2 Simulation 091029

Result obtained for the experiment 091029 is displayed below:

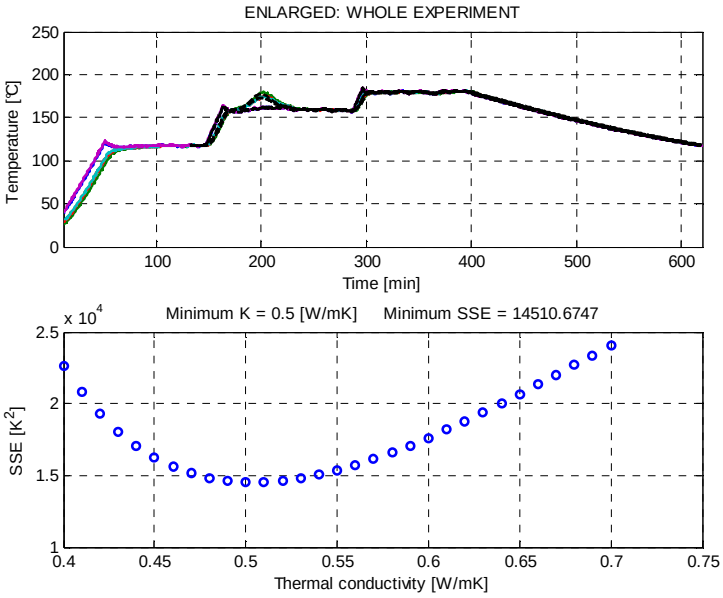

Fig. 115

The optimal thermal conductivity value is $0.5\ [W/mK]$ and its error is 14510.6747.

10.3 Simulation 091104

Result obtained for the experiment 091104 is displayed below:

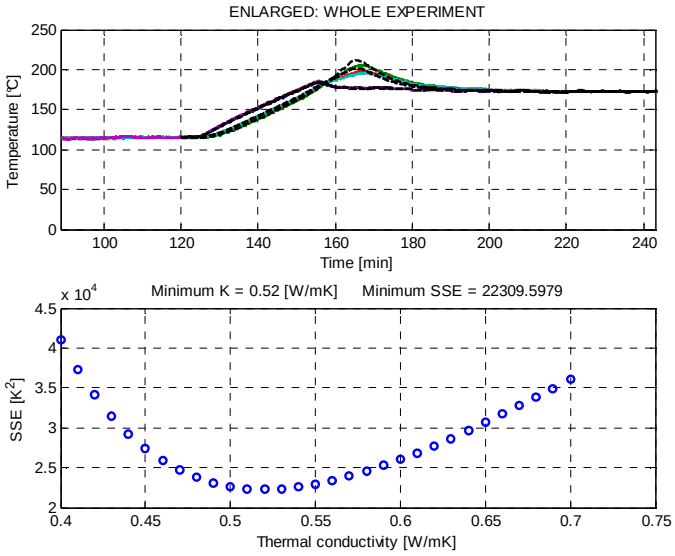

Fig. 116

The optimal thermal conductivity value is $0.52\,[W/mK]$ and its error is 22309.5979.

10.4 Simulation 091110

Result obtained for the experiment 091110 is displayed below:

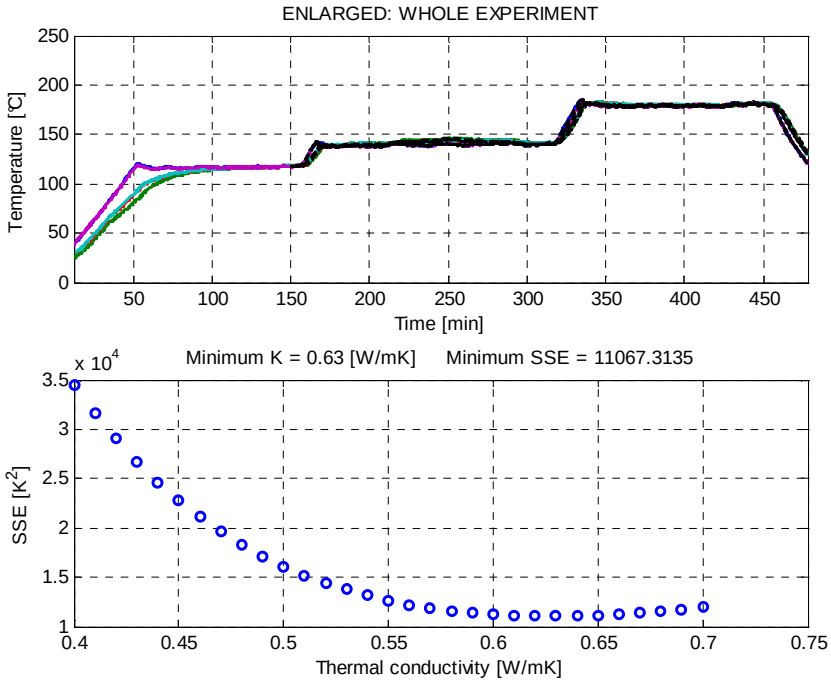

Fig. 117

The optimal thermal conductivity value is $0.63\,[W/mK]$ and its error is 11067.3135.

10.5 Simulation 091202

Result obtained for the experiment 091202 is displayed below:

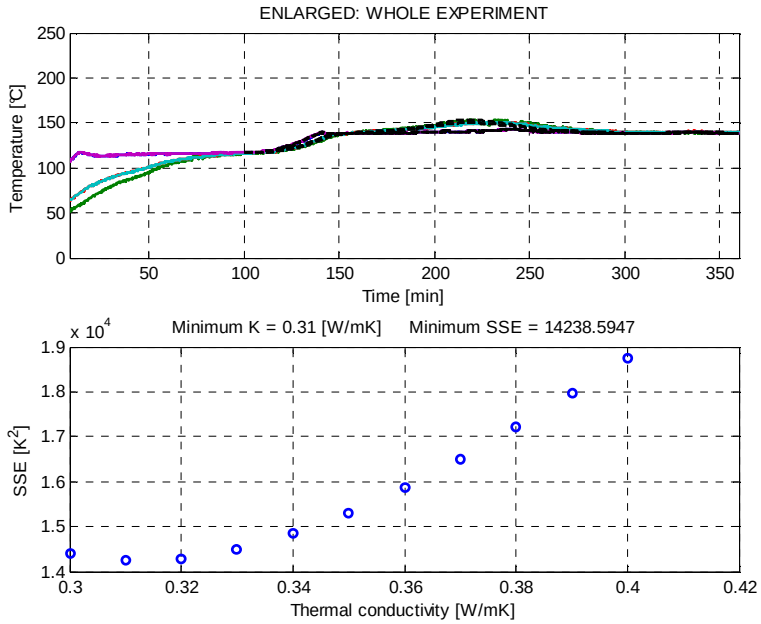

Fig. 118

The optimal thermal conductivity value is $0.31\,[W/mK]$ and its error is 14238.5947.

10.6 Simulation 100210

Result obtained for the experiment 100226 is displayed below:

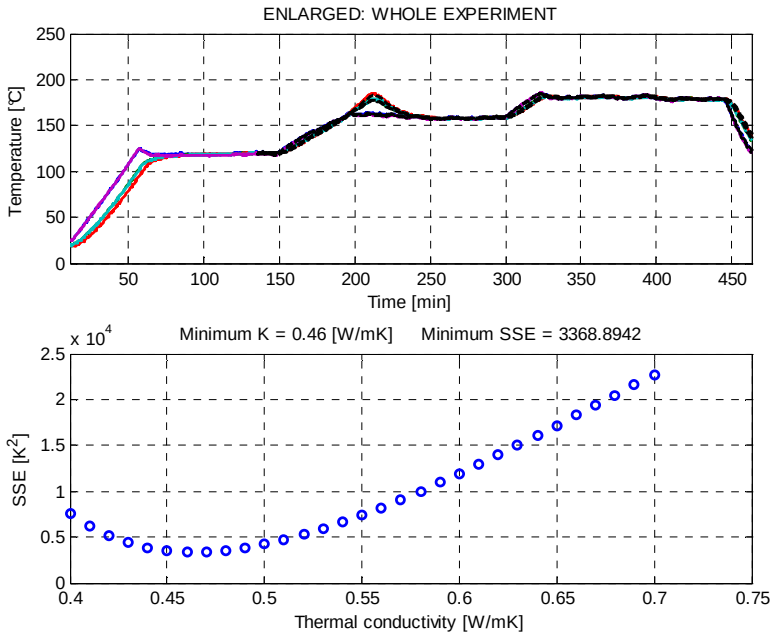

Fig. 119

The optimal thermal conductivity value is $0.46\ [W/mK]$ and its error is 3368.8942.

10.7 Simulation 100216

Result obtained for the experiment 100226 is displayed below:

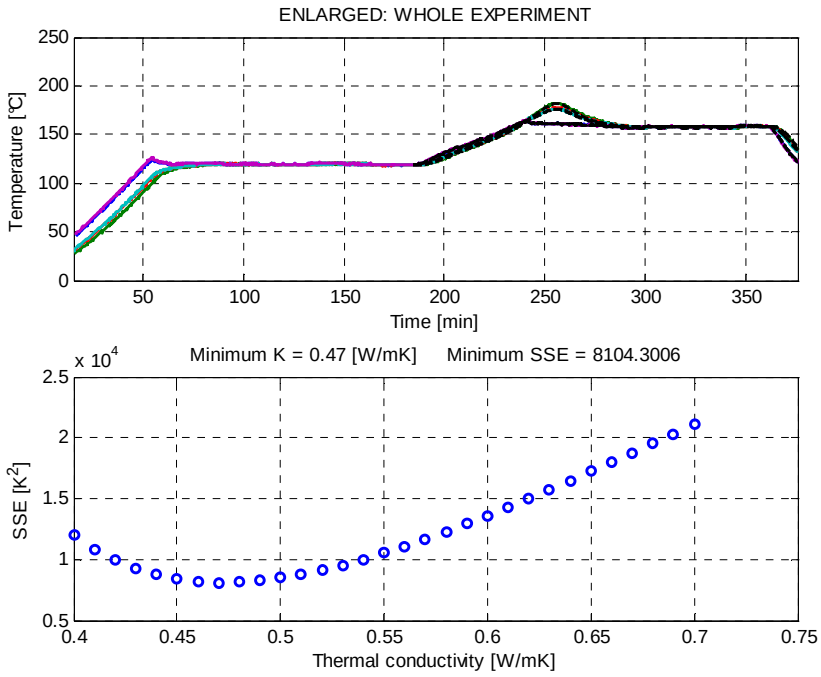

Fig. 120

The optimal thermal conductivity value is $0.47\ [W/mK]$ and its error is 8104.3006.

11 References

11.1 Numbered references:

[1] J.M. Balvers, H.E.N. Bersee, A. Beukers and K.M.B. Jansen. “Determination of cure dependent properties for curing simulation of thick-walled composites”. *Proceeding of the 49th AIAA/ASME/ASCE/AHS/ASC Structures, Structural Dynamics, and Materials Conference*, April 2008, Schaumburg, IL, USA.

[2] E. Ruiz and F. Trochu. “Numerical analysis of cure temperature and internal stresses in thin and thick RTM parts”. *Composites*: Part A 36 (2005): 806-826.

[3] S.C. Joshi, X.L. Liu and Y.C. Lam. “A numerical approach to the modeling of polymer curing in fibre-reinforced composites”. *Composite science and Technology*: 59 (1999): 1103-1113.

[4] P. Dufour, D.J. Michaud, Y. Toure and P.S. Dhurjati. “A partial differential equation model predictive control strategy: application to autoclave composite processing”. *Computers and Chemical Engineering*: xxx (2003) xxx-xxx.

[5] H. Chiu, B. Yu, S.C. Chen and L.J. Lee. “Heat transfer during flow and resin reaction through fiber reinforcement”. *Chemical Engineering Science*: 55 (2000): 3365-3376.

[6] T. Behzad and M. Sain. “Finite element modeling of polymer curing in natural fibre reinforced composites”. *Composites Science and Technology*: 67 (2007) 1666-1673.

[7] V.A.F. Costa and A.C.M. Sousa. “Modeling of flow and thermo-kinetics during the cure of thick laminated composites.” *International Journal of Thermal Sciences*: 42 (2003) 15-22.

[8] M. Grujicic, K.M. Chittajallu and Shawn Walsh. “Non-isothermal preform infiltration during the vacuum-assisted resin transfer molding (VARTM) process”. *Applied Surface Science*: 245 (2005): 51-64.

[9] D. Rouison, M. Sain and M. Couturier. “Resin transfer moulding of natural fibre reinforced composites: cure simulation”. *Composites Science and Technology*: 64 (2004) 629-644.

[10] J.H. Oh and D.G. Lee. “Cure cycle for thick glass/epoxy composite laminates”. *Journal Composites Materials*: 36 (2002) (1): 19–45.

[11] M. Jinno, S. Sakai, K. Osaka and T. Fukuda. “Smart autoclave processing of thermoset resin matrix composites based on temperature and internal strain monitoring”. *Advanced Composite Materials*: Vol. 12, No 1.(2003): 57-72.

[12] Z. Ghuo, Shanyi Du and B. Zhang. “Temperature field of thick thermoset composite laminates during cure process”. *Composites Science and Technology*: 65 (2005): 517-523.

[13] Rolfes R. and Hammerschmidt. “Transverse thermal conductivity of CFRP laminates: A numerical and experimental validation of approximation formulae”. *Composites Science and Technology*: 54 (1995): 45-54.

[14] T. Behzad and M. Sain. “Finite element modeling of polymer curing in natural fibre reinforced composites”. *Composites Science and Technology*: 67 (2007): 1666-1673.

[15] S. C. Joshi and Y.C. Lam. “Three-dimensional finite-element/nodal-control-volume simulation of the pultrusion process with the temperature-dependent material properties including resin shrinkage”. *Composites Science and Technology*: 61 (2001): 1539-1547.

[16] D. Rouison, M. Sain and M. Couturier. “Resin transfer molding of natural fiber reinforced composites: cure simulation”.*Composites Science and Technology*: 64 (2004) 629-644.

[17] M. Henne, P. Ermanni, M. Deleglise and P. Krawczak. “Heat transfer of fibre beds in resin transfer moulding: an experimental approach”. *Composites Science and Technology*: 64 (2004): 1941-1202.

[18] D. Kumlutas, I. H. Tavman and M.T. Coban. “Thermal conductivity of particle filled polyethylene composite materials”. *Composites Science and Technology*: 63 (2003): 113-117.

[19] T. B. Lewis and L. E. Nielsen. “Dynamic Mechanical Properties of Particulate-
Filled Composites”. *Journal of applied polymer science:* 14 (1970): 1449-1471.

[20] V. Antonucci, M. Giordano, K. Hsiao and S. G. Advani. “A methodology to reduce thermal gradients due to the exothermic reactions in composites processing”. *International Journal of heat and mass transfer*: 45 (2002): 1675-1684.

[21] A.A. Skordos and I.K. Partridge. “Inverse heat transfer for optimization and on-line thermal properties estimation in composites curing”. *Inverse problems in engineering*: 200, 00, 0: 1-16.

[22] E.Ruiz and F. Trochu. “Multi-criteria thermal optimization in liquid composite moulding to reduce processing stresses and cycle time”. *Composites Part A: Applied Science and Manufacturing*: 37 (2006) 913-924.

[23] J. M. Balvers. “Cure Kinetics of Bicomponent RTM6 System”. 2009.

11.2 Non-numbered references:

[a] K.F. Schoch, Jr., P.A. Panackal and P.P. Frank. “Real-time measurement of resin shrinkage during cure”. *Thermochimica Acta*: 417 (2004): 115-118.

[b] D.H. Lee, S.K. Kim, W. II Lee, S.K. Ha and S.W. Tsai. “Smart cure of thick composite filament wound structures to minimize the development of residual stresses”. *Applied Science and Manufacturing*: Vol. 37, Issue 4 (2006): 530-537.

[c] T. Behzad and M. Sain. “Finite element modeling of polymer curing in natural fiber reinforced composites”. *Composites Science and Technology*: 67 (2007) 1666-1673.

[d] A. Shojaei, S.R. Ghaffarian and S.M.H. Karimian. “Simulation of the three-dimensional non-isothermal mold filling process in resin transfer moulding”. *Composites Science and Technology*: 63 (2003): 1931-1948.

[e] V. Antonucci, M. Giordano, K. Hsiao and S. G. Advani. “A methodology to reduce thermal gradients due to the exothermic reactions in composites processing*”. International Journal of Heat and Mass Transfer*: 45 (2002): 1675-1684.

[f] H. C. Park and S. W. Lee. “Cure simulation of thick composite structures using the finite element method”. *Journal of Composite Materials*: 35, No. 03/2001.

[g] Z.S. Guo, S. Du and B. Zhang. “Temperature field of thick thermoset composite laminates during cure process”. *Composites Science and Technology*: 65 (2005): 517-523.

[h] M. LeGrand and V. Bellenger. “The cure optimisation of carbon/epoxy prepregs”. *Composites Science and Technology*: 58 (1998): 639-644.